Economical and Environmentally Friendly Geocast Routing in Vehicular Networks

by

Maazen Sulaiman Alsabaan

A thesis
presented to the University of Waterloo
in fulfillment of the
thesis requirement for the degree of
Doctor of Philosophy
in
Electrical and Computer Engineering

Waterloo, Ontario, Canada, 2013

I hereby declare that I am the sole author of this thesis. This is a true copy of the thesis, including any required final revisions, as accepted by my examiners.

I understand that my thesis may be made electronically available to the public.

Abstract

The volatile world economy has greatly affected fuel prices, while pollution and gas emissions are increasing to negatively impact global warming. Rising fuel costs have made drivers more concerned about how much of their monthly budgets are allocated for gasoline. In terms of the air pollution problem, greenhouse gas (GHG) emissions from vehicles are considered to be one of the main contributing sources. Carbon dioxide (CO_2) is the largest component of GHG emissions. As a result, it is important to develop and implement effective strategies to reduce fuel expenditure and prevent the expected increase of CO_2 emission from vehicles.

Vehicular networks offer a promising approach that can be applied in transportation systems to reduce fuel consumption and emissions. One of the major applications of vehicular networks is intelligent transportation systems (ITS). To exchange and distribute messages, geocast routing protocols have been proposed for ITS applications. Most of these protocols focus on improving network-centric performance measures (e.g., message delay, packet delivery ratio, etc.) instead of focusing on improving the performance measures that are meaningful to both the scientific community and the general public (e.g., fuel consumption and CO_2 emission).

Stop-and-go conditions, high acceleration, and unnecessary speed are uneconomical and environmentally unfriendly (UEU) actions that increase the amount of vehicle fuel consumed and the CO_2 emission. These actions can happen frequently for vehicles approaching a traffic light signal (TLS). This thesis proposes a new protocol named Economical and Environmentally Friendly Geocast (EEFG), which focuses on minimizing CO_2 emission and fuel consumption from vehicles approaching a TLS. The goal of this protocol is to deliver useful information to approaching vehicles inside the regions of interest (ROIs). Based on the information sent, the vehicle receiving the message adapts its speed to a recommended speed (S_R), which helps the vehicle reduce its UEU actions.

To determine the value of S_R, a comprehensive optimization model that is applicable in both vehicle-to-vehicle (V2V) communication and traffic light signal-to-vehicle (TLS2V) communication is developed. The objective function is to minimize fuel consumption by and emissions from vehicles. The speed that can achieve this goal is the optimum S_R (S_R^*). The thesis also proposes efficient heuristic expressions to compute the optimum or near-optimum value of S_R.

An extensive performance study of the EEFG protocol is performed. It shows the impact of using EEFG in a modeled real-world network for urban and suburban areas in the city of Waterloo, Ontario, Canada. Four case studies have been considered: (1) a suburban environment at the maximum traffic volume hour of the day; (2) a suburban environment at the minimum traffic volume hour of the day; (3) an urban environment at the maximum traffic volume hour of the day; (4) an urban environment at the minimum traffic volume hour of the day. The results show that EEFG saves fuel and CO_2 emission in all four cases. In addition, the thesis studies the effect of communication parameters (e.g., transmission range, packet delay, and packet dropping rate) on vehicle fuel consumption and CO_2 emission. Having high transmission range, low packet delay, and low packet dropping rate, can save more fuel and CO_2 emission.

Acknowledgements

All praise is to Allah for giving me the ability and knowledge to accomplish this thesis.

Several people deserve sincere recognition. I am deeply grateful to my advisor, Prof. Kshirasagar Naik, for his guidance, support, patience, and encouragement. He was always available, professional, and friendly. I have learned from him to think differently, be optimistic, and be self motivated. This work would have not been done without his advice and valuable comments.

I would like to thank Prof. Mahesh Pandey, Prof. Otman Basir, Prof. Catherine Gebotys, and Prof. Roch Glitho for serving as the committee members for my thesis. I am grateful to them for their fruitful discussions and comments.

Special acknowledgment is due to King Saud University and the Saudi Arabian Cultural Bureau in Canada for their financial support to complete my PhD degree. Thanks to the Regional Municipality of Waterloo for sharing with me useful data. I would like also to thank Prof. Hesham Rakha of Civil and Environmental Engineering at Virginia Tech for providing a spreadsheet with the VT-Micro model coefficients.

My sincere gratitude goes to all my colleagues from the Network Programming Lab, Tarek Khalifa, Majid Al-Tamimi, Tamer Abdelkader, Abdurhman Albasir and Abdulhakim Abogharaf. It has been my pleasure to work in this cooperative group. I sincerely thank Mary McPherson at the Writing Centre for her help and expert advice. Many thanks also go to the administration support staff in the Electrical and Computer Engineering Department for their help and efforts. I thank my dear friends Waleed Alasmary, Suhail Aldharrab, Nizar Alsharif, Omar Binhomaid, Abdullah Bin Humayd, Khalid Alsubhi, Olzhas Tazabekov, Mohamed El massad, and all my other friends, who make my life colorful and enjoyable.

I am forever indebted to my family for for their encouragement, continuing support, prayers, and love. My father, Mr. Sulaiman Alsabaan and my mother, Nora Al-Ateeq, and my siblings, Majid, Mohammed, Moatez, Mansour, Montaha, Roba, Meshary and Lamo, have been the greatest supporters in my life. I also cannot forget the unconditional love of my deceased grandfather, Khamees Alsabaan. May Allah grant him paradise. Thanks to my grandparents, uncles, aunts, and cousins for their prayers and encouragement.

Finally, I thank all my teachers, colleagues and friends who have helped and supported me in different ways throughout my work.

This thesis is dedicated

to my father, Sulaimn;

to my mother, Nora;

and to my brothers, Majid, Mohammed, Moatez, Mansour,and Meshary, and my sisteres, Montaha, Roba, and Lama

Table of Contents

List of Tables

List of Figures

List of Abbreviations

AU	Application Unit
OBU	On-Board Unit
PDA	Personal Digital Assistant
IVC	Inter-Vehicle Communication
HVC	Hybrid Vehicle Communication
VANETs	Vehicular Ad Hoc Networks
V2V	Vehicle-to-Vehicle
WLAN	Wireless Local Area Network
ITS	Intelligent Transportation System
IVG	Inter-Vehicle Geocast
HVG	Hybrid Vehicle Geocast
EEFG	Economical and Environmentally Friendly Geocast
GHG	Greenhouse Gas
CO_2	Carbon dioxide

ROI	Region of Interest
TLS2V	traffic light signal-to-vehicle
LBM	Location Based Multicast
EMDV	Emergency Message Dissemination for Vehicular environment
RC	Retransmission Counter
EEF	Economical and Environmentally Friendly
CMEM	Comprehensive Modal Emissions Model
VT-Micro	Virginia Tech Microscopic model
LDV	Light-Duty Vehicle
HDT	Heavy-Duty Truck
MEC	Model Emission Cycle
ORNL	Oak Ridge National Laboratory
EPA	Environmental Protection Agency
CA	Cellular automata
SUMO	Simulation of Urban Mobility
VSL	Variable Speed Limit
FC-VSL	Carbon-footprint/Fuel-consumption-aware Variable Speed Limit
TCS	Traffic Control System
VTL	Virtual Traffic Light

DSRC	Dedicated Short Range Communications
CCH	Control Channel
SCH	Service Channel
WSM	Wave Short Message
TLS	Traffic Light Signal
RSU	Road Side Unit
GPS	Global Positioning Systems
C2C-CC	Car-to-Car Communication Consortium
MAC	Medium Access Control
PHY	Physical
UEU	Uneconomical and Environmentally Unfriendly
MOE	Measures of effectiveness

Chapter 1

Introduction

1.1 Vehicular Networks

Vehicular networks consist of nodes (vehicles) equipped with an application unit (AU) and an on-board Unit (OBU) [1], which are connected to each other. An AU is an in-vehicle entity that runs applications such as a navigation system with communication capabilities. There are two types of AUs: the first type is embedded into a vehicle and permanently connected to an OBU. The second one is dynamically plugged into the in-vehicle network by means such as laptops and personal digital assistants (PDAs). In addition to an AU, an OBU is another in-vehicle entity and is responsible for wireless communication such as vehicle-to-vehicle and vehicle-to-infrastructure communications. An OBU is equipped with a (short-range) wireless communication device that is based on radio technology.

There are three possible network architectures for vehicular networks: inter-vehicle communication (IVC), infrastructure-based vehicle communication, and hybrid vehicle communication (HVC) as shown in Figure 1.1. IVC is a form of direct radio communication between vehicles without control centers. Thus, vehicles need to be equipped with network devices that are based on a radio technology capable of organizing access to channels in a decentralized manner (e.g., IEEE 802.11 and IEEE 802.11p). In addition, multi-hop routing protocols are required in order to forward messages to any destinations out of the sender's transmission range. IVC is also called vehicular ad hoc network (VANET) and vehicle-to-vehicle (V2V) communication. In infrastructure-based vehicle communication, fixed gateways, such as access points in a wireless local area network (WLAN), are used for communication. This network architecture could provide different application types and

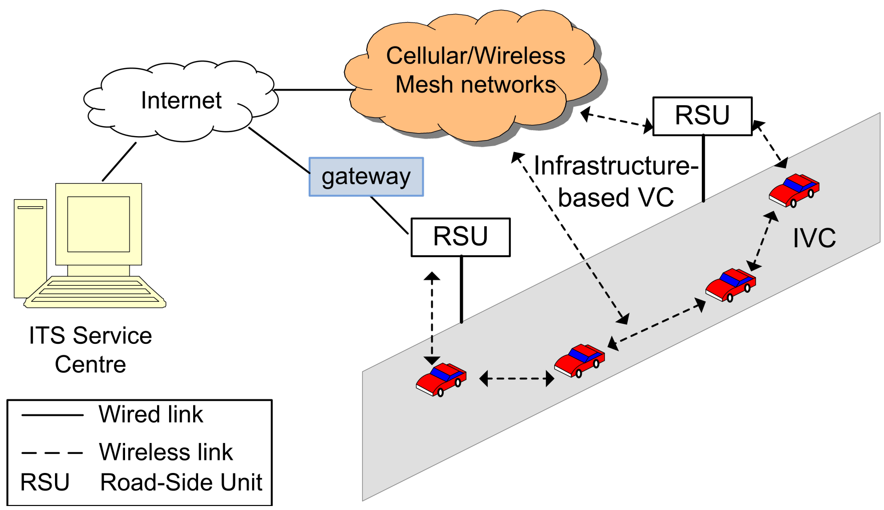

Figure 1.1: An ITS application architecture with vehicular networks

large coverage. However, the infrastructure cost has to be taken into consideration. Last is HVC, an integration of IVC with infrastructure-based communications.

Vehicular networks are a promising research area in intelligent transportation systems (ITSs) applications [2]. With vehicular networks, drivers can be informed about many kinds of events and conditions that can impact their travel. Applications for vehicular networks can be classified into safety and non-safety applications. The safety applications are intended to reduce the number of fatalities on roads. For example, a vehicle can identify itself as crashed by vehicular sensors that detect events like airbag inflation. Then, it sends a warning message to nearby vehicles. After receiving the message, drivers are aware of the crash; therefore, they can take an action such as choosing a different route or slowing down their cars gradually. The non-safety applications are available to comfort drivers and their passengers. Examples of non-safety applications are toll service and internet access[1].

Vehicular networks share some characteristics with ad hoc networks. However, vehicular networks can be distinguished from other kinds of ad hoc networks by their highly dynamic topology, frequently disconnected network, sufficient energy and storage, various communications environments, strict delay constraints, and interaction with on-board devices [3]. Some of these characteristics create many challenging issues that need to be addressed. For instance, the network layer has the challenge of finding and maintaining routes in vehicular networks, because of the network nodes' behavior that makes links change all the time or may even make no links available.

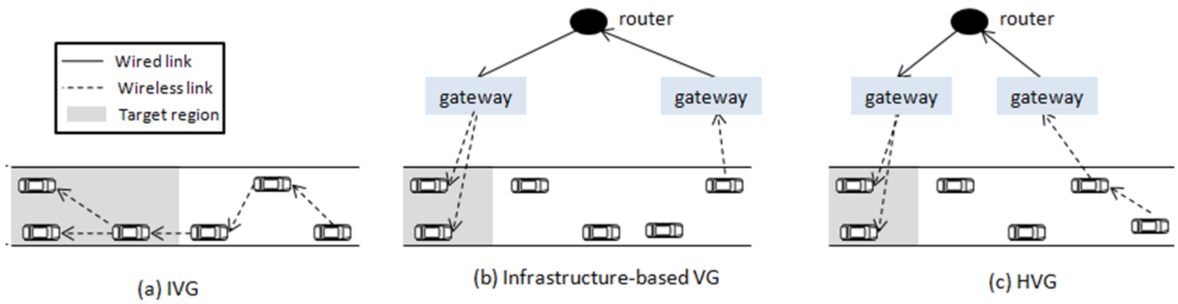

Figure 1.2: Vehicular networks architectures

1.2 Geocast Routing in Vehicular Networks

Geocast is a network protocol that aims to deliver data packets from a source node to all nodes that currently reside in selected geographical regions. Essentially, geocast provides two functions: geographical addressing and geographical forwarding. In geocast, a destination address is restricted within a position or a geographical region. It is assumed in geocast that every node knows its location and its neighbors' topology. Based on this information and the packet destination address, a node forwards the received packet. A geocast routing approach is useful in vehicular networks for two reasons: (1) position information for vehicles is made available by their navigation systems, which promises more efficient routing protocols; (2) many applications address their destinations by positions rather than identifiers. In vehicular networks, the possible network architectures for geocast can be classified into Inter-Vehicle Geocast (IVG), infrastructure-based vehicle geocast, and hybrid vehicle geocast (HVG) as shown in Figure 1.2. Table 1.1 compares these architectures in terms of cost, coverage, and applications.

Some important benefits from geocast protocols can be introduced to vehicular network applications. Using safety applications as an example, suppose a vehicle can identify itself as crashed by vehicular sensors that detect events like airbag inflation. Then, it sends a warning message targeting following vehicles within 500 m of the accident site. In this situation, vehicles outside the geocast region are not alerted. An example for non-safety applications is traveler information support such as a gas station advertising its existence and prices to approaching vehicles.

In many applications foreseen for vehicular networks, the one-time dissemination of information to all vehicles in a geographical region is rather inappropriate. For instance, it is clear that crashed vehicles will not be removed instantly after the accident happens. In this case, the warning message has to be valid until the accident site has been cleared.

Table 1.1: Comparison of vehicular networks' architectures

	IVG	Infrastructure-based VG	HVG
Cost	Low	High	Less infrastructure
Coverage	Based on the vehicle density	High	High, but it is not guaranteed in scenarios with low vehicle density
Main applications	Safety	Non-safety	Both safety and non-safety

Consequently, a new concept of geocast called "time-stable" or "abiding geocast" has been introduced [4, 5, 6, 7, 8]. A time-stable geocast protocol delivers a message to the users in the geocast region for a specific duration of time.

Almost all proposed geocast protocols evaluate network performance level (e.g., by message delays, packet delivery ratio, etc.), instead of evaluating the impact of the protocol on the vehicular system (e.g., on fuel consumption, emissions, travel time, etc.) [9]. This thesis presents a geocast protocol designed for minimizing vehicle fuel consumption and emissions. This protocol has been named the "Economical and Environmentally Friendly Geocast" (EEFG). To the best of our knowledge, our attempt is a first in the field. EEFG protocol aims to alleviate the main factors that affect increases in vehicle fuel consumption and emissions. Since the goals of the EEFG protocol are different from the existing geocast protocols, the required exchange of information and the functions of such an EEFG protocol differ.

1.3 Research Motivation and Objectives

The detrimental effects of air pollution and concerns about global warming are being increasingly reported by the media. In many countries, fuel prices have risen considerably. For instance, the gasoline price in western Canada increased around 150%, from about 53 cents/liter in 1998, to 127 cents/liter in 2012 [10]. As for air pollution, greenhouse gas (GHG) emissions from vehicles are considered one of the main contributing sources. Carbon dioxide (CO_2) is the largest component of GHG emissions. For example, in the European Union (EU), in 2009, CO_2 emission from the transport sector were about 25%

of the entire EU's CO_2 emission [11]. The Kyoto Protocol aims to stabilize the GHG concentrations in the atmosphere at a level that would prevent dangerous alterations to regional and global climates [12]. As a result, it is important to develop and implement effective strategies to reduce fuel expenditure and prevent the expected increase in CO_2 emission from vehicles.

This research has been motivated by the fact that geocast protocols in vehicular networks can play a key role in reducing vehicle fuel consumption and CO_2 emission. Stop-and-go condition, unnecessary high speed, high acceleration, and congestion are uneconomical and environmentally unfriendly (UEU) actions that increase the amount of vehicle fuel consumption and CO_2 emission. Some of these actions happen frequently with vehicles approaching a traffic light signal (TLS). For this scenario, our objective is to propose a new protocol named Economical and Environmentally Friendly Geocast (EEFG), which focuses on minimizing CO_2 emission and fuel consumption from vehicles. The goal of the protocol is to deliver required information to vehicles inside the region of interest (ROI). Based on the information sent, the vehicle receiving the message adapts its speed to the optimum recommended speed (S_R^*), which helps the vehicle reduce some of the UEU actions. As a result, minimum vehicle fuel consumption and CO_2 emission are achieved.

1.4 Summary of Contributions

This thesis makes the following contributions:

- It studies in-depth the use of vehicular communication networks to provide green solutions. It shows how to apply a fuel consumption and emission model to vehicular networks. Moreover, it identifies a suitable scenario wherein applying vehicular geocast protocols will significantly reduce vehicle fuel consumption and CO_2 emission. This scenario involves vehicles approaching a TLS where the main UEU actions that can occur are stop-and-go conditions, unnecessarily excessive speed, and unnecessarily high acceleration. The key parameter that controls the relation between vehicular networks and energy saving is vehicular traffic mobility as summarized in Figure 1.3.

- It develops a new geocast routing protocol for vehicular networks, named Economical and Environmentally Friendly Geocast (EEFG), that has the following attributes:
  - The objective functions are to reduce fuel consumption and CO_2 emission by vehicles approaching a TLS;

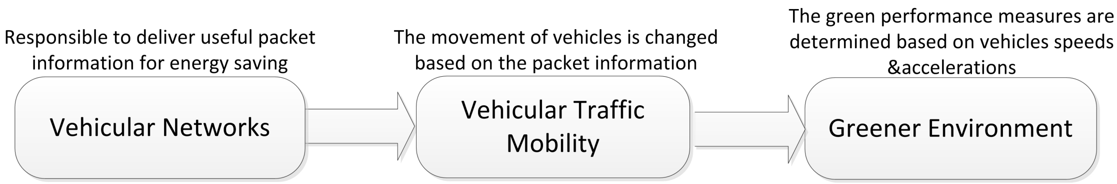

Figure 1.3: Relation between vehicular networks and energy saving

  - The ROIs are determined and adapted according to the aforementioned objective functions. Moreover, the packet contents and message delivery are developed to achieve the same goal.

- It develops a comprehensive optimization model that is applicable in both V2V communication and traffic light signal-to-vehicle (TLS2V) communication as a special case, with the objective function of minimizing fuel consumption and emissions of vehicles approaching a TLS. This model determines the value of the optimum recommended speed (S_R^*) that will lead to the maximum reduction of fuel use and emissions. Therefore, this objective is achieved by controlling the vehicle speed to S_R^*, which helps the vehicle avoid having to stop, making lengthy accelerations, and running at unnecessarily excessive speed. This thesis shows that, in most cases, S_R^* equals the recommended speed of the leading vehicle (S_{Rl}) if the follower, once it increases its speed to more than S_{Rl}, will be affected by its leader; S_R^* equals the minimum speed limit (S_{min}) if the vehicle has to stop anyway; S_R^* is within the range $S_{Rl} \leq S_R^* \leq S_{max}$ if the vehicle is able to increase its speed to more than S_{Rl} without being affected by its leader. The minimum fuel consumption and CO_2 emissions can be achieved if the vehicle travels at S_R^*.

- It proposes heuristic expressions to compute the optimum or near-optimum recommended speed (S_R) of vehicles approaching a TLS. These expressions have been proposed based on the observations drawn from optimization results presented in Chapter 5: (1) the optimum S_R should be the maximum possible speed that allows the vehicle to pass the TLS without idling or decelerating; (2) if the vehicle has to stop, the result of the optimum S_R equals S_{min}; (3) the optimum S_R must equal the maximum speed limit (S_{max}) if the vehicle is close to a green TLS and can catch it. In the case of TLS2V communication, the optimization and heuristic expressions give the same S_R results. However, the results might slightly differ if V2V communication is involved because of many factors, including speed limitation, current speed value, S_{Rl} value, distance between vehicles, distance to the TLS, TLS phase times, time of idling, and time of deceleration. These factors are considered in the optimization model.

- It studies the effect of communication parameters (e.g., transmission range, packet delay, and packet dropping rate) on vehicle fuel consumption and CO_2 emission.

- It provides extensive performance studies using a modeled real-world network for urban and suburban areas in the city of Waterloo, Ontario, Canada. Four case studies have been considered in this thesis to evaluate the EEFG protocol: (1) a suburban environment at the maximum traffic volume (peak) hour of the day; (2) a suburban environment at the minimum traffic volume (off-peak) hour of the day; (3) an urban environment at the maximum traffic volume hour of the day; (4) an urban environment at the minimum traffic volume hour of the day. The results show that EEFG saves fuel and CO_2 emission in all four cases.

1.5 Thesis Organization

This thesis is organized as follows:

- Chapter 2 provides the background material for this research. The research requires integration of fuel consumption and emission models with vehicular networks. The key parameter that controls the relation between vehicular networks and energy saving is the vehicular traffic mobility. Therefore, this chapter covers three different research areas: (1) geocast protocols in vehicular networks; (2) vehicle fuel consumption and emission models; (3) traffic flow models. The chapter also reviews other research efforts that have used vehicular networks to reduce vehicle fuel consumption and emissions.

- Chapter 3 presents the system model, assumptions, and the problem definition. It also identifies strategy and steps to achieve a solution.

- Chapter 4 describes the mechanism of the proposed EEFG protocol for vehicles approaching a TLS. It defines the regions of interest and develops mathematical formulations to determine these regions. Additionally, the chapter provides details on data dissemination to deliver packets containing useful information with the objective of reducing vehicle fuel consumption and CO_2 emission.

- Chapter 5 develops an optimization model that is applicable in both TLS2V and V2V communications. This model determines the value of S_R that leads to the maximum reduction of fuel use and emissions. Analytical results for a leading and following vehicle in different cases have been studied in this chapter.

- Chapter 6 proposes heuristic expressions to compute the optimum or near-optimum S_R of the leading and following vehicles. It compares the results of the expression to those using the optimization model.

- Chapter 7 presents results of a scale-up simulation study using a modeled real-world network of urban and suburban environments. In each environment, the chapter evaluates the EEFG protocol during the peak and the off-peak hour of the day. It shows the benefit of using EEFG and the effect of the communication measures on fuel consumption and CO_2 emission. Moreover, the results show the amount of fuel and CO_2 emission when vehicles travel at optimum and computed S_R.

- Chapter 8 summarizes the thesis work and provides interesting and challenging directions for future research.

Chapter 2

Background and Literature Survey

This research brings together three key areas:

1. Geocast protocols in vehicular networks;
2. Vehicle fuel consumption and emission models;
3. Traffic flow models.

2.1 Geocast protocols in Vehicular Networks

Geocast protocols provide the capability to transmit a packet to all nodes within a geographic region. The geocast region is defined based on the applications. For instance, a message to alert drivers about congestion on a highway may be useful to vehicles approaching an upcoming exit prior to the obstruction, yet unnecessary to vehicles already in the congested area. This region in all protocols proposed in the literature is assumed to be fixed without the consideration of an objective function; also it is not known how the region is calculated. These protocols are classified based on the forwarding types, which are either simple flooding, efficient flooding, or forwarding without flooding [9] in order to reduce latency or increase reliability. In this thesis, we want to draw the attention of researchers in the field of communication to designing geocast protocols intended to reduce vehicle fuel consumption and emissions. Therefore, we classify the geocast protocols based on performance measures as in the following subsections.

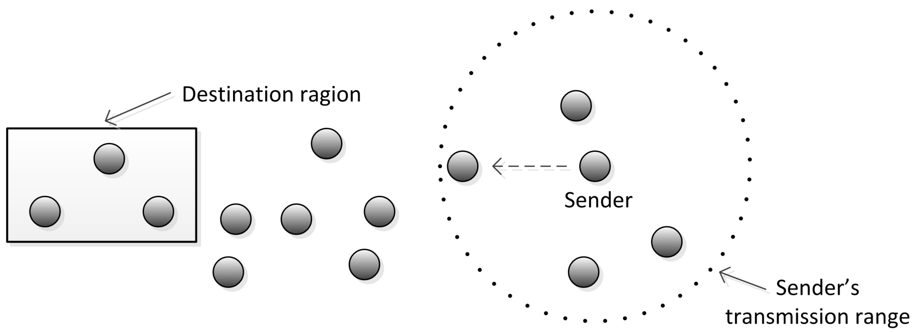

Figure 2.1: An example of greedy forwarding

2.1.1 Geocast protocols to minimize message latency

Message latency can be defined as the delay of message delivery. A higher number of wireless hops causes an increase in message latency. Greedy forwarding can be used to reduce the number of hops used to transmit a packet from a sender to a destination [13]. In this approach, a packet is forwarded by a node to a neighbor located closer to the destination, as depicted in Figure 2.1. Contention period strategy can potentially minimize message latency. In reference [14], when a node receives a packet, it waits for a certain time before rebroadcasting. This waiting time depends on the distance between the node and the sender; as such, the waiting time is shorter for a more distant receiver. The node will rebroadcast the packet if the waiting time expires and the node has not received the same packet from another node. Otherwise, the packet will be discarded.

2.1.2 Geocast protocols to increase dissemination reliability

One of the main problems associated with geocast routing protocols is that they do not guarantee reliability, thus not all nodes inside a geographic area can be reached. Simple flooding forwarding can achieve a high delivery success ratio because it has high transmission redundancy. However, the delivery ratio will worsen with increased network size. Also, frequent broadcasting in simple flooding causes message overhead and collisions. To limit the inefficiency of the simple flooding approach, directed flooding approaches have been proposed that define a forwarding zone and apply a controlled packet retransmission scheme within the dissemination area [15][16][17].

Location Based Multicast (LBM) protocols are based on flooding in which a forwarding zone is defined. In reference [15], two LBM protocols have been proposed. The first protocol defines the forwarding zone as the smallest rectangular shape that includes the sender and destination region. The second, a distance-based forwarding zone, defines the forwarding zone by the coordinates of sender, destination region, and distance of a node to the center of the destination region. An intermediate node broadcasts a received packet only if it is inside the forwarding zone. The Emergency Message Dissemination for Vehicular environment (EMDV) protocol requires the forwarding zone to be shorter than the communication range and to lie in the direction of dissemination [16]. The forwarding range is adjusted according to the probability of reception of a single hop broadcast message. In this case, high reception probability near the boundary of the range can be achieved.

A retransmission counter (RC) is proposed as a packet retransmission scheme [16]. When nodes receive a packet, they cache it, increment the RC and start a timer. RC=0 means the node did not receive the packet correctly. The packet will be rebroadcast if the time is expired. Moreover, the packet will be discarded if the RC reaches a threshold.

For small networks, temporary caching can potentially increase the reliability [17]. The caching of geounicast packets is used to prevent the loss of packets in case of forwarding failures. Another type of caching is for geobroadcast, which is used to keep information inside a geographical area alive for a certain time.

2.1.3 Geocast protocols to reduce vehicle fuel consumption and emissions

To the best of our knowledge, most existing protocols focus on improving network-centric performance measures (e.g., message delay and packet delivery ratio) instead of improving the performance measures that are meaningful to both the scientific community and the general public (e.g., fuel consumption and CO_2 emissions). The key performance measures of this thesis are vehicle fuel consumption and CO_2 emissions. These can be called economical and environmentally friendly (EEF) measures.

Improving the network measures will improve the EEF measures. However, the existing protocols are not EEF because their delivery approach and provided information are not designed to assist vehicles in reducing uneconomical and environmentally unfriendly (UEU) actions such as high acceleration, stop-and-go conditions, congestion, high speeds, indirect routing, and idling. Moreover, navigation systems may choose routes that later become congested and inefficient after drivers commit to that path. In [18][19], we studied how vehicular networks can be used to reduce fuel consumption and CO_2 emission in a city and a highway environment. This thesis introduces a protocol called Economical and Environmentally Friendly Geocast (EEFG) that can deliver useful information to approaching

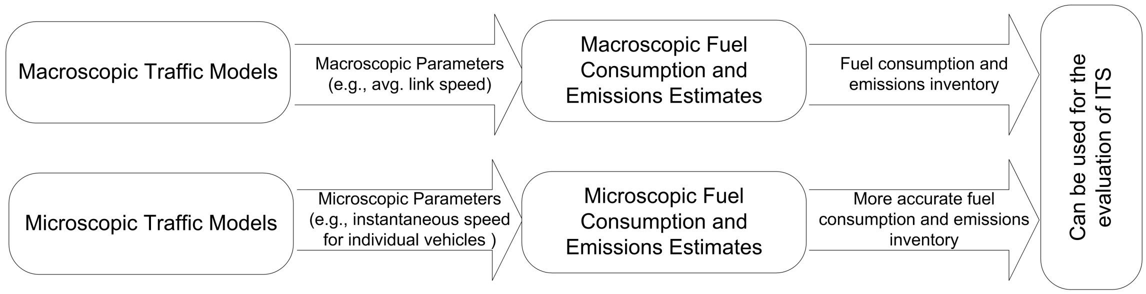

Figure 2.2: Summary of the link between traffic flow and fuel consumption and emission models.

vehicles. Based on that information, fuel consumption and CO_2 emissions are reduced if vehicles travel at the recommended speed (S_R).

2.2 Fuel Consumption and Emission Models

Environment and automotive engineers have proposed several models for vehicle fuel consumption and emissions. Essentially, two classes of models have been developed: macroscopic [20][21] and microscopic [22][23]. The macroscopic models estimate fuel consumption and emissions based on average link speeds. This class of models is relatively simple, but it has only limited accuracy. Meanwhile, microscopic models address this limitation by providing fuel consumption and emission levels based on instantaneous speed and acceleration. Thus, they predict changes more precisely. An evaluation study has been applied on a macroscopic model called MOBILE6 and two microscopic models: the Comprehensive Modal Emissions Model (CMEM) and the Virginia Tech Microscopic model (VT-Micro) [23]. It has been demonstrated that the VT-Micro and CMEM models produce more reliable fuel consumption and emissions estimates than MOBILE6 [20]. Figure 2.2 shows the link between transportation models and fuel consumption and emissions estimates.

Microscopic models are well suited for ITS applications since these models are concerned with computing fuel consumption and emission by tracking individual vehicles instantaneously. The following subsections briefly describe two widely used microscopic models.

2.2.1 CMEM Model

The development of CMEM began in 1996, with researchers at the University of California, Riverside. The term "comprehensive" is utilized to reflect the ability of the model to predict fuel consumption and emissions for a wide variety of vehicles under various conditions. CMEM was developed as a power-demand model. It estimates about 30 vehicle/technology categories, from the smallest Light-Duty Vehicles (LDVs) to class 8 Heavy-Duty Trucks (HDTs) [22]. The required inputs for CMEM include vehicle operational variables (e.g., second-by-second speed and acceleration) and model-calibrated parameters (e.g., cold-start coefficients and engine-out emission indices). The cold-start coefficients measure the emissions that are produced when vehicles start operation, while engine-out emission indices are the amount of engine-out emissions in grams per one gram of fuel consumed [22][24]. The CMEM model was developed using vehicle fuel consumption and emission testing data collected from over 300 vehicles on three driving cycles, following the Federal Test Procedure (FTP), US06, and the Model Emission Cycle (MEC). Both second-by-second engine-out and tailpipe emissions were measured.

2.2.2 VT-Micro Model

VT-Micro ia a statistical model developed based on testing data collected at the Oak Ridge National Laboratory (ORNL) and the Environmental Protection Agency (EPA) of the United States. These data include fuel consumption and emission rate measurements as a function of the vehicle's instantaneous speed and acceleration levels. Therefore, the input variables of this model are the vehicle's instantaneous speed and acceleration. The model was finalized as a regression model from experimentation with numerous polynomial combinations of speed and acceleration levels, as shown in the following equation.

$$\ln(MOE_e) = \begin{cases} \sum_{i=0}^{3}\sum_{j=0}^{3}(L_{i,j}^{e} \times s^i \times a^j), & \text{for } a \geqslant 0 \\ \sum_{i=0}^{3}\sum_{j=0}^{3}(M_{i,j}^{e} \times s^i \times a^j), & \text{for } a < 0 \end{cases} \tag{2.1}$$

where

$\ln(y)$: Natural logarithm function of y, where y is a real number;

s: Instantaneous vehicle speed (km/h);

a: Instantaneous vehicle acceleration (km/h/s);

MOE_e: Instantaneous fuel consumption or emission rate (L/s or mg/s);

e: An index denoting fuel consumption or emission type, such as CO_2, HC, and NO_x emissions. e is not an exponential function;

$M^e_{i,j}$: Model regression coefficient for MOE_e at speed power i and acceleration power j for negative accelerations;

$L^e_{i,j}$: Model regression coefficient for MOE_e at speed power i and acceleration power j for positive accelerations.

As noticed from the above equation, the model is separated for positive and negative accelerations because vehicles exert power in positive accelerations, but do not exert power in negative accelerations. The VT-Micro model is inserted into a microscopic traffic simulator called "INTEGRATION" to compute vehicles' fuel consumption and emissions [25]. This model has been used in this research due to its simplicity and high accuracy since it produces vehicle emissions and fuel consumption that are consistent with the ORNL data. The correlation coefficient between the ORNL data and the model predicted values ranges from 92% to 99% [26].

Example of using the VT-Micro Model

Sample model coefficients for estimating CO_2 emission for a composite vehicle are introduced in Table 2.1. The vehicle was derived as an average across eight light duty vehicles (LDVs). The required input parameters of the model are $s, a, L^e_{i,j}$, and $M^e_{i,j}$.

In this example, the effect of speed and acceleration on the vehicle CO_2 emissions is studied. To study the impact of vehicle speed, the vehicle acceleration is set to a constant value (say 0 kph/s). After that, the CO_2 emissions are computed with different values of speed using the VT-Micro model. Figure 2.3(a) shows that CO_2 emissions increase with high speeds. Similarly, to show the effect of vehicle acceleration, the vehicle speed is set to 30 kph. Then, the CO_2 emissions are calculated with different values of accelerations. Figure 2.3(b) demonstrates that negative accelerations do not affect the CO_2 emissions much because vehicles do not exert power in negative accelerations. On the other hand, the amount of CO_2 emissions increases with high acceleration.

Table 2.1: VT-Micro model coefficients for estimating CO_2 emission

Coefficients	s^0	s^1	s^2	s^3
Positive a				
a^0	6.91	2.75E-02	-2.07E-04	9.80E-07
a^1	0.22	9.68E-03	-1.01E-04	3.66E-07
a^2	2.35E-04	-1.75E-03	1.97E-05	-1.08E-07
a^3	-3.64E-04	8.35E-05	-1.02E-06	8.50E-09
Negative a				
a^0	6.91	2.84E-02	-2.27E-04	1.11E-06
a^1	-3.20E-02	8.53E-03	-6.59E-05	3.20E-07
a^2	-9.17E-03	1.15E-03	-1.29E-05	7.56E-08
a^3	-2.89E-04	-3.06E-06	-2.68E-07	2.95E-09

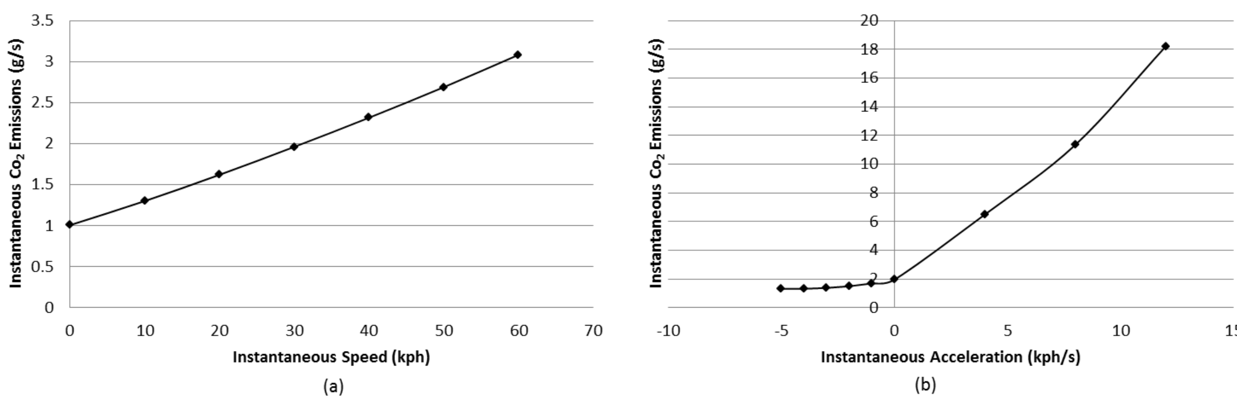

Figure 2.3: The impact of speed and acceleration on vehicle CO_2 emissions

2.3 Traffic Flow Models

One of the critical factors in traffic engineering is traffic density (known in the communication field as node density). Node density is an important factor that significantly affects vehicles' movement on the road, the communication protocols' performance, and the resulting green measures. Vehicular networks have been widely used to estimate or calculate the number of vehicles on the road. However, such methods have two inherent problems: their inaccuracy and their complexity.

Most decisions on ITS applications involve the number of vehicles, especially in road congestion, which plays a significant role in vehicular communication protocols [27] [28] [29] [30]. Vehicle mobility greatly affects the green measures. Gasoline consumption changes due to differences in speeds, accelerations, stop-and-go times, routes, and traffic congestion levels [18] [19] [31]. Thus, designing a green vehicular network protocol requires an understanding of vehicles' mobility model and the relation to the network protocol. Below is a brief description of each traffic flow parameter.

Speed (S): the distance traveled during a given period of time. Speed can be expressed in kilometers per hour (km/h), feet per second (ft/s), and miles per hour (ml/h). There are two essential speed parameters: the free-flow speed (S_F) and the speed-at-capacity (S_c). According to [32], the free-flow speed has mainly two definitions: (1) the maximum speed that is attained when density approaches zero, which means only one vehicle is present; (2) the average speed of vehicles under the condition of low traffic volume over a road segment that is not interrupted by external devices such as traffic light signals and STOP signs. The second parameter is speed-at-capacity, which can be defined as the traffic stream speed at the maximum sustainable flow rate.

Flow / Volume (q): the number of vehicles passing a particular point on a roadway during a unit of time. Traffic volume is expressed as vehicles per hour (vph) or vehicles per hour per lane (vph/lane). There is an essential flow parameter called "Basic saturation flow (q_m)", which is the maximum number of vehicles that would have passed a road segment after one hour. q_m is the capacity of a roadway section.

Density (k): the number of vehicles occupying a unit length of a road segment at a given instant in time, typically expressed as vehicles per kilometer (v/km) or vehicles per mile (v/ml). Two important density parameters are the density-at-capacity (k_c) and the jam density (k_j). Similar to S_c, k_c can be defined as the traffic density at the maximum sustainable flow rate. The jam density, on the other hand, is the highest density that occurs when all vehicle movement has stopped. In this case, the speed and flow of the traffic stream approach zero.

Headway: a microscopic measure, there are two types: space headway and time headway. Space headway is the distance between two successive vehicles in meters or feet. Time headway is the time interval in seconds between two successive vehicles as they arrive at a point on the roadway.

The above parameters are related to each other as follows:

$$flow = speed \times density \tag{2.2}$$

$$\text{space headway } (m) = \frac{1000}{density(v/km)} \tag{2.3}$$

$$\text{time headway } (s) = \frac{3600 \times \text{space headway } (m)}{speed(km/h) \times 1000} \tag{2.4}$$

Figure 2.4 shows the general shapes of the relationships between the traffic flow parameters. Regarding these relationships, hypotheses can be made as follows:

1. **For the speed-flow relationship**

   - When the value for flow equals zero, speed will equal the free-flow speed;
   - As flow increases, speed decreases;
   - Flow will reach its maximum value when speed equals speed-at-capacity;
   - After traffic reaches the maximum flow, any further vehicles will result in a reduction in the number of vehicles passing a particular point on a roadway during a unit of time;
   - Congestion will happen when speed and flow approach zero.

2. **For flow-density relationship**

   - Flow will be zero if the number of vehicles occupying a unit length of a road segment is zero;
   - Continuous increase in density will result in a continuous increase in flow up to a maximum value;
   - Then, flow decreases with increasing density;

- Flow becomes zero when jam density is reached.

3. **For speed-density relationship**
   - When density equals zero, speed will equal the free-flow speed;
   - As density increases, speed decreases;
   - When density reaches jam density, speed will be zero.

4. **For speed-headway relationship**
   - As the space headway becomes small and approaches the jam density headway, vehicles will decelerate until a complete stop is reached;
   - At large space headway, vehicles can attain high speeds.

Traffic mobility models are classified into macroscopic and microscopic. The macroscopic ones are developed to seek simplicity and measure a single value (e.g., average speed) for the whole traffic flow [33]. However, they do not consider transient changes in a vehicle's speed and acceleration levels. To overcome this limitation, microscopic models have been proposed that measure a single value for each vehicle [34]. They are concerned with describing the flow by tracking individual vehicles instantaneously. As a result, microscopic traffic flow models are well suited for ITS applications. These models are either car-following or cellular automata.

2.3.1 Car-following Models

Car-following models are time-continuous [34]. All these models describe how one vehicle follows another vehicle. The car-following parameter is headway, which is either space headway or time headway. Space headway is the distance between two successive vehicles. Time headway is the time interval between two successive vehicles as they arrive at a point on the roadway. Figure 4.1 shows a comprehensive set of notations used to describe the car-following theory. Definitions of these notations are as follows:

n: Leading vehicle;

$n+1$: Following vehicle;

L_n: Length of leading vehicle;

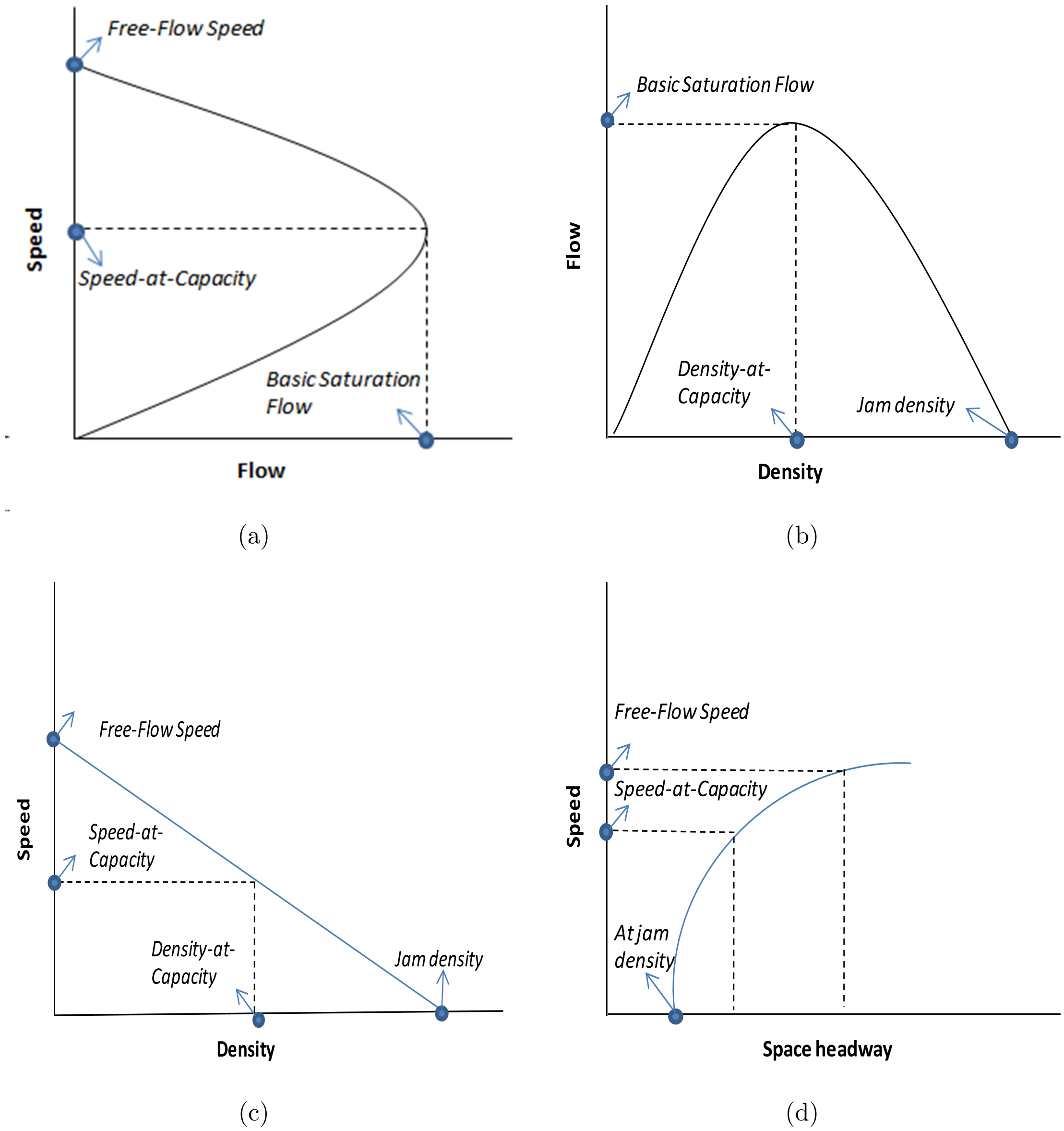

Figure 2.4: Traffic flow parameters relationships

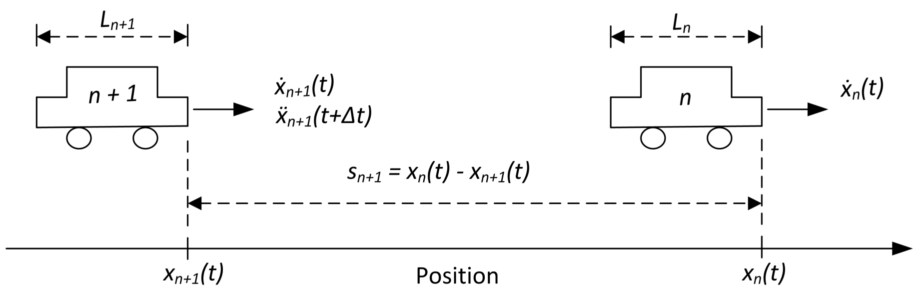

Figure 2.5: Car-Following theory notations.

L_{n+1}: Length of following vehicle;

$x_n(t)$: Position of leading vehicle at time t;

$\dot{x}_n(t)$: Speed of leading vehicle at time t;

$\dot{x}_{n+1}(t)$: Speed of following vehicle at time t;

$\ddot{x}_{n+1}(t)$: Acceleration or deceleration rate of the following vehicle at time $t + \Delta t$;

Δt: Reaction time;

s_{n+1}: Space headway of following vehicle.

The acceleration or deceleration rate occurs at time $t + \Delta t$. The reaction time is the time between t and the time the driver of the following vehicle decides to accelerate or decelerate. The time headway of the following vehicle can be determined as

$$h_{n+1} = s_{n+1}/\dot{x}_{n+1} \tag{2.5}$$

$[\dot{x}_n(t) - \dot{x}_{n+1}(t)]$ is the relative speed of the leading vehicle and the following vehicle. The space headway will increase if the leading vehicle has a higher speed than the following vehicle. This implies that the relative speed is positive. On the other hand, if the relative speed is negative, the leading vehicle has a lower speed than the following vehicle and the space headway is decreasing.

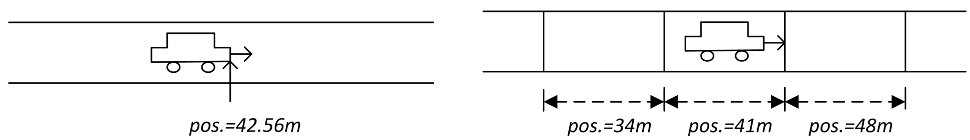

(a) Space-continuous (b) Space-discrete

Figure 2.6: The difference between space-continuous and space-discrete models.

2.3.2 Cellular Automata Models

Cellular automata (CA) models are dynamic ones in which space and time are discrete. A cellular automaton consists of a grid of cells. Each cell can be in one of a finite number of states, which are updated synchronously in discrete time steps according to a rule. The rule is the same for each cell and does not change over time. Moreover, the rule is local which means the state of a cell is determined by the previous states of a surrounding neighborhood of cells. CA has been applied to many traffic engineering software packages, including Simulation of Urban Mobility (SUMO) [35], TRANSIM [36], MMTS [37], and RoadSim [38]. CA is simpler than car-following; however, it is less accurate and the locality of the rules makes drivers short-sighted, meaning that they do not know if the leading vehicle will move or stop. Figure 2.6 shows the difference between space-continuous and space-discrete models.

Example of a cellular automata model of car traffic

The model in this example is for a one-way street with one lane. The street is divided into cells. Each cell can be in one of two states (s): an empty cell is denoted by a “0”, while an occupied cell is denoted by a “1”. The movements of the vehicles are simulated as they jump from one cell to another ($i \rightarrow i+1$). The rule is that a vehicle jumps only if the next cell is empty. Consequently, the state of a cell is determined based on the states of its neighbors. In this model, each cell has two neighbors: one in front and one behind. The car motion rule is explained in Table 2.2. For example, when all states ($i-1$, i, and $i+1$) equal “1”, which means each cell is occupied by a vehicle, cell i will still have the vehicle for the next time step. An example of the grid configuration over one time step is shown in Table 2.3. At t = 0, position 1 is occupied by car A, while position 2 is empty. Therefore, car A can move to position 2 at the next time step (t = 1). Similarly, car B and C are able to move at t = 1.

The fraction of cars able to move is the number of motions divided by the total number of cars. For instance, in Table 2.3 at t=0, the number of motions is the same as the total

Table 2.2: An example of CA rule table for updating the grid

$(s_{i-1}s_is_{i+1})_t$:	111	110	101	100	011	010	001	000
$(s_i)_{t+1}$:	1	0	1	1	1	0	0	0

Table 2.3: An example of grid configuration over one time step

Position⇒ Time⇓	Pos. 1	Pos. 2	Pos. 3	Pos. 4	Pos. 5	Pos. 6	Pos. 7	Pos. 8
$t = 0$	car A (1)	empty (0)	empty (0)	car B (1)	empty (0)	car C (1)	empty (0)	empty (0)
$t = 1$	empty (0)	car A (1)	empty (0)	empty (0)	car B (1)	empty (0)	car C (1)	empty (0)

number of cars; it is equal to three. As a result, the fraction of cars that can move equals one. This indicates that the traffic is low in the system, and all the cars are able to move.

2.4 Related Work

Related work can be divided into two categories: Geocast protocols and the attempts of applying vehicular networks at signalized intersections for green purposes. In terms of Geocast, the existing protocols focus on improving network-centric performance measures such as message delay and packet delivery ratio. They do not focus on how to assist vehicles to avoid the UEU actions.

Different research efforts have used vehicular communications networks to reduce vehicle fuel consumption and emissions. In [39], the authors attempted to shorten the time needed for a vehicle to find an available parking space. The authors proposed a reservation protocol using vehicular ad hoc networks (VANETs) to disseminate and efficiently allocate parking places to drivers. The protocol was evaluated in terms of the average time drivers needed to park but not in terms of vehicle fuel consumption and emissions. In the area of variable speed limit (VSL), vehicular networks have been used to conserve fuel and reduce pollution. In [40], a carbon-footprint/fuel-consumption-aware variable speed limit (FC-VSL) scheme has been designed for freeways under real-time conditions such as accidents, visibility, and wind speed. The system architecture uses vehicular communication networks for speed sensing and transmitting vehicles' information to a traffic control system (TCS) through road side units (RSUs). The TCS performs data analysis and calculates a vehicle trajectory with minimum fuel consumption and emissions. Vehicular networks are also used to send the optimum trajectory to vehicles to determine a new speed limit.

At intersections, vehicular networks are used to reduce fuel consumption and emissions. For un-signalized intersections, Ferreira *et al.* in [11] present the concept of virtual traffic lights (VTLs) using VANETs. Each vehicle approaching the intersection periodically broadcasts beacons to advertise its location. Beaconing and location tables are used to determine whether a VTL needs to be created or has been already created by election of a vehicle as the intersection leader responsible for controlling the VTL. In this case, the VTL must be obeyed by vehicles approaching the intersection. Simulation results show an almost 20% reduction of CO_2 emissions when using VTLs under high density traffic. Research on using vehicular networks at signalized intersections to reduce fuel consumption and emissions can be classified into two types: (1) controlling a TLS based on information transmitted from approaching vehicles [41]; (2) controlling vehicles based on information transmitted from the TLS ahead.

A few studies have been conducted to minimize vehicle fuel consumption and emissions by utilizing the information received from TLSs. Tielert *et al.* studied the effect of gear choices on minimizing vehicle fuel consumption and emissions [42]. The authors used traffic light signal-to-vehicle (TLS2V) communication to deliver TLS information to approaching vehicles. Based on that information, vehicles chose the preferred gear that enhances vehicle fuel consumption and emissions. However, authors did not develop an optimization model in order to help vehicles achieve the maximum reduction of fuel and emissions. TLS2V communication has been used in [43] to decrease the average idling time at TLSs. As a result, vehicle fuel consumption and emission will be reduced. Although reducing idling time results in the reduction of fuel and emissions, it is not proven if this reduction is the maximum. Another attempt presented by Rakha *et al.* in [44] is using TLS2V to highlight the importance of microscopic fuel consumption models in minimizing fuel and emissions.

The aforementioned studies consider only TLS2V communication and no ROIs are defined. Moreover, they do not guarantee if the achieved reductions are the optimum. This thesis develops a new geocast routing protocol for vehicular networks, named Economical and Environmentally Friendly Geocast (EEFG), that has the following attributes:

- The objective functions are to reduce fuel consumption and CO_2 emission by vehicles approaching a TLS;
- The ROIs are determined and adapted according to the aforementioned objective functions. Moreover, the packet contents and message delivery are developed to achieve the same goal.

In addition, this thesis develops a comprehensive optimization model that is applicable in both V2V communication and traffic light signal-to-vehicle (TLS2V) communication as a special case, with the objective function of minimizing fuel consumption and emissions of vehicles approaching a TLS.

2.5 Summary

In this chapter, three research areas have been briefly surveyed: geocast protocols, vehicle fuel consumption and emission models, and traffic flow models. Geocast protocols in vehicular networks have been examined. The protocols have been classified based on their performance measures. To the best of our knowledge, almost all of these protocols evaluate network-centric performance measures, instead of evaluating the impact of the protocol on the vehicular system. The key performance measures of this thesis are vehicle fuel consumption and CO_2 emissions. To be able to calculate these performance measures, two microscopic vehicle fuel consumption and emission models are presented: the CMEM model and VT-Micro model. It has been reported that the VT-Micro model is superior to other models for its accuracy. After that, traffic flow parameters are described and car-following and cellular automata concepts are reviewed. Although car-following models are more accurate and widely used than CA models, CA is simpler to implement. Research efforts that have used vehicular networks to reduce vehicle fuel consumption and emissions are discussed.

Chapter 3

System Model, Problem Definition, and Solution Strategy

3.1 System Model

Since this work is quite interdisciplinary, models from different areas have to be considered. The system model includes (1) communication model: represents the communication components and technologies that can be used for such an application; (2) traffic model: represents the characteristics of the road network; (3) mobility model: represents the the movement of vehicles, and how their location, velocity and acceleration change over time; (4) fuel consumption and emission model: estimates the amount of fuel consumption and CO_2 emissions from vehicles. We use VT-Micro model as in Subsection 2.2.2.

3.1.1 Communication Model

The Dedicated Short Range Communications (DSRC) spectrum enables wireless devices to use different services via seven channels, a control channel (CCH) and six service channels (SCHs). CCH is dedicated for safety communications, while the others are used for non-safety transmissions (e.g., Internet access and real-time audio/video streaming). Vehicles that intend to use DSRC should be equipped with IEEE 802.11p and WAVE devices.

The IEEE 802.11p is based on the well-established IEEE 802.11a standard for wireless access [45]. However, IEEE 802.11p is enhanced for mobile access and short-to-medium range communications. To coordinate the wireless access for safety messages and other services, the IEEE 1609.4 standard [46] is defined for multichannel operation. The IEEE 1609.4 provides a split-phase multichannel medium access control protocol with a dedicated control channel. The IEEE 1609.4 standard is a split-phase since – typically – nodes keep switching alternately between CCH and one of the SCHs. Figure 3.1 illustrates the operation of multichannel switching in IEEE 1609.4. Other functionalities such as security, networking and resource management are also defined in the IEEE 1609 family of standards.

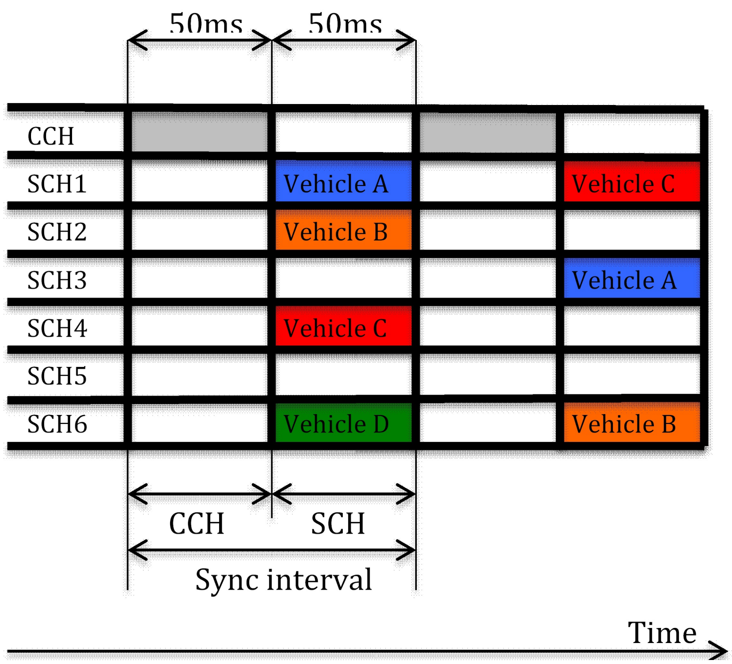

Figure 3.1: Example of multichannel operation of IEEE 1609.4

A DSRC operating device typically works as follows. Its radio is tuned to the CCH for half of the frame time (i.e., 50ms). During this phase, each vehicle generates a beacon message, which contains information regarding vehicle speed, position coordinates, etc. The generation rate of beacons is 10Hz (i.e., one every 100ms). Beacons are broadcast in nature. Moreover, vehicles may also generate event-based emergency messages as needed during the same interval. At the end of the CCH interval, nodes may optionally switch to any of the six SCHs and conduct other services. To access one of the SCHs, a vehicle must perform a negotiation process via CCH. The process includes transmitting a wave short message (WSM) to advertise the service and reply with an acknowledgement. At the end of the CCH interval, all successful negotiations may switch to the SCHs to provide the services. It is clear that CCH is the bottleneck in vehicular network communications. Beacons, event-based messages, and WSM advertisement are broadcast via CCH. As a result, bottleneck congestion and high load in the channel can be introduced.

The system of VANETs has been described as a cyber-physical system (CPS) [47][48], which has a tight combination of cyber and physical elements. In VANETs for safety applications as an example, vehicles periodically broadcast their physical parameters (e.g., location and speed) to keep nearby vehicles aware of road conditions. The cyber elements in this system involve communication processes and the tracking of other vehicles' processes, while the physical element is the vehicles' movement.

Several suggested models and architecture are discussed in the literature. However, a generic system model is needed that includes a high-level view and provides the necessary communication perspective. A general road network includes a suburban and an urban environment. At the intersections, there are traffic light signals (TLSs) or road side units (RSUs), as shown in Figure 3.2. Moreover, for communication purposes, RSUs are placed in between intersections separated by a long distance. A RSU is an entity equipped with at least a short range wireless network device. RSUs are likely equipped with other network devices so as to be able to communicate with an infrastructure network. Sensors are distributed on the road network to detect traffic information (e.g., average speed of vehicles) that helps to estimate average vehicle emissions and fuel consumption. The nodes in the road network are (1) mobile nodes: vehicles and (2) fixed nodes: TLSs and RSUs. Wireless communications consist of vehicle-to-vehicle (V2V) communication, vehicle-to-TLS/RSU communication, and TLS/RSU-to-TLS/RSU communication. In this thesis, the focus is on wireless communication that involves V2V and TLS2V. In this case, the communication model can be summarized as follows:

- Assume that the TLSs and vehicles are equipped with an on-board unit (OBU), an entity responsible for vehicular communication such as wireless radio access, geographical ad hoc routing, network congestion control, etc. The assumption is made that the OBU is equipped with a (short range) wireless communication device.

- In addition to the OBU, vehicles and TLSs are equipped with an Application Unit (AU), an entity that runs applications. It is assumed in this study that the AU in vehicles is equipped with highly accurate position data [49] and an electronic road map. Therefore, the vehicles know their locations and the location of the TLSs. Figure 3.3 shows some required components for the OBU and AU:

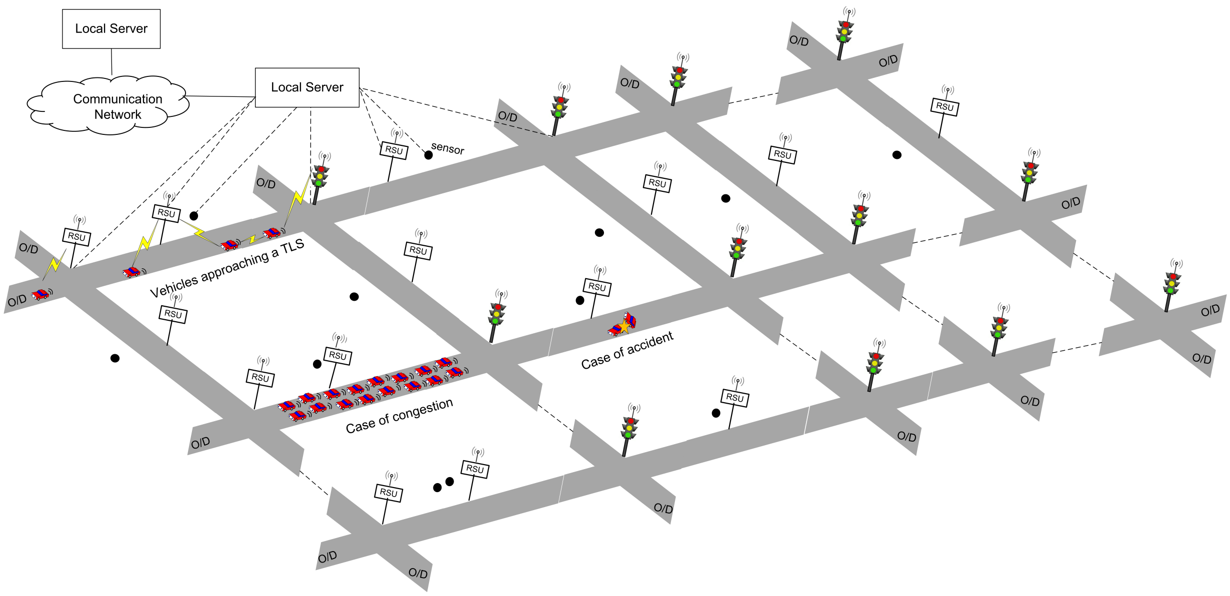

Figure 3.2: A general system model

1. Short Range Wireless Device: It is based on a radio technology capable of organizing access to channels in a decentralized manner (e.g., IEEE 802.11 and IEEE 802.11p).
2. Human Machine Interface: Its main functions is to provide information to the driver through audio or visual display.
3. Navigation System: Any navigation system includes three components: (1) a Global Positioning Systems (GPS) receiver; (2) electronic maps. It is assumed that maximum speed-limit information is provided with maps; (3) software capable of selecting a route from the current location to a specified destination.
4. TLS Controller: It is a system to control TLSs. TLS controllers can be divided into two groups: static and dynamic signals. Static TLSs are controlled by fixed-cycle controllers, regardless of current traffic volumes. On the other hand, the operation of dynamic signal controllers varies based on the observed traffic volume [50][51].

- Vehicles exchange (X, Y) location coordinates periodically every 100 ms.
- An ideal Medium Access Control (MAC) layer and Physical (PHY) layer are assumed where a packet arriving at network layer gets transmitted immediately without any

contention at the MAC layer, and the transmitted packets arrive at the intended destination without error.

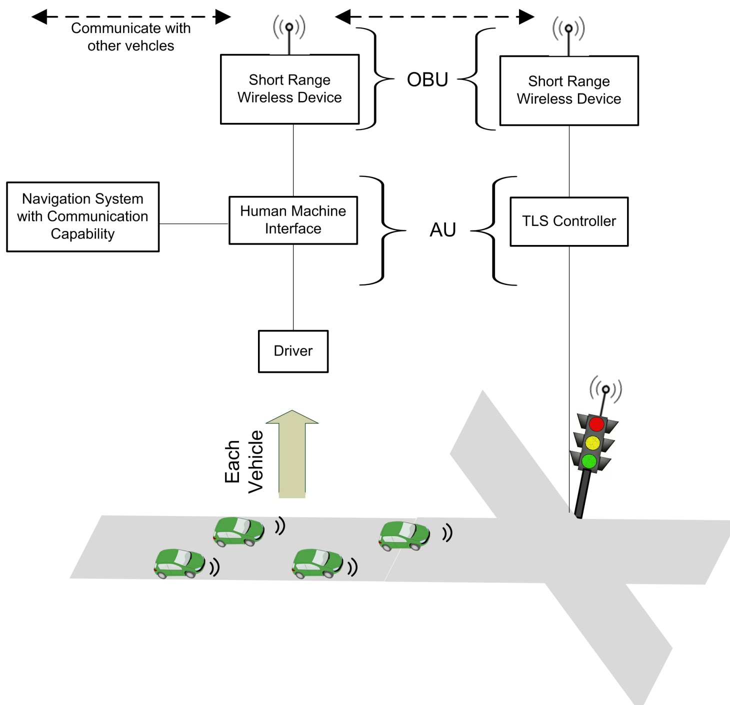

Figure 3.3: Main components for the OBU and AU

For geo-addressed applications (e.g. safety applications), the protocol stack considered by the Car-to-Car Communication Consortium (C2C-CC) is shown in Figure 3.4. Application and transport layers are defined by C2C-CC [1]. The specifications of these protocols are currently under discussion. Geographical routing provides ad hoc communication among vehicles, as well as between vehicles and RSUs or TLSs over IEEE 802.11p in the MAC and PHY layer. The work in this research is in the network layer, for which a geocast routing protocol that aims to reduce vehicle fuel consumption and CO_2 emission is proposed.

Data Dissemination

VANETs have essentially been proposed for use in the transmission of safety messages, which are exchanged between mobile vehicles within a limited deadline. Essentially, broad-

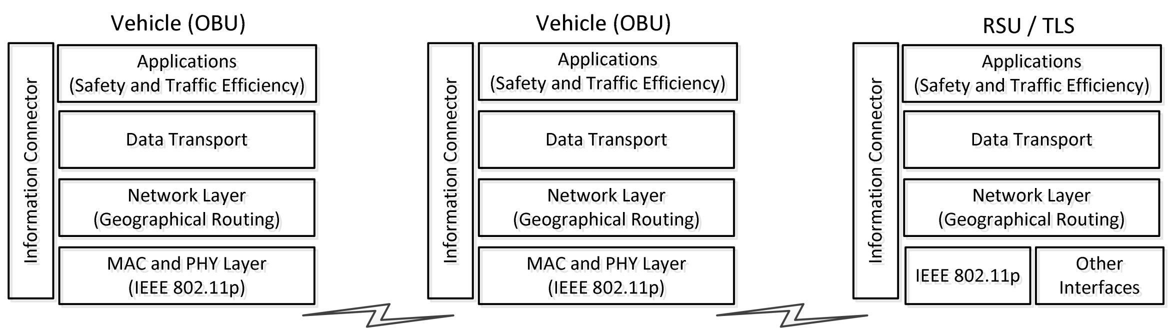

Figure 3.4: Protocol stack

cast protocols are proposed for such an application. DSRC-operated vehicles periodically exchange a variety of information (e.g., node ID, location). However, during certain situations, not all vehicles receive the intended safety messages. For example, broadcasting messages to leading vehicles to inform them about an accident is not compulsory in safety communications. Similarly, vehicles traveling in lanes going the opposite direction may not need these messages. Consequently, geocast routing protocols have been proposed for VANETs. In a geocast protocol, the message is supposed to be delivered to a group of nodes within a specific geographical location. For example, a TLS would be used to geocast messages to vehicles that have not yet passed by it. Similarly, multicasting can be used based on the requirement of the networking protocol.

Region of Interest (ROI)

A critical part of the vehicular network design is the transmission range of each vehicle. Interestingly, the region of interest (ROI) – defined as the range that covers all the intended receivers of a message – is also critical. A green protocol also has its own ROI, which might include special characteristics. For example, the protocol used for a three-lane road that has an accident in one of its lanes might be a travel-congestion avoidance protocol. If the protocol sends a message informing vehicles that the farthest lane is the optimal one and all vehicles change lanes to that one, then it will very likely become congested as well. Therefore, the ROI is not only about how far the message should go [52], but also about who should receive it.

3.1.2 Traffic Model

The Origin (O) and the Destination (D) are specified as shown in Figure 3.2. O and D for each vehicle are determined arbitrarily. In the road network, each segment contains a maximum speed limit (S_{max}), minimum speed limit (S_{min}), N-lane with length L and is two directions. TLSs are placed at intersections. Two categories of consecutive signalized intersections exist: (1) those with coordinated systems, with TLSs timed so that traveling vehicles need not stop at each intersection. These intersections are usually close to one another, such as those in urban areas; (2) isolated intersections, which are not close to each other and are independent (e.g., suburban areas). We consider a predominant TLS model where TLSs have three phases: green "g", yellow "y", and red "r". The phase duration is T_g, T_y, and T_r for green, yellow, and red, respectively. Other TLS models such as flashing and arrow signals can be incorporated into the predominant model [53]. The arrival of vehicles is modeled as a Poisson process with a rate of λ vph/lane [54][34]. We make a few assumptions for simplicity: no lane change is considered; vehicles do not exceed speed limits; and they do not pass through red TLSs.

3.1.3 Mobility Model

Microscopic traffic flow models are well suited for intelligent transportation systems (ITS) applications. These models are either car-following or cellular automata [34, 55, 56]. More details are discussed in Chapter 2. In this work, the car-following concept is considered due to its accuracy. We use the car-following behavior that has been used in the well known traffic simulator called INTEGRATION [25]. The movements of the vehicles are adapted according to the space headway. Vehicles travel at the free flow speed. Each vehicle estimates the space headway between itself and a vehicle driving ahead of it (its leader), or the space headway between itself and a red or yellow TLS. When this space headway reaches the minimum safe space headway (h_{min}), the vehicle has to be decelerated. The value h_{min} is calculated as the time a vehicle has to comfortably decelerate from its current speed to the speed of its leader multiplied by the average speed of the vehicle and its leader. The calculation can be represented in the following equation [25]:

$$h_{min} = (\frac{S_f + S_l}{2}) \cdot (\frac{S_f - S_l}{\delta}) \tag{3.1}$$

where S_f and S_l represent the speed of the following and leading vehicles, respectively and δ is the maximum comfortable deceleration rate that can be applied in the VT-Micro

Model (δ = 1.38 m/s^2) [23]. VT-Micro is based on ORNL data that provides fuel consumption and emissions rates for a range of speeds from 0 to 120 km/h and for a range of accelerations from -1.38 m/s^2 to 3.6 m/s^2 [23]. Therefore, speed, acceleration, and deceleration have to be determined inside the ranges.

For example, consider a vehicle at a position of 30 m traveling at 20 m/s approaching another vehicle at apposition of 100 m traveling at 15 m/s. At this instant, the space headway of the following vehicle and the leading vehicle is 70 m and h_{min} is 58.33 m. In this case, the following vehicle will continue at its speed until the time when the space headway of the following vehicle and the leading vehicle reaches h_{min}; then, it starts deceleration.

The following vehicle would accelerate if the leading vehicle were accelerating, as the increase of the space headway to the leading vehicle would cause the following vehicle to increase its speed. The acceleration rate is governed by vehicle dynamics. A vehicle wanting to increase its speed will attempt to accelerate at the maximum possible rate. The maximum possible rate is subject to the maximum acceleration rate, which is derived from a constant vehicle power. This power is a function of speed. A regression model was developed to identify the relationship between maximum acceleration and vehicle speed as in Equation 3.2 [25][57]. This linear relationship provides a reasonable approximation with what was observed in the ORNL data.

$$A = -0.00003 \cdot S^3 + 0.00801 \cdot S^2 - 0.80333 \cdot S + 35.19284 \tag{3.2}$$

where S is the speed (km/h) and A is the acceleration (km/h/s).

3.1.4 Performance Measures

The performance measures of this research are divided into three parts:

Economical and Environmentally-Friendly (EEF) Measures: Vehicles' fuel consumption and CO_2 emission;

Quality of Travel Measures: Vehicles' idling time;

Communication System Measures: Message delay and delivery success ratio.

Our focus in this research is on minimizing vehicles' fuel consumption and CO_2 emission. The measures of the quality of a travel and communication system have an impact on the EEF measures.

3.2 Problem Definition

The detrimental effects of air pollution and concerns about global warming are being increasingly reported by the media. In many countries, fuel prices have risen considerably. For instance, the gasoline price in western Canada increased around 150%, from about 53 cents/liter in 1998 to 127 cents/liter in 2012 [10]. As for air pollution, greenhouse gas (GHG) emissions from vehicles are considered one of the main contributing sources. CO_2 is the largest component of GHG emissions. For example, in the European Union (EU), in 2009, CO_2 emission from the transport sector were about 25% of the entire EU CO_2 emission [11]. The Kyoto Protocol aims to stabilize the GHG concentrations in the atmosphere at a level that would prevent dangerous alterations to regional and global climates [12].

With the increasing public awareness of the need to reduce GHG emissions and fuel consumption by vehicles, it is important to start effectively using information technology. For example, utilizing the functionalities of GPS in cell phones for location services and traffic prediction and estimation [58][59], which help improve the efficiency of transportation systems in terms of GHG emissions and fuel consumption. One area of study – namely, vehicular networks – is expected to provide a variety of applications resulting in excellent networking performance [2][60]. Indeed, vehicular networks have been used to improve vehicular traffic along roads, resulting in the field of ITS, which incorporate wireless communication, transportation engineering, and computer software and hardware [33]. Geocast protocols in vehicular network technologies are a promising research area in ITS. The main uneconomical and environmentally unfriendly (UEU) actions contributing to increased emissions and fuel consumption include high acceleration, stop-and-go conditions, congestion, high speeds, indirect routing, and idling. Moreover, navigation systems may choose routes that later become congested and inefficient after drivers commit to that path. The question then becomes, "what role can geocast protocols play in vehicular networks to reduce the impact of some of these actions?".

Applications for vehicular networks are classified into those that aim to reduce the number of fatalities on roads and those that aim to comfort drivers and their passengers [1]. In this research, we consider new applications that aim to save the environment and drivers' money.

The effect of speed and acceleration on a vehicle's fuel consumption and CO_2 emission can be investigated by using a fuel consumption and emission model. Fuel consumption and emission models have been discussed in Section 2.2. The VT-Micro model is superior to the others in its accuracy [61]. To study the impact of vehicle speed, the vehicle acceleration is set to a constant value (say 0 kph/s). After that, the CO_2 emission and fuel consumption are computed with different values of speed using VT-Micro model [23]. Figures 3.5a and 3.5b show that CO_2 emission and fuel consumption increase with high speeds. Similarly, to show the effect of vehicle acceleration, the vehicle speed is set to a constant value (e.g., 30 kph). Then, the CO_2 emission and fuel consumption are calculated with different values of accelerations. Figures 3.5c and 3.5d demonstrate that negative accelerations (decelerations) do not have much effect on the CO_2 emission and fuel consumption because vehicles do not exert power in negative accelerations. On the other hand, the amount of vehicle fuel consumption and CO_2 emission increases with increased the vehicle acceleration. As a result, it is logical to consider existing scenarios where the uneconomical and environmentally unfriendly (UEU) actions (e.g., stop-and-go conditions, high speed, high acceleration, and congestion) happen frequently. Based on these scenarios, the capability of information technology has to be utilized to help avoid or reduce these actions. Figure 3.2 shows three main scenarios where the UEU actions happen frequently: (1) vehicles approaching a TLS; (2) a road segment with an accident; (3) congestion. In this thesis, the focus is on the scenario where vehicles are approaching a TLS. The main UEU actions that can occur for these vehicles are as follows:

1. Stop-and-go conditions: Vehicles may stop at a red signal. Then, they go when the signal switches to green.

2. Unnecessary excessive speed: Suppose a vehicle stops at a TLS if it travels at the maximum allowed speed (S_{max}) and at the minimum acceptable speed (S_{min}). In this case, a vehicle may travel at the maximum allowed speed instead of traveling at the minimum acceptable speed, although it will stop at both speeds.

3. High acceleration: Suppose a vehicle passes through a TLS without stopping. In this case, the vehicle may travel at a speed less than S_{max} to pass the TLS. Therefore, after passing the TLS, the vehicle will return to S_{max} with higher acceleration than if the vehicle had traveled at S_{max} to pass the TLS without stopping.

Statement:
This research has been inspired by the fact that rising fuel costs and CO_2 emission are increasingly recognized as global challenges. Geocast protocols in vehicular networks can play a key role in reducing vehicle fuel consumption and CO_2 emission.
Stop-and-go condition, unnecessary high speed, high acceleration, and congestion are

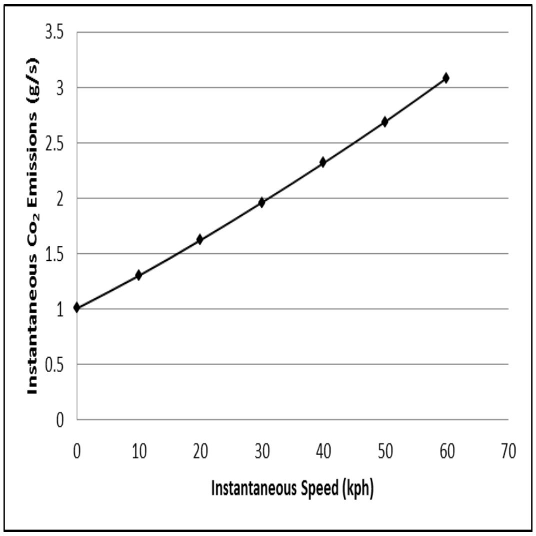

(a)

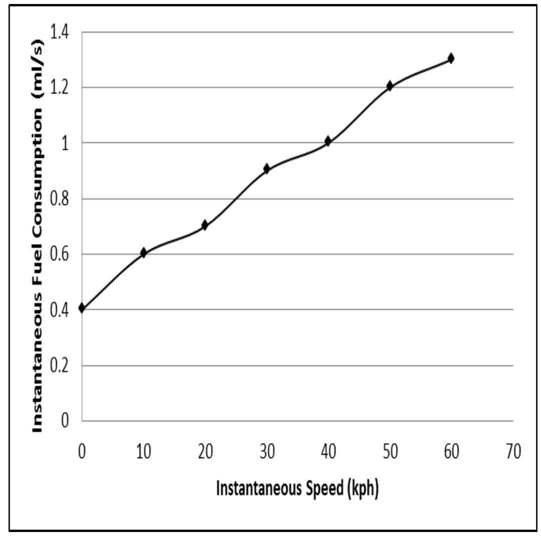

(b)

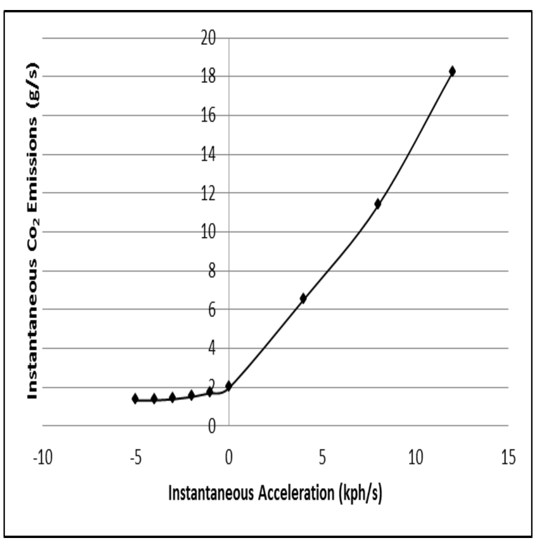

(c)

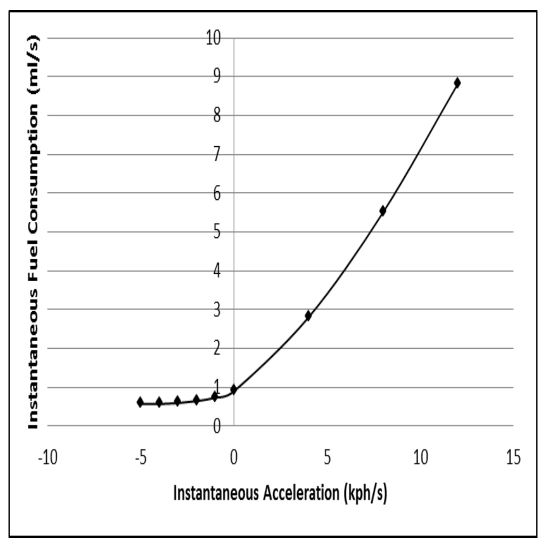

(d)

Figure 3.5: The impact of speed and acceleration on vehicle fuel consumption and CO_2 emission

actions that increase the amount of vehicle fuel consumption and CO_2 emission. Some of these actions can happen frequently for vehicles approaching a TLS. For this scenario, our objective is to propose a new protocol named Economical and Environmentally Friendly Geocast (EEFG), which focuses on minimizing CO_2 emission and fuel consumption from vehicles. The goal of the protocol is to deliver required information to vehicles inside the ROI. Based on that information, vehicles control their behavior so as to reduce these actions. Therefore, greater fuel and CO_2 emission reductions can be achieved.

3.3 Solution Strategy

Geocast protocols in vehicular-network technologies are a promising research area in ITS applications. The goal of this research is to develop a new Economical and Environmentally Friendly Geocast (EEFG) protocol that focuses on minimizing vehicle fuel consumption and CO_2 emission. The objective of the protocol is to deliver useful information to vehicles so that they can reduce fuel consumption and CO_2 emission. EEFG delivers useful information to vehicles approaching a TLS. Based on that information, reduction of fuel consumption and CO_2 emission is achieved by controlling the speed of the vehicles to a speed named the recommended economical and environmentally friendly (EEF) speed (S_R) that helps vehicles:

1. avoid having to stop: a vehicle may avoid a stop by adapting its speed to (S_R), such that $S_{min} \leq S_R \leq S_{max}$, where S_{min} is the minimum speed limit and S_{max} is the maximum speed limit.

2. prevent unnecessarily excessive speed: a vehicle adjusts its speed to S_{min} in order to avoid unnecessarily high speeds if the vehicle has to stop for the TLS.

3. avoid high acceleration: this can be achieved by calculating S_R as the maximum possible speed for the vehicle to pass the TLS. Thus, after passing the TLS, the vehicle returns to S_{max} with low acceleration.

3.3.1 Solution Steps

The steps of the solution can be summarized as follows:

1. Define the Regions of Interest (ROIs) based on whether a vehicle will benefit from the information or not;
2. Specify what types of information a packet has to contain;
3. Deliver a packet with required information to targeted vehicles;
4. Utilize the idea of VANETs;
5. develop an optimization model to determine the value of S_R that leads to the maximum reduction of fuel use and emissions. This model must be applicable in both signal-to-vehicle (TLS2V) and vehicle-to-vehicle (V2V) communications;
6. Integrate a fuel consumption and emission model with vehicular networks. As a result, the high-level performance measures (fuel consumption and CO_2 emission) can be calculated.

3.4 Summary

This chapter has presented the system model, assumptions, and the problem definition. Also, it has identified the solution strategy. The system model includes the communication model, traffic model, mobility model, and performance measures. The uneconomically and environmentally unfriendly actions can happen frequently for vehicles approaching a TLS. For this scenario, our objective is to propose a new protocol named Economical and Environmentally Friendly Geocast (EEFG) that focuses on minimizing CO_2 emission from and fuel consumption by vehicles. The goal of the protocol is to deliver required information to vehicles inside the ROI. Based on that information, vehicles control their behavior in such away that these actions are reduced. Therefore, fuel and CO_2 emission reductions can be achieved.

Chapter 4

Proposed Economical and Environmentally Friendly Geocast Protocol for Vehicles approaching a TLS

The material of this chapter has been published in [62]. The main goal of the proposed Economical and Environmentally Friendly Geocast (EEFG) protocol is to reduce CO_2 emission from and fuel consumption by vehicles approaching a traffic light signal (TLS) by avoiding certain uneconomical and environmentally unfriendly (UEU) actions such as:

1. stop-and-go conditions: a vehicle may avoid a stop by adapting its speed to (S_R), such that $S_{min} \leq S_R \leq S_{max}$, where S_{min} is the minimum speed-limit and S_{max} is the maximum speed-limit.
2. high acceleration: a vehicle can avoid high acceleration by calculating S_R as the maximum possible speed for the vehicle to pass the TLS. Thus, after passing the TLS, the vehicle returns to S_{max} with low acceleration.
3. unnecessary speed: a vehicle can avoid unnecessary high speeds by slowing down if the vehicle has to stop anyway for the TLS.

The main idea of the EEFG protocol is to deliver useful information to approaching vehicles inside the regions of interest (ROIs). Based on that information, the recommended

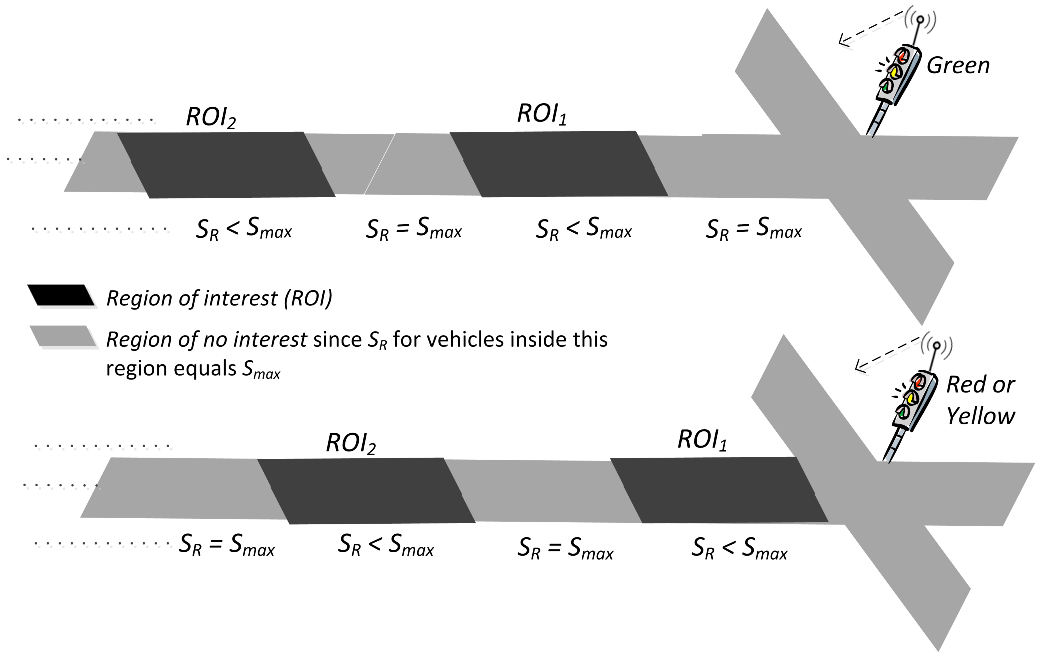

Figure 4.1: S_R and ROI when the current phase is green, red, or yellow

speed (S_R) is advised, UEU actions are avoided, and CO_2 emission and fuel consumption are consequently reduced.

Before presenting the message delivery protocol, destination regions or regions of interest (ROI) have to be defined as in the next section.

4.1 Defining the Geocast Destination Regions or ROI

Regions of interest (ROIs) refer to those sections along the road in which the suggested S_R results in fuel and CO_2 emission reduction (Figure 4.1). For example, if a vehicle is close to a green TLS, it is good for the vehicle to travel at S_{max} in order to catch the green light. However, if the vehicle is a little further away and it will not catch the green light even if it travels at S_{max}, a speed (S_R) less than S_{max} will be recommended to the vehicle so that it passes the TLS in the next cycle. Figure 4.1 shows intuitively what the S_R and ROIs will be when the current phase is green, red, or yellow. Table 4.1 defines the main notations that have been used.

Table 4.1: Definition of the notations

L_g	Time remaining to switch from green to yellow
L_y	Time remaining to switch from yellow to red
L_r	Time remaining to switch from red to green
T_g	Full green phase time
T_y	Full yellow phase time
T_r	Full red phase time
C_L	TLS cycle length
S_{max}	Maximum speed-limit
S_{min}	Minimum speed-limit
S_R	Recommended speed
β	Acceleration time
A	Maximum acceleration rate
$v(t)$	Vehicle speed at time t
$a(t)$	Vehicle acceleration at time t
$y(t)$	Maximum possible vehicle acceleration at time t. The expression of $y(t)$ is a regression model developed in [26] as follows: $y(t) = -0.00003 \cdot v(t-1)^3 + 0.00801 \cdot v(t-1)^2 - 0.80333 \cdot v(t-1) + 35.19284$ (km/h/s)
δ	Deceleration rate

Since we assume that the application unit (AU) in vehicles has an electronic map with roads' speed-limits, the S_R for vehicles that do not receive a packet is considered to be S_{max}. Therefore, it is not necessary to geocast in a region where $S_R = S_{max}$. Thus, ROIs are the regions where $S_R < S_{max}$. To calculate these regions, we need to determine the range of the distance (d) between vehicles with $S_R < S_{max}$ and the TLS.

4.1.1 If the current phase is green

As shown in Figure 4.2.a, d for vehicles that have $S_R < S_{max}$ is in the following range:

$$(L_g + (n-1) \cdot C_L) \cdot S_{max} < d < (L_g + T_y + T_r + (n-1) \cdot C_L) \cdot S_{max} + h_{min}$$

where $1 \leq n \leq \tau$. n is the region's ID number, and τ is the last region's number. Defining τ depends on d_s, which is the distance between a TLS and the preceding one minus the acceleration distance from idling to S_{max} ($d_{acc_{0-S_{max}}}$) such as $\tau = \lceil \frac{d_s - L_g \cdot S_{max}}{C_L \cdot S_{max}} \rceil$. $d_{acc_{0-S_{max}}}$ has been introduced to avoid affecting the motion of vehicles at intersections as shown in Figure 4.3. It can be calculated using the SUVAT equation as follows: $d_{acc_{0-S_{max}}}(t) = v(t) + 0.5 \cdot a(t)$. As a result,

$$d_{acc0-S_{max}} = \sum_{t=1}^{\beta} d_{acc_{0-S_{max}}}(t) \cdot \frac{a(t)}{y(t)} \tag{4.1}$$

where $\beta = \lceil \frac{S_{max}}{A} \rceil$; $t = 1, 2, .., \beta$ sec; $v(0) = 0$;
$a(t) = \min(y(t), S_{max} - v(t-1))$;
$v(t) = \min(S_{max}, v(t-1) + a(t))$.

The center of each ROI is as follows:

$$Cen(ROI_n) = \frac{S_{max} \cdot (T_y + T_r) + h_{min}}{2} + (L_g + (n-1) \cdot C_L) \cdot S_{max}$$

where $Cen(ROI_n)$ is defined as the distance between the TLS and the center of ROI_n. Generally, h_{min} is the minimum space headway. Here, h_{min} is the minmum space headway of a vehicle traveling at S_{max} and a red TLS such as $h_{min} = (S_{max}/2) \cdot (S_{max}/\delta)$. In Figure 4.3, if TLS 1 is inside the last ROI (ROI_τ) of TLS 2, the center and diameter of ROI_τ will be as follows:

$$Cen(ROI_\tau) = \tfrac{d_s - (L_g + (\tau-1) \cdot C_L) \cdot S_{max}}{2} + (L_g + (\tau - 1) \cdot C_L) \cdot S_{max} \tag{4.2}$$

$$Dia(ROI_\tau) = d_s - (L_g + (\tau - 1) \cdot C_L) \cdot S_{max} \tag{4.3}$$

4.1.2 If the current phase is red

As shown in Figure 4.2.b, d for vehicles that have $S_R < S_{max}$ is in the following range:

$0 < d < L_r \cdot S_{max} + h_{min}$ if the vehicle is inside ROI_1; otherwise,

the range is $(L_r + T_g + (n-1) \cdot C_L) \cdot S_{max} < d < (L_r + n \cdot C_L) \cdot S_{max} + h_{min}$

$$Cen(ROI_1) = \frac{L_r \cdot S_{max} + h_{min}}{2} \tag{4.4}$$

$$Cen(ROI_{n+1}) = \frac{(T_y + T_r) \cdot S_{max} + h_{min}}{2} + (L_r + T_g + n \cdot C_L) \cdot S_{max} \tag{4.5}$$

where $\tau = \lceil \frac{d_s - (L_r + T_g) \cdot S_{max}}{C_L \cdot S_{max}} \rceil + 1$. As shown in Figure 4.3, if TLS 1 is inside ROI_τ, the center of ROI_τ will be as follows:
When $\tau = 1$,

$$Cen(ROI_1) = \frac{d_s}{2} \tag{4.6}$$

$$Dia(ROI_1) = d_s \tag{4.7}$$

Otherwise,

$$Cen(ROI_\tau) = \frac{d_s - (L_r + T_g + (\tau - 1) \cdot C_L) \cdot S_{max}}{2} + (L_r + T_g + (\tau - 1) \cdot C_L) \cdot S_{max} \tag{4.8}$$

$$Dia(ROI_\tau) = d_s - (L_r + T_g + (\tau - 1) \cdot C_L) \cdot S_{max} \tag{4.9}$$

4.1.3 If the current phase is yellow

As shown in Figure 4.2.c, d for vehicles that have $S_R < S_{max}$ is in the following range:

$0 < d < (L_y + T_r) \cdot S_{max} + h_{min}$ if the vehicle is inside ROI_1; otherwise, the range is $(L_y + T_r + T_g + (n-1) \cdot C_L) \cdot S_{max} < d < (L_y + T_r + n \cdot C_L) \cdot S_{max} + h_{min}$

$$Cen(ROI_1) = \frac{(L_y + T_r) \cdot S_{max} + h_{min}}{2} \tag{4.10}$$

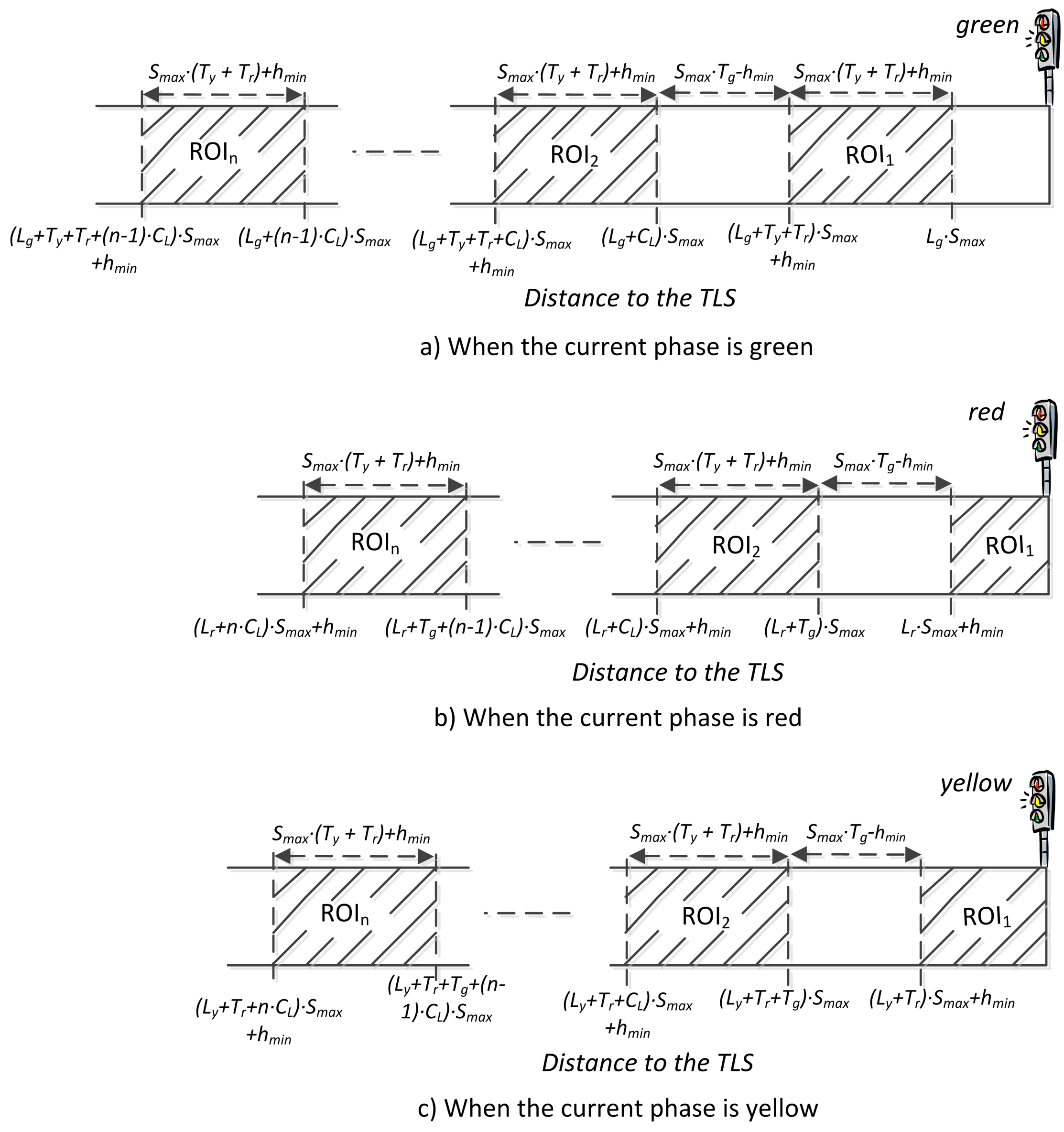

Figure 4.2: Distances between ROI and a green, red, and yellow TLS

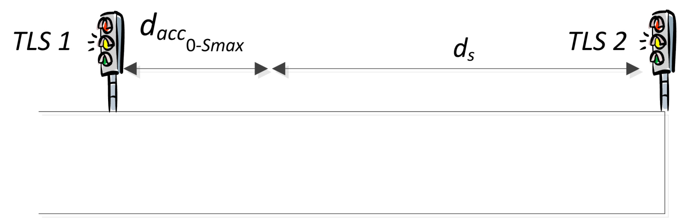

Figure 4.3: Two consecutive TLSs

$$Cen(ROI_{n+1}) = \frac{(T_y + T_r) \cdot S_{max} + h_{min}}{2} + (L_y + T_r + T_g + n \cdot C_L) \cdot S_{max} \tag{4.11}$$

where $\tau = \lceil \frac{d_s - (L_y + T_r + T_g) \cdot S_{max}}{C_L \cdot S_{max}} \rceil + 1$. As in Figure 4.3, if TLS 1 is inside ROI$_\tau$, the center of ROI$_\tau$ will be as follows:
When $\tau = 1$,

$$Cen(ROI_1) = \frac{d_s}{2} \tag{4.12}$$

$$Dia(ROI_1) = d_s \tag{4.13}$$

Otherwise,

$$Cen(ROI_\tau) = \frac{d_s - (L_y + T_r + T_g + (\tau - 1) \cdot C_L) \cdot S_{max}}{2} + (L_y + T_r + T_g + (\tau - 1) \cdot C_L) \cdot S_{max} \tag{4.14}$$

$$Dia(ROI_\tau) = d_s - (L_y + T_r + T_g + (\tau - 1) \cdot C_L) \cdot S_{max} \tag{4.15}$$

Figure 4.2 shows that for all green, red, and yellow lights, the diameters of the ROI are fixed to $S_{max} \cdot (T_y + T_r) + h_{min}$ except ROI_1 when the current phase is red or yellow; however, it would equal $S_{max} \cdot (T_y + T_r) + h_{min}$ if $L_r = T_y + T_r$ and $L_y = T_y$. On the other hand, the centers are changed based on the value of L_g, L_y, or L_r.

For low traffic, a fixed ROI might work well. However, with higher traffic, the ROI must be adaptive. With EEFG, the ROI is determined at the beginning as above to define the destination of the TLS. Then, the ROI can be extended by means of vehicle-to-vehicle (V2V) communication if necessary. The extension of a ROI depends on the recommended speed of a vehicle (to be discussed in Subsection 4.2.2).

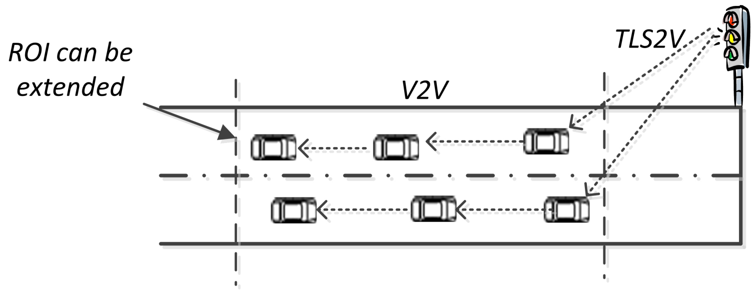

Figure 4.4: Message delivery from a TLS to vehicles and from vehicle to vehicle

4.2 Message Delivery

The TLS uses a geocast routing protocol to deliver its information to the destination regions. Three kinds of communications occur in our system model, summarized in Figure 4.5, as follows: (1) TLS-to-vehicles; (2) vehicle-to-vehicle; (3) vehicles-to-TLS.

4.2.1 From a TLS to vehicles (TLS2V)

A TLS sends (geomulticasts) a packet to the first vehicle in each lane inside a ROI. A geomulticast sends a packet to a group (not all) of nodes (vehicles) in a geographical area as shown in Figure 4.4. The packet contains four types of information: (1) the type of the current phase; (2) the time remaining to switch from the current phase; (3) the TLS schedule; (4) the geographical address of the destination node, which is the first vehicle in each lane inside a ROI. Since a TLS communication range could covers a ROI or part of it, the TLS can sense (X, Y) coordinates from vehicles inside its coverage. Therefore, a TLS can know the location of the first vehicle inside the ROI in each lane. Since each vehicle knows its own location, a vehicle itself can recognize whether it is the destination node or not. A vehicle discards the packet if it is not the destination node. Otherwise, the vehicle calculates and adjusts its speed to the optimum S_R (S_R^*), which is determined using our optimization model (to be discussed in Chapter 5).

4.2.2 Vehicle to Vehicle Communication (V2V)

As discussed in Subsection 4.2.1, the TLS sends the information to the first approaching vehicle (V_1) in each lane. The vehicle then calculates and adjusts its speed to S_R^*. Next, as shown in Figure 4.4, V_1 unicasts a packet to the vehicle behind it (following) on the same lane (V_2), its (V_1's) speed, time to reach and pass the TLS, and idling time at the TLS, as well as that vehicle's (V_2's) geographical location and the TLS schedule. V_2 receives the packet if it is within the V_1 transmission range. Based on the packet information, V_2 calculates and adjusts its speed to S_R^* using the optimization model (to be discussed in Chapter 5). If S_R^* is less than S_{max}, it means that V_2 is inside the ROI. Therefore, the unicast approach is repeated to the vehicle behind it (say V_3). In this case, V_2 becomes the leader and V_3 is the follower. The communication pattern continues in the same manner for the vehicles behind; a following vehicle becomes a leader and so on. This unicast based mechanism is used because the movement of each vehicle depends on the movement of the vehicle in front of it, meaning that each vehicle must know its immediate leader's information.

4.2.3 From vehicles to a TLS

When a vehicle receives a packet, it adjusts the speed to S_R^*, then unicasts the packet to its following vehicle if that vehicle is inside the transmission range. Otherwise, the packet has to be buffered until the following vehicle enters the transmission range. However, a vehicle might reach a TLS while it still has the packet. In this case, the vehicle notifies the TLS. As a result, the TLS sends a new packet as explained in Subsection 4.2.1.

4.3 Summary

This chapter has introduced the proposed EEFG protocol for vehicles approaching a TLS. Based on the sent information, the vehicles calculate their recommended EEF speed in order to avoid having to stop, to prevent unnecessary excessive speed, and to avoid accelerations. Geocast destination regions have been defined based on whether a vehicle will benefit from the TLS information or not. The proposed message-delivery aims to deliver the EEF message from a TLS to vehicles inside the geocast destination regions. The message delivery has been divided into three parts: (1) From a TLS to vehicles; (2) Vehicle-to-vehicle communication; (3) From vehicles to a TLS.

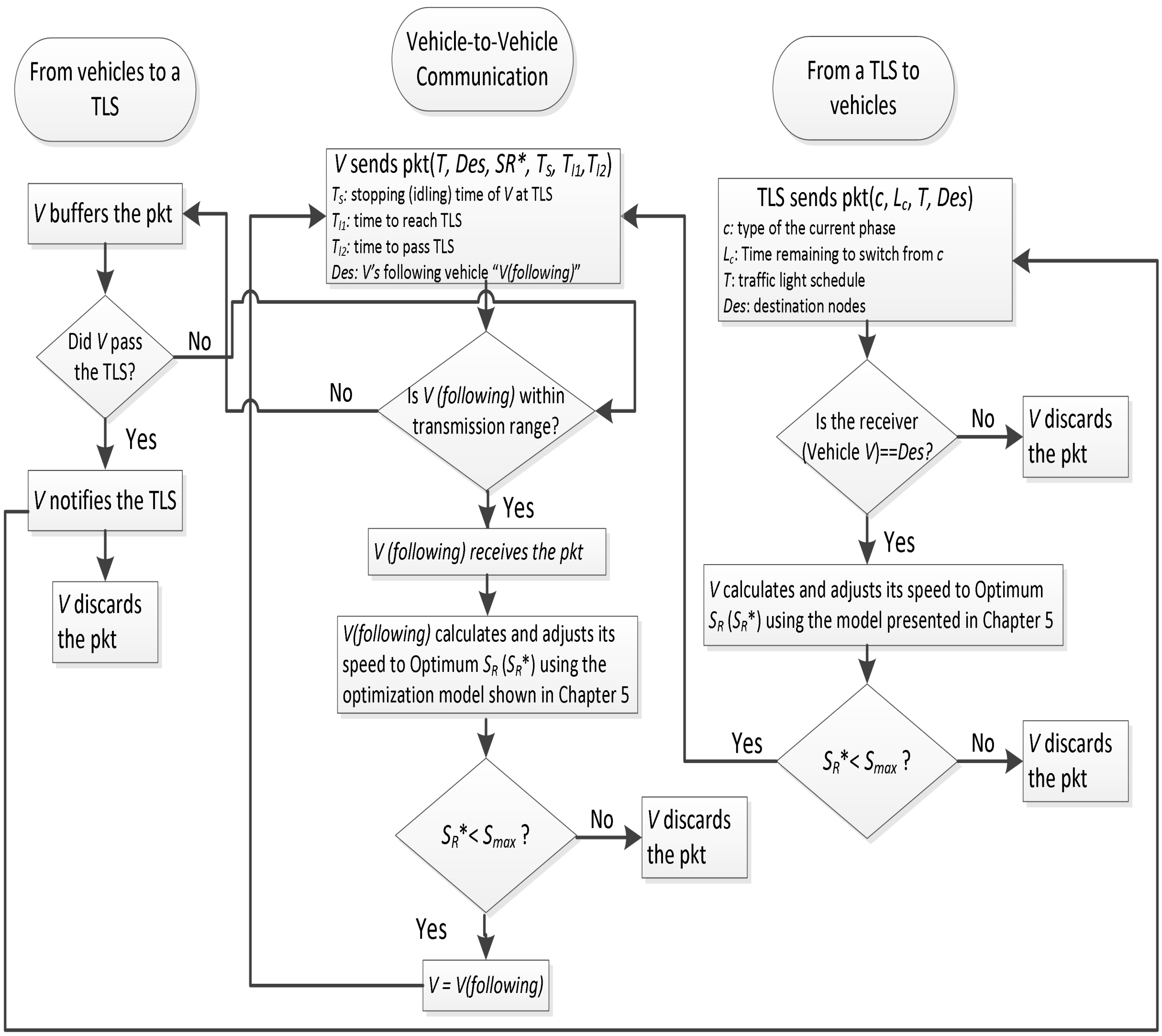

Figure 4.5: Flowchart for the EEFG protocol

Chapter 5

Optimization of Fuel Cost and Emissions with Vehicular Networks at Traffic Intersections

This chapter develops an optimization model that is applicable in both vehicle-to-vehicle (V2V) and signal-to-vehicle (TLS2V) communications. This model determines the value of the recommended speed (S_R) that leads to the maximum reduction of fuel use and emissions. We have published this work as a journal paper in IEEE Transactions on Intelligent Transportation Systems [63] and a conference paper in IEEE Intelligent Transportation Systems Conference [64].

5.1 Methodological Approach

The fact that controlling the speed of vehicles can lead to the maximum reduction of fuel consumption and emissions has motivated us to develop an optimization model. We use VT-Micro to estimate the total fuel consumption and emissions, as discussed in Chapter 3. There are two cases for a vehicle approaching a traffic light signal (TLS): (1) the vehicle has one or more vehicles in front of it; and (2) the vehicle is the closest one to the TLS. In the first case, the vehicle might be forced to decelerate its speed to that of the leading vehicle. In the second case, the vehicle might be forced to stop or decelerate at the TLS. Therefore, one of four scenarios, summarized in Figure 5.1, can happen for a vehicle approaching a TLS:

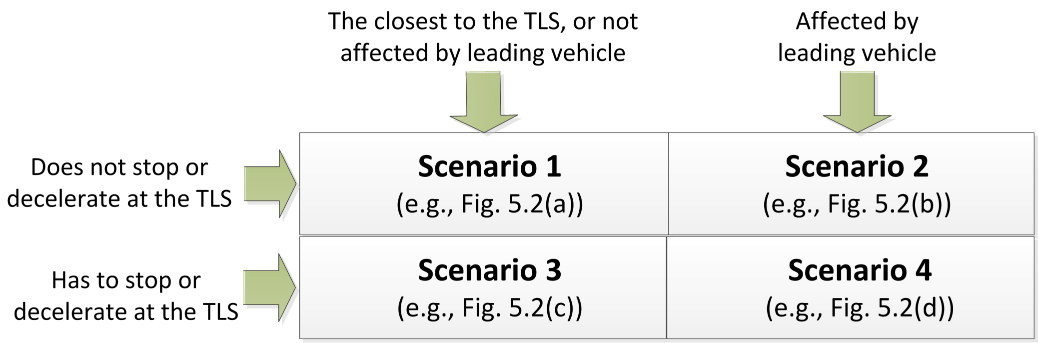

Figure 5.1: Scenarios for a vehicle approaching a TLS

1. The vehicle does not stop and does not decelerate at the TLS, nor is it affected by its leading vehicle (or it has no leading vehicle).
2. The vehicle does not stop at the TLS; however, it is affected by its leading vehicle (leader).
3. The vehicle has to stop or decelerate at the TLS.
4. The vehicle stops at the TLS, but before it reaches the TLS, is affected by its leader.

As discussed in Chapter 4, S_R equals S_{max} for a vehicle outside the ROI. Therefore, a vehicle travels at S_{max} if it has not received a message from the TLS or from its leading vehicle, or if it has already passed the TLS. Figure 5.2 illustrates the vehicle movements in each scenario, from when the vehicle receives a message until it reaches the destination.

In Figure 5.2 (a), as an example, when the vehicle receives a message from the TLS, it adapts its speed to (S_R), such that $S_{min} \leq S_R \leq S_{max}$. In the first action, the vehicle decelerates to S_R, then continues traveling at S_R until it reaches the TLS. After that, the vehicle accelerates to S_{max}. Finally, it continues at S_{max} to the destination. The two lines in Figure 5.2 represent possible vehicle movements in the range of S_R ($S_{min} \leq S_R \leq S_{max}$). For instance, in Figure 5.2 (b), if the vehicle travels at S_{max}, it must decelerate to S_{Rl}, as shown in the upper line because it is affected by the vehicle in front of it. On the other hand, if the vehicle travels at S_{min}, it needs no deceleration because $S_{min} < S_{Rl}$, as shown in the lower line. Measures of effectiveness (MOE_e), either fuel or emissions, are indicated in Figure 5.2 as follows:

$MOEe_1$: Total fuel consumption or emissions during the deceleration time from the current speed (S_{max}) to S_R.

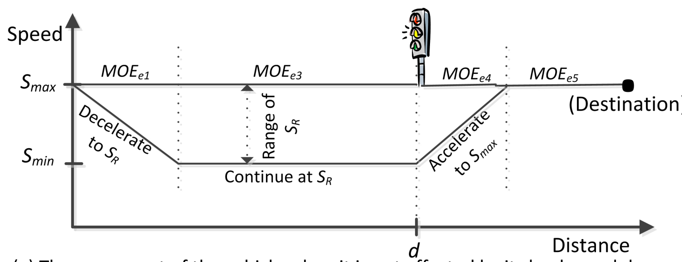

(a) The movement of the vehicle when it is not affected by its leader and does not stop or decelerate at the TLS.

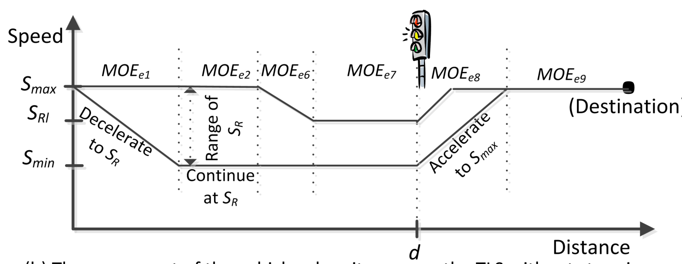

(b) The movement of the vehicle when it can pass the TLS without stopping but has to decelerate because of a vehicle in front of it

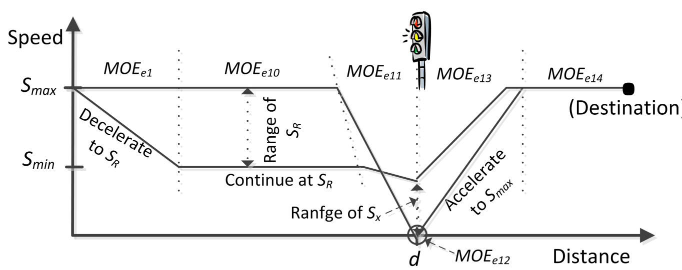

(c) The movement of the vehicle when it has to stop or decelerate at the TLS. The vehicle could be the closest to the TLS, or affected by a leading vehicle that is already stopped or decelerating at the TLS

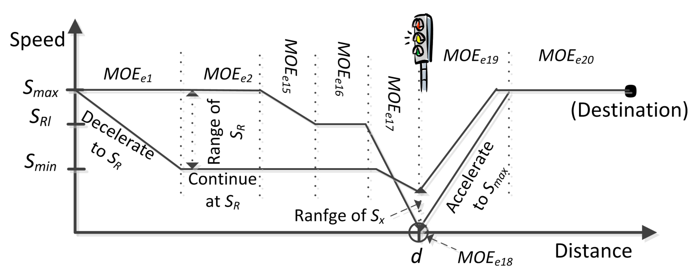

(d) The movement of the vehicle when it stops or decelerates at the TLS and is affected by its leader before it reaches the TLS

Figure 5.2: Possible scenarios for a vehicle approaching a TLS

$MOEe_2$: Total fuel consumption or emissions for the time interval the vehicle travels at S_R until the distance between the following and leading vehicles reaches h_{min}, or the following vehicle reaches the TLS.

$MOEe_3$ and $MOEe_{10}$: Total fuel consumption or emissions for the time interval the vehicle travels at S_R until it reaches the TLS.

$MOEe_4$: Total fuel consumption or emissions during the acceleration from S_R to S_{max}, which is the maximum speed limit after passing the TLS.

$MOEe_5$, $MOEe_9$, $MOEe_{14}$ and $MOEe_{20}$: Total fuel consumption or emissions for the time interval the vehicle travels at S_{max} to the destination.

$MOEe_6$ and $MOEe_{15}$: Total fuel consumption or emissions during the deceleration from S_R to S_{Rl}, which is the recommended speed of the leading vehicle. This case occurs if the space headway reaches h_{min} before the leading vehicle has reached the TLS.

$MOEe_7$ and $MOEe_{16}$: Total fuel consumption or emissions for the time interval that the following vehicle travels at S_{Rl} after the space headway reaches h_{min} and until the vehicle reaches the TLS.

$MOEe_8$: Total fuel consumption or emissions during the acceleration from S_{Rl} to S_{max}.

$MOEe_{11}$: Total fuel consumption or emissions during the deceleration from S_R to S_x or zero, where S_x is the minimum speed that the vehicle will reach before it accelerates.

$MOEe_{12}$ and $MOEe_{18}$: Total fuel consumption or emissions when the vehicle idles at the TLS;

$MOEe_{13}$ and $MOEe_{19}$: Total fuel consumption or emissions during the acceleration from S_x or idling to S_{max};

$MOEe_{17}$: Total fuel consumption or emissions during the deceleration from S_{Rl} to S_x or zero;

As a result, the total fuel consumption or emissions for each scenario is as follows:

- *Scenario 1:* $MOEe_T = MOEe_1 + \sum_{m=3}^{5} MOEe_m$;
- *Scenario 2:* $MOEe_T = \sum_{m=1}^{2} MOEe_m + \sum_{m=6}^{9} MOEe_m$,
- *Scenario 3:* $MOEe_T = MOEe_1 + \sum_{m=10}^{14} MOEe_m$;
- *Scenario 4:* $MOEe_T = \sum_{m=1}^{2} MOEe_m + \sum_{m=15}^{20} MOEe_m$.

Some $MOEe_m$ have the same definition; however, the calculations are different. For example, both $MOEe_5$ and $MOEe_{20}$ are defined as the total fuel consumption or emissions for the time interval the vehicle travels at S_{max} to the destination. However, calculating the time interval is different in each case because it depends on the acceleration length of the vehicle after it passes the TLS. Section 5.3 includes details for computing the values of $MOEe_m$.

5.2 Optimization Model

We develop an optimization model to determine the optimum S_R. The model consists of an objective function to be minimized and constraints to be satisfied. The objective is to minimize the total measure of effectiveness ($MOEe_T$), where e is an index denoting fuel consumption or emissions. This function is written as

$$Min\ MOEe_T \tag{5.1}$$

where

$$\begin{aligned} MOEe_T = &\sum_{m=1}^{2} MOEe_m + (1-x)[(1-z_1)\cdot((1-z_2)\sum_{m=3}^{5} MOEe_m + z_2 \sum_{m=10}^{14} MOEe_m) \\ &+z_1\cdot((1-z_3)\sum_{m=6}^{9} MOEe_m + z_3 \sum_{m=15}^{20} MOEe_m)] + x[(1-z)z_2 \sum_{m=10}^{14} MOEe_m \\ &+z_1(1-z_2)\cdot((1-z_3)\sum_{m=6}^{9} MOEe_m + z_3 \sum_{m=15}^{20} MOEe_m) + (1-z_1)(1-z_2) \\ &\sum_{m=3}^{5} MOEe_m] \end{aligned}$$

$MOEe_T$ is a function of S_R, x, z_1, z_2, z_3, v, and u. These are the decision variables. S_R, v, and u might be difficult to find in Equation 5.1. However, they are used in the formulas for calculating $MOEe_m$, where $m = 1, 2, .., 20$, as will be shown in Section 5.3. The binary variables x, z_1, z_2, z_3, v, and u are introduced to select the measures based on the scenarios (to be discussed). Notations used in this section are defined in Table 5.1 and calculated as in Section 5.3.

Constraints

1. Recommended Speed (S_R) limitation

$$S_{min} \leq S_R \leq S_{max} \tag{5.2}$$

S_R must not be larger than S_{max} or less than S_{min}.

2. Binary

a) x is a binary variable that indicates whether the leading vehicle will stop or not at the TLS. It depends on the value of T_s of the leading vehicle (T_{sl}). This information is sent from the leader to the follower.

$$x = \begin{cases} 1 & \text{if } T_{sl} > 0, \text{ leading vehicle stops at the TLS} \\ 0 & \text{if } T_{sl} \leq 0, \text{ leading vehicle does not stop} \end{cases} \tag{5.3}$$

This constraint is equivalent to
$T_{sl} - \mathtt{M}_{big}(x - 1) > 0$, and $T_{sl} - \mathtt{M}_{big}x \leq 0$
where $\mathtt{M}_{big}$ is some big constant [65].

b) z_1 is a binary variable indicating whether the vehicle will be affected by its leader while the latter is moving at S_{Rl}.

$$z_1 = \begin{cases} 1 & \text{if } 0 < T_{h_{min_1}} < T_{l_1}, \text{ will be affected by the moving lead vehicle} \\ 0 & \text{otherwise, } \quad\quad \text{will not be affected by the moving lead vehicle} \end{cases} \tag{5.4}$$

To model the equivalent constraints of this condition, we introduce a new binary variable (τ_1) defined as:

$$\tau_1 = \begin{cases} 1 & \text{if } T_{h_{min_1}} \leq 0 \\ 0 & \text{if } T_{h_{min_1}} \geq T_{l_1} \end{cases} \tag{5.5}$$

As a result, the equivalent constraints are
$\mathtt{M}_{big}(z_1 - 1) + T_{h_{min_1}} < T_{l_1}$,
$\mathtt{M}_{big}(1 - z_1) + T_{h_{min_1}} > 0$,
$T_{h_{min_1}} - \mathtt{M}_{big} z_1 \leq \mathtt{M}_{big}(1 - \tau_1)$, and
$\mathtt{M}_{big} z_1 + T_{h_{min_1}} \geq T_{l_1} - \mathtt{M}_{big}\tau_1$

c) v is a binary variable that indicates whether S_R is less than S_{Rl}.

$$v = \begin{cases} 1 & \text{if } S_R > S_{Rl} \\ 0 & \text{if } S_R \leq S_{Rl} \end{cases} \tag{5.6}$$

This constraint is equivalent to
$S_R - \mathtt{M}_{big}(v - 1) > S_{Rl}$, and
$S_R - \mathtt{M}_{big} v \leq S_{Rl}$

d) u is a binary variable that indicates whether d_{fln} is longer than h_{min_1}. If yes, the following vehicle is either not affected instantly or not affected at all by its leader. Otherwise, the following vehicle has to decelerate instantly if $d_{fln} < h_{min_1}$.

$$u = \begin{cases} 1 & \text{if } d_{fln} \geq h_{min_1} \text{ instant action not required} \\ 0 & \text{if } d_{fln} < h_{min_1} \text{ instant action required} \end{cases} \tag{5.7}$$

Similarly, this constraint is equivalent to
$d_{fln} - \mathtt{M}_{big}(u - 1) \geq h_{min_1}$, and
$d_{fln} - \mathtt{M}_{big} u < h_{min_1}$

e) z_2 is a binary variable indicating whether the vehicle will be affected by a stopped or decelerating leading vehicle at the TLS, but not affected by its leader while the latter is moving at S_{Rl}. Note: z_1 and z_2 cannot both equal 1, because if $z_1 = 1$, the vehicle follows Scenario 4 and z_2 should be 0. On the other hand, if $z_1 = 0$, z_2 can be 1 (Scenario 3) or 0 (Scenario 1).

$$z_2 = \begin{cases} 1 - z_1 & \text{if } T_{h_{min_2}} < T_{l_2} \\ 0 & \text{if } T_{h_{min_2}} \geq T_{l_2} \end{cases} \tag{5.8}$$

This constraint is equivalent to

$T_{h_{min_2}} + \mathtt{M}_{big}(z_2 - 1) < T_{l_2}$, and
$T_{h_{min_2}} + \mathtt{M}_{big} z_2 \geq T_{l_2}$

f) z_3 is a binary variable indicating whether the vehicle will be affected by its leader twice in a row: first, while the leader is traveling at S_{Rl}; next, while the leader is decelerating at the TLS.

$$z_3 = \begin{cases} 1 & \text{if } T_{h_{min_3}} < T_{l_2}, \text{ will be affected by lead vehicle twice} \\ 0 & \text{otherwise, } \qquad\quad \text{will not be affected by lead vehicle twice} \end{cases} \tag{5.9}$$

This constraint is equivalent to
$T_{h_{min_3}} + \mathtt{M}_{big}(z_3 - 1) < T_{l_2}$, and
$T_{h_{min_3}} + \mathtt{M}_{big} z_3 \geq T_{l_2}$

3. Non-negativity constraint
x, z_1, z_2, z_3, v, and u are binary variables, and S_R is not negative, as shown in the first constraint.

5.2.1 Special case: TLS2V

As discussed in Chapter 4, a TLS sends its packet to the first vehicle in each lane inside the ROI, named the $V_{1_{ROI}}$. Those vehicles do not receive a packet from their leading vehicles and are not affected by them. In this case, the model considers that a $V_{1_{ROI}}$ has a virtual leading vehicle that travels at S_{max} and has the same location as the $V_{1_{ROI}}$. Thus, $d_{fl} = 0$ and $S_{Rl} = S_{max}$.

By applying this case to the model: (1) x can be 0 or 1, thereby indicating whether the virtual leading vehicle will stop or not; (2) the values of z_1, z_3 and v are always 0, which means that a V_{ROI_1} is never affected by a virtual leading vehicle in motion; (3) the u value is always 1 since no instant action is required; (4) z_2 can be 0 or 1. $V_{1_{ROI}}$ follows Scenario 1 if z_2 is equal to zero and Scenario 3 if z_2 equals 1. V_{ROI_1} will stop if $S_x = 0$. When $0 < S_x < S_{max}$, V_{ROI_1} will decelerate prior to the TLS becoming green, but the vehicle will accelerate when the TLS switches to green before it stops.

Table 5.1: Definition of notations.

T_{l_1}	Time for a leading vehicle to reach the TLS (s). It is sent by the leading vehicle based on its selected scenario
T_{l_2}	Time for a leading vehicle to pass the TLS (s). It is sent by the leading vehicle based on its selected scenario
h_{min_1}	Minimum safe space headway when the following vehicle travels at S_R and the leading vehicle travels at S_{Rl} (m)
h_{min_2}	Minimum safe space headway when the following vehicle travels at S_R and the leader is stopped or decelerating (m)
h_{min_3}	Minimum safe space headway when the following vehicle travels at S_{Rl} and the leader is decelerating or idling (m)
$T_{h_{min_i}}$	Time the following vehicle needs so that the space headway reaches h_{min_i} (i = 1, 2 ,3 and 4) (s)
α_1	Required time to decelerate from S_{max} to S_R (s)
d_{dec_1}	Deceleration distance from S_{max} to S_R (m)
d_{fl}	Distance between the following and the leading vehicles (m) once the former receives the packet
d_{fl_n}	Distance between the following and the leading vehicles (m) after the the former adjusts its speed to S_R
d	Distance between the vehicle and the TLS (m) at the time of receiving the packet (given by GPS)
δ	Deceleration rate (kph/s)
S_{Rl}	Recommended speed of the leading vehicle (km/h)
S_{max}	Maximum speed limit (km/h)
S_{min}	Minimum speed limit (km/h)
L_g	Time remaining to switch from green to yellow (s)
L_y	Time remaining to switch from yellow to red (s)
L_r	Time remaining to switch from red to green (s)
T_g	Full green phase time (s)
T_y	Full yellow phase time (s)
T_r	Full red phase time (s)
C_L	TLS cycle length (s). $C_L = T_g + T_y + T_r$.
T_s	Stopping (idling) time (s). T_s formula is different based on the scenario that will be followed
S_x	Minimum speed that a vehicle will reach at the TLS before it accelerates. S_x formula is different based on the scenario that will be followed
S_{xl}	S_x of the leading vehicle

5.3 Formulas to calculate Measures of Effectiveness (MOE_e)

This section shows the computation of Measures of Effectiveness (MOE_e), either fuel or emissions, that are used in the optimization model and presented in Figure 5.2. All notations are defined in Tables 5.1 and 5.2.

1. $MOEe_1$: **Total fuel consumption or emissions during the deceleration time from the current speed (S_{max}) to S_R.**

$$MOEe_1 = \sum_{t_1=1}^{\alpha_{1c}} e^{\sum_{i=0}^{3}\sum_{j=0}^{3}(N_{i,j}^{e} \times v_1(t_1)^i \times na_1(t_1)^j)} \cdot \frac{na_1(t_1)}{\delta} \tag{5.10}$$

where
$\alpha_1 = \frac{S_{max}-S_R}{\delta}$; $\alpha_{1c} = \lceil \alpha_1 \rceil$; $t_1 = 1, 2, .., \alpha_{1c}$ sec; $v_1(0) = S_{max}$;
$na_1(t_1) = \min(\delta, v_1(t_1-1) - S_R)$;
$v_1(t_1) = \max(v_1(t_1-1) - na_1(t_1), S_R)$;
To calculate the deceleration distance from S_{max} to S_R, named d_{dec_1}, we use the SUVAT equations (equations of motion) as follows: $d_{dec_1}(t_1) = v_1(t_1) + \frac{1}{2} \cdot na_1(t_1)$. As a result,

$$d_{dec_1} = \sum_{t_1=1}^{\alpha_{1c}} d_{dec_1}(t_1) \cdot \frac{na_1(t_1)}{\delta} \tag{5.11}$$

2. $MOEe_2$: **Total fuel consumption or emissions for the time interval the vehicle travels at S_R until the distance between the following and leading vehicles reaches h_{min}, or the following vehicle reaches the TLS.**

$$MOEe_2 = (e^{\sum_{i=0}^{3} L_{i,0}^{e} \times S_R^i}) \times T_2 \tag{5.12}$$

where
$T_2 = z_1 \cdot min(T_{h_{min_1}}, T_{TLS}) + x \cdot (1-z_1) \cdot z_2 \cdot min(T_{h_{min_2}}, T_{TLS})$;
$T_{TLS} = \frac{d - d_{dec_1} - (x \cdot z_1 + x \cdot z_2) \cdot d_{dec_{11}}}{S_R}$;
$T_{h_{min_1}} = \frac{v \cdot u \cdot (d_{fl_n} - h_{min_1})}{(S_R - v \cdot S_{Rl})}$;

Table 5.2: Definition of notations.

$v_k(t_k)$	Vehicle speed at time t_k $(k = 1, 4, 6, 8, 11, 13\&17)$
$na_k(t_k)$	Vehicle deceleration at time t_k $(k = 1, 6, 11\&17)$
$a_k(t_k)$	Vehicle acceleration at time t_k $(k = 4, 8, \&13)$
$y_k(t_k)$	Maximum possible vehicle acceleration (km/h/s) at time t_k $(k = 4, 8, \&13)$. The expression of $y_k(t_k)$ is a regression model developed in [26] as follows: $y_k(t_k) = -0.00003 \cdot v_k(t_k - 1)^3 + 0.00801 \cdot v_k(t_k - 1)^2 - 0.80333 \cdot v_k(t_k - 1) + 35.19284$
$N^e_{i,j}$	$= M^e_{i,j}$ if $na_k(t_k) < 0$; else $N^e_{i,j} = L^e_{i,j}$ $(k = 1, 6\&17)$
α_6	Required time to decelerate from S_R to S_{Rl}
α_{11}	Required time to decelerate from S_R to S_x or 0
α_{17}	Required time to decelerate from S_{Rl} to 0
β_4	Required time to accelerate from S_R to S_{max}
β_8	Required time to accelerate from S_{Rl} to S_{max}
β_{13}	Required time to accelerate from S_x or 0 to S_{max}
L	Distance between the vehicle and the destination at the time of receiving the packet (given by GPS)
l	index referring to the leading vehicle (e.g., d_l is the d value of the leading vehicle)
A	Maximum acceleration rate = 3.6 m/s^2
T_{TLS}	Time interval a vehicle needs to reach the TLS
T_2	Time interval that the vehicle travels at S_R until the distance b/w following and leading vehicles reaches a min. space headway or the following vehicle reaches the TLS
T_7	Time interval that the following vehicle travels at S_{Rl} after the space headway reaches h_{min_1} until the vehicle reaches the TLS
N_g	Light cycles that will be completed before passing the TLS if the message is sent when the TLS is green
T_{14}	Time interval that the vehicle travels at S_{max} to the destination
D	packet delay (s), defined as the difference between the time of receiving the packet and the time of initiating the packet from the TLS

$T_{h_{min_2}} = \frac{u \cdot (d - d_{dec_1} - h_{min_2})}{S_R} + \alpha_1$;
$d_{fl_n} = \max(d_{fl} - d_{dec_1} + S_{Rl} \cdot \alpha_1, 0)$;
$h_{min_1} = (\frac{v \cdot (S_R + S_{Rl})}{2}) \cdot (\frac{S_R - S_{Rl}}{\delta})$;
$h_{min_2} = \frac{S_R + S_{xl}}{2} \cdot \frac{S_R - S_{xl}}{\delta}$

3. $MOEe_3$: **Total fuel consumption or emissions for the time interval the vehicle travels at S_R until it reaches the TLS.**

$$MOEe_3 = (e^{\sum_{i=0}^{3} L_{i,0}^{e} \times S_R^i}) \times (T_{TLS} - T_2) \quad (5.13)$$

4. $MOEe_4$: **Total fuel consumption or emissions during the acceleration from S_R to S_{max}, which is the maximum speed limit after passing the TLS.**

$$MOEe_4 = \sum_{t_4=1}^{\beta_4} (e^{\sum_{i=0}^{3} \sum_{j=0}^{3} (L_{i,j}^{e} \times v_4(t_4)^i \times a_4(t_4)^j)}) \cdot \frac{a_4(t_4)}{y_4(t_4)} \quad (5.14)$$

where
$\beta_4 = \lceil \frac{S_{max} - S_R}{A} \rceil$; $t_4 = 1, 2, .., \beta_4$ sec;
$v_4(0) = S_R$;
$a_4(t_4) = \min(y_4(t_4), S_{max} - v_4(t_4 - 1))$;
$v_4(t_4) = \min(S_{max}, v_4(t_4 - 1) + a_4(t_4))$
To calculate the acceleration distance from S_R to S_{max}, named d_{acc_4}, we use the SUVAT equation as follows: $d_{acc_4}(t_4) = v_4(t_4) + 0.5 \cdot a_4(t_4)$. As a result,

$$d_{acc_4} = \sum_{t_4=1}^{\beta_4} d_{acc_4}(t_4) \cdot \frac{a_4(t_4)}{y_4(t_4)} \quad (5.15)$$

5. $MOEe_5$: **Total fuel consumption or emissions for the time interval the vehicle travels at S_{max} to the destination.**

$$MOEe_5 = [e^{\sum_{i=0}^{3} L_{i,0}^{e} \times S_{max}^i}] \times (\frac{L - d - d_{acc_4}}{S_{max}}) \quad (5.16)$$

6. $MOEe_6$: **Total fuel consumption or emissions during the deceleration from**

S_R to S_{Rl}, which is the recommended speed of the leading vehicle. This case occurs if the space headway reaches h_{min} before the leading vehicle has reached the TLS.

$$MOEe_6 = \sum_{t_6=1}^{\alpha_{6c}} e^{\sum_{i=0}^{3}\sum_{j=0}^{3}(N_{i,j}^{e}\times v_6(t_6)^i\times na_6(t_6)^j)} \cdot \frac{na_6(t_6)}{\delta} \tag{5.17}$$

where
$\alpha_6 = \frac{S_R - S_{Rl}}{\delta}$; $\alpha_{6c} = \lceil \alpha_6 \rceil$; $t_6 = 1, 2, .., \alpha_{6c}$ sec;
$v_6(0) = S_R$;
$na_6(t_6) = \min(\delta, v_6(t_6 - 1) - S_{Rl})$
$v_6(t_6) = \max(v_6(t_6 - 1) - na_6(t_6), S_{Rl})$
To calculate the deceleration distance from S_R to S_{Rl}, named d_{dec_6}, we use the SUVAT equations as follows: $d_{dec_6}(t_6) = v_6(t_6) + \frac{1}{2} \cdot na_6(t_6)$. As a result,

$$d_{dec_6} = \sum_{t_6=1}^{\alpha_{6c}} d_{dec_6}(t_6) \cdot \frac{na_6(t_6)}{\delta} \tag{5.18}$$

7. $MOEe_7$**: Total fuel consumption or emissions for the time interval that the following vehicle travels at S_{Rl} after the space headway reaches h_{min} and until the vehicle reaches the TLS.**

$$MOEe_7 = (e^{\sum_{i=0}^{3} L_{i,0}^{e}\times S_{Rl}^{i}}) \times T_7 \tag{5.19}$$

where
$T_7 = \frac{d - (d_{dec_1} + S_R \cdot T_2 + d_{dec_6} + (x \cdot z_1 + x \cdot z_2) \cdot d_{dec_{17}})}{S_{Rl}}$

8. $MOEe_8$**: Total fuel consumption or emissions during the acceleration from S_{Rl} to S_{max}.**

$$MOEe_8 = \sum_{t_8=1}^{\beta_8} (e^{\sum_{i=0}^{3}\sum_{j=0}^{3}(L_{i,j}^{e}\times v_8(t_8)^i\times a_8(t_8)^j)}) \cdot \frac{a_8(t_8)}{y_8(t_8)} \tag{5.20}$$

where
$\beta_8 = \lceil \frac{S_{max} - S_{Rl}}{A} \rceil$; $t_8 = 1, 2, .., \beta_8$ sec;

$v_8(0) = S_{Rl}$;
$a_8(t_8) = \min(y_8(t_8), S_{max} - v_8(t_8-1))$;
$v_8(t_8) = \min(S_{max}, v_8(t_8-1) + a_8(t_8))$
To calculate the acceleration distance from S_R to S_{max}, named d_{acc_8}, we use the SUVAT equation as follows: $d_{acc_8}(t_8) = v_8(t_8) + 0.5 \cdot a_8(t_8)$. As a result,

$$d_{acc_8} = \sum_{t_8=1}^{\beta_8} d_{acc_8}(t_8) \cdot \frac{a_8(t_8)}{y_8(t_8)} \tag{5.21}$$

9. $MOEe_9$**: Total fuel consumption or emissions for the time interval the vehicle travels at S_{max} to the destination in Scenario 2**

$$MOEe_9 \;=\; [e^{\sum_{i=0}^{3} L_{i,0}^{e} \times S_{max}^{i}}] \times (\frac{L-d-d_{acc_8}}{S_{max}}) \tag{5.22}$$

10. $MOEe_{10}$**: has the same definition and formulas as $MOEe_3$.**

$$MOEe_{10} \;=\; MOEe_3 \tag{5.23}$$

11. $MOEe_{11}$**: Total fuel consumption or emissions during the deceleration from S_R to S_x or zero, where S_x is the minimum speed that the vehicle will reach before it accelerates.**

$$MOEe_{11} \;=\; \sum_{t_{11}=1}^{\alpha_{11c}} e^{\sum_{i=0}^{3}\sum_{j=0}^{3}(M_{i,j}^{e} \times v_{11}(t_{11})^{i} \times na_{11}(t_{11})^{j})} \cdot \frac{na_{11}(t_{11})}{\delta} \tag{5.24}$$

where
$\alpha_{11} = \frac{S_R - S_x}{\delta}$; $\alpha_{11c} = \lceil \alpha_{11} \rceil$; $t_{11} = 1, 2, .., \alpha_{11c}$ sec;
$v_{11}(0) = S_R$;
$na_{11}(t_{11}) = \min(\delta, v_{11}(t_{11}-1) - S_x)$;
$v_{11}(t_{11}) = \max(v_{11}(t_{11}-1) - na_{11}(t_{11}), S_x)$;
$S_x = min(max(0, S_R - (T_{l_2} - \alpha_1 - T_{h_{min_2}}) \cdot \delta), S_R)$;
To calculate the deceleration distance from S_R to S_x or zero, named $d_{dec_{11}}$, we use the SUVAT equations as follows: $d_{dec_{11}}(t_{11}) = v_{11}(t_{11}) + \frac{1}{2} \cdot na_{11}(t_{11})$. As a result,

$$d_{dec_{11}} = \sum_{t_{11}=1}^{\alpha_{11c}} d_{dec_{11}}(t_{11}) \cdot \frac{na_{11}(t_{11})}{\delta} \tag{5.25}$$

12. $MOEe_{12}$**: Total fuel consumption or emissions when the vehicle idles at the TLS.**

$$MOEe_{12} \quad = \quad e^{L^e_{0,0}} \times T_s \tag{5.26}$$

where
$T_s = \max(0, (N_g - 1) \cdot C_L + L_g + T_y + T_r - D - (\frac{d - d_{dec_1} - d_{dec_{11}}}{S_R} + \alpha_1 + \alpha_{11}))$

13. $MOEe_{13}$**: Total fuel consumption or emissions during the acceleration from** S_x **or idling to** S_{max}**.**

$$MOEe_{13} \quad = \quad \sum_{t_{13}=1}^{\beta_{13}} e^{\sum_{i=0}^{3}\sum_{j=0}^{3}(L^e_{i,j} \times v_{13}(t_{13})^i \times a_{13}(t_{13})^j)} \cdot \frac{a_{13}(t_{13})}{y_{13}(t_{13})} \tag{5.27}$$

where
$\beta_{13} = \lceil \frac{S_{max} - S_x}{A} \rceil$; $t_{13} = 1, 2, .., \beta_{13}$ sec;
$v_{13}(0) = \ell \cdot S_x$;
$a_{13}(t_{13}) = \min(y(t_{13}), S_{max} - v_{13}(t_{13} - 1))$;
$v_{13}(t_{13}) = \min(S_{max}, v_{13}(t_{13} - 1) + a_{13}(t_{13}))$
To calculate the acceleration distance from zero to S_{max}, named $d_{acc_{13}}$, we use the SUVAT equation as follows: $d_{acc_{13}}(t_{13}) = v_{13}(t_{13}) + 0.5 \cdot a_{13}(t_{13})$. As a result,

$$d_{acc_{13}} = \sum_{t_{13}=1}^{\beta_{13}} d_{acc_{13}}(t_{13}) \cdot \frac{a_{13}(t_{13})}{y_{13}(t_{13})} \tag{5.28}$$

14. $MOEe_{14}$**: Total fuel consumption or emissions for the time interval the vehicle travels at** S_{max} **to the destination in Scenario 3.**

$$MOEe_{14} \quad = \quad [e^{\sum_{i=0}^{3} L^e_{i,0} \times S^i_{max}}] \times T_{14} \tag{5.29}$$

where
$T_{14} = \frac{[L-(d_{dec_1}+S_R \cdot T_2+S_R \cdot (T_{TLS}-T_2)+d_{dec_{11}}+d_{acc_{13}})]}{S_{max}}$

15. $MOEe_{15}$**: has the same definition and formulas as** $MOEe_6$**.**

$$MOEe_{15} \quad = \quad MOEe_6 \tag{5.30}$$

16. $MOEe_{16}$**: has the same definition and formulas as** $MOEe_7$**.**

$$MOEe_{16} \quad = \quad MOEe_7 \tag{5.31}$$

17. $MOEe_{17}$**: Total fuel consumption or emissions during the deceleration from** S_{Rl} **to** S_x **or zero**

$$MOEe_{17} \quad = \quad \sum_{t_{17}=1}^{\alpha_{17_c}} e^{\sum_{i=0}^{3}\sum_{j=0}^{3}(N_{i,j}^{e} \times v_{17}(t_{17})^i \times na_{17}(t_{17})^j)} \cdot \frac{na_{17}(t_{17})}{\delta} \tag{5.32}$$

where
$\alpha_{17} = \frac{S_{Rl}-S_x}{\delta}$; $\alpha_{17_c} = \lceil \alpha_{17} \rceil$; $t_{17} = 1, 2, .., \alpha_{17c}$ sec;
$v_{17}(0) = S_{Rl}$;
$na_{17}(t_{17}) = \min(\delta, v_{17}(t_{17}-1) - S_x)$;
$v_{17}(t_{17}) = \max(v_{17}(t_{17}-1) - na_{17}(t_{17}), S_x)$;
$S_x = min(max(0, S_{Rl} - (T_{l_2} - T_{h_{min_3}}) \cdot \delta), S_{Rl})$;
$T_{h_{min_3}} = \frac{d_{fl_{S_{Rl}-S_{Rl}}} - h_{min_3}}{S_{Rl}-S_{xl}} + \alpha_1 + \alpha_6 + T_2$;
where $d_{fl_{S_{Rl}-S_{Rl}}} = h_{min_1} - d_{dec_6} + S_{Rl} \cdot \alpha_6$, which is the distance between the following and leading vehicles after the former adjusts its speed to S_{Rl}.
To calculate the deceleration distance from S_{Rl} to S_x, named $d_{dec_{17}}$, we use the SUVAT equations as follows: $d_{dec_{17}}(t_{17}) = v_{17}(t_{17}) + \frac{1}{2} \cdot na_{17}(t_{17})$. As a result,

$$d_{dec_{17}} = \sum_{t_{17}=1}^{\alpha_{17_c}} d_{dec_{17}}(t_{17}) \cdot \frac{na_{17}(t_{17})}{\delta} \tag{5.33}$$

18. $MOEe_{18}$**: Total fuel consumption or emissions when the vehicle idles at the TLS**

$$MOEe_{18} = e^{L^e_{0,0}} \times T_s \tag{5.34}$$

where
$T_s = \max(0, (N_g - 1) \cdot C_L + L_g + T_y + T_r - D - (T_2 + T_7 + \alpha_1 + \alpha_6 + \alpha_{17}))$

19. $MOEe_{19}$**: has the same definition and formulas as** $MOEe_{13}$**.**

$$MOEe_{19} = MOEe_{13} \tag{5.35}$$

20. $MOEe_{20}$**: Total fuel consumption or emissions for the time interval the vehicle travels at** S_{max} **to the destination in Scenario 4.**

$$MOEe_{14} = [e^{\sum_{i=0}^{3} L^e_{i,0} \times S^i_{max}}] \times T_{20} \tag{5.36}$$

where
$T_{20} = \frac{[L-(d_{dec_1}+S_R \cdot T_2+d_{dec_{15}}+S_{Rl} \cdot T_{16}+d_{dec_{17}}+d_{acc_{19}})]}{S_{max}}$

5.4 Results and Discussions

This section presents an example to show the results of the optimum S_R (S_R^*), which can achieve the minimum vehicle fuel consumption and CO_2 emission. The model presented in Section 5.2 is solved using an exhaustive search from S_{min} to S_{max} with an increment of 0.1 km/h. Having less than 0.1 km/h (e.g., 0.01 km/h) is not practical because adjusting the speed (e.g., to 40.01 km/h) would be hard. Exhaustive search is used because the search space from S_{min} to S_{max} is small.

Consider two vehicles V_1 and V_2 approaching a TLS as shown in Figure 5.3. Table 5.3 determines some parameters. We consider that the packet is sent as the TLS turns green, V_1 is within the transmission range of the TLS, and V_2 is within the transmission range of V_1. Based on the EEFG protocol, V_1 receives a packet from the TLS and adjusts its speed to S_R^*. Then, V_1 sends its information to V_2.

Figure 5.4 shows the total fuel consumption and CO_2 emission for V_1 versus S_R with different values of d, where d is the distance between the vehicle and the TLS. At $d = 0.5$ km, the vehicle, at all possible values of S_R (40 km/h $\leq S_R \leq$ 60 km/h), can pass the

Table 5.3: Parameters.

S_{max}	60 km/h	T_y	5 s
S_{min}	40 km/h	T_r	50 s
L_g	45 s	T_g	45 s
D	0 s	δ	-5 kph/s

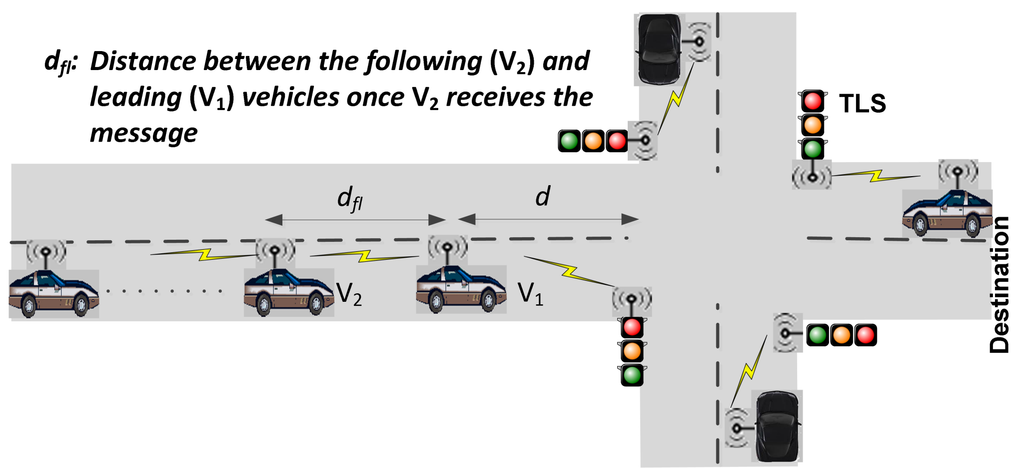

Figure 5.3: Vehicles V_1 and V_2 approaching a TLS

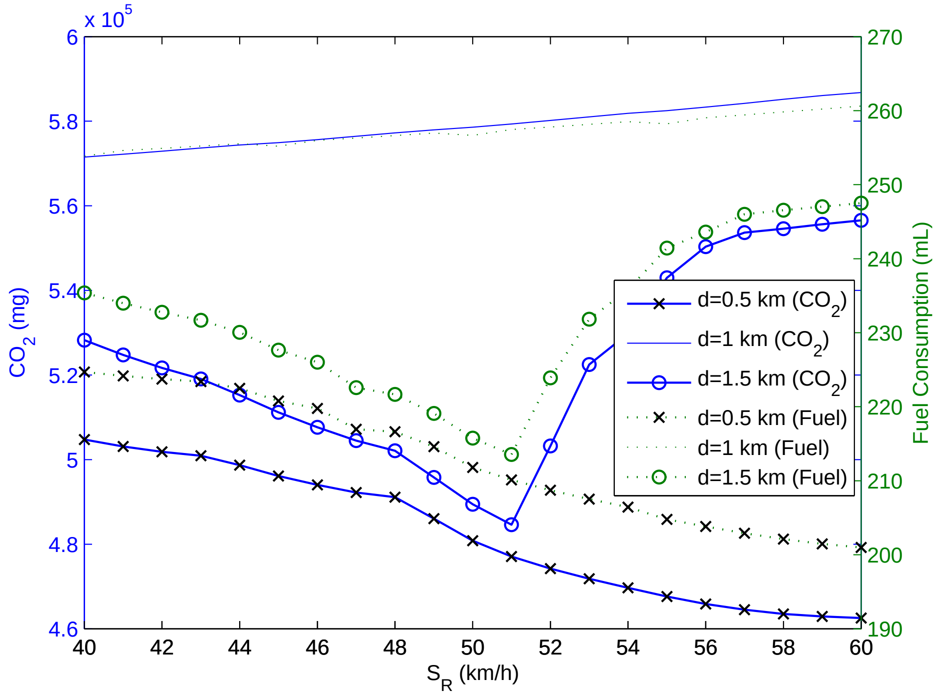

Figure 5.4: Total vehicle CO_2 emission and fuel consumption versus the recommended speed of V_1

green TLS. However, $S_R = 60$ km/h is the best value since it gives the minimum fuel consumption and CO_2 emission. At $d = 1$ km, the vehicle has to stop at the TLS for all possible values of S_R since the green light will switch to red at the time the vehicle reaches the TLS. The optimum value is when $S_R = 40$ km/h. At $d = 1.5$ km, the fuel consumption and CO_2 emission decrease until $S_R = 51.1$ km/h, which is the optimum speed; then, they increase. The decrease represents Scenario 1 since the vehicle that travels at S_R can pass the green light for the next phase of the TLS. A high S_R leads to low acceleration to S_{max} after passing the TLS. Therefore, fuel consumption and CO_2 emission decrease with increasing S_R. On the other hand, the increase part represents Scenario 3. High S_R results in low S_x, which leads to high acceleration to S_{max}. Thus, fuel consumption and CO_2 emission increase with increasing S_R.

After V_1 adjusts its speed to S_R^*, it sends a packet to V_2. Since the movement of V_2 depends on V_1, we discuss the CO_2 and fuel results of V_2 in two cases. First, V_1 will not stop at the TLS. That happens when $d = 0.5$ and 1.5 km, as discussed. At $d = 0.5$ km, V_1

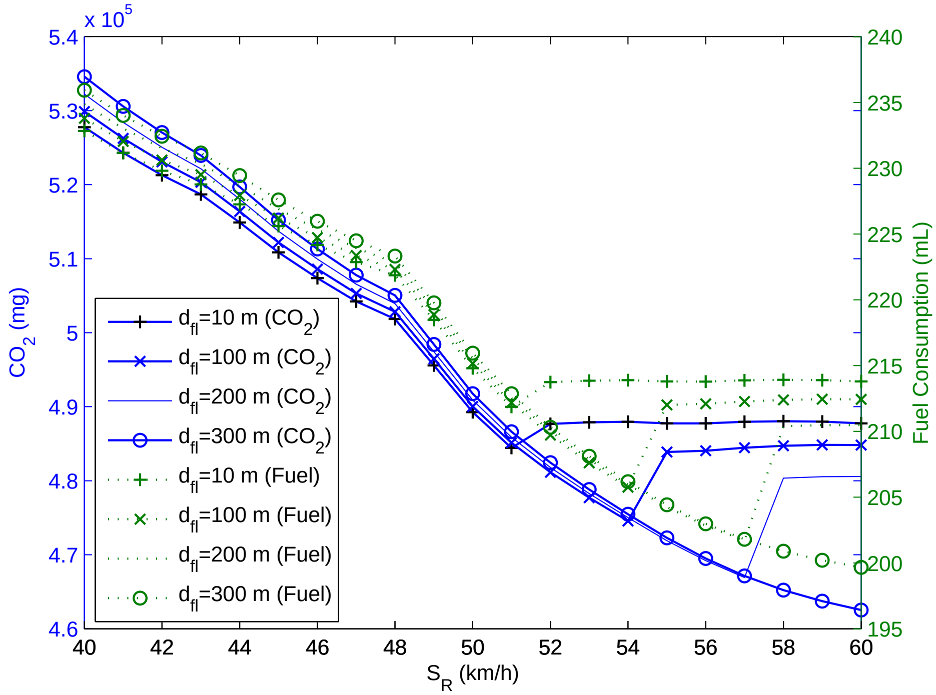

Figure 5.5: Total vehicle CO_2 emission and fuel consumption versus the recommended speed of V_2 if the leading vehicle will not stop at the TLS

is out of ROI since $S_R^* = S_{max}$. Therefore, V_1 does not need to send its information to its follower, as discussed in Chapter 4. However, at $d = 1.5$ km, V_1 sends its information to V_2. The results of V_2 in this case will be discussed in the following subsection. A second case arises when V_1 will stop at the TLS. In this case, $S_R^* = 40$ km/h as shown in Figure 5.4 at $d = 1$ km.

5.4.1 If the leading vehicle will not stop at the TLS

Figure 5.5 shows the effect of S_R and d_{fl} on the total CO_2 emission and fuel consumption. At $d_{fl} = 10$ m, a short distance between the following and leading vehicles, the following vehicle will be affected by the leading vehicle once the former increases its speed to more than S_{Rl}. Therefore, the best value of S_R, giving the minimum CO_2 emission and fuel consumption, equals S_{Rl}, as shown in the figure. Note that S_{Rl} is the S_R^* of V_1. As d_{fl} increases, the following vehicle will be able to increase its speed to more than S_{Rl} and not be affected by its leader. CO_2 emission and fuel consumption decrease with increasing S_R until a certain value; then, they increase. While decreasing, the following vehicle is not affected by the leading vehicle. In this case, the CO_2 emission and fuel consumption from the following vehicle decrease with increasing S_R, because high speed will save on acceleration after a vehicle passes the TLS. The increase indicates that the following vehicle has been affected by the leading one. In this case, the following vehicle would have to reduce its speed to S_{Rl}, then accelerate to S_{max} after passing the TLS. The constant phase occurs because acceleration after passing the TLS is the same in all cases since the speed would have to be changed to S_{Rl} at any values of S_R. It might be argued that since the following vehicle will travel at S_R before it is affected by its leader, traveling at higher S_R should result in more CO_2 emission and fuel use than lower S_R with zero acceleration; however, they are almost constant. The answer is that the periods of traveling at S_R and S_{Rl} are different. For example, when $d_{fl} = 100$ m, the time needed for the following vehicle to reach h_{min_1} if it travels at $S_R = 55$ km/h will be longer than that time if it traveled at $S_R = 60$ km/h. Consequently, the time the vehicle travels at S_{Rl} will be shorter in the first case (when $S_R = 55$ km/h).

5.4.2 If the leading vehicle will stop at the TLS

Figure 5.6 shows the effect of S_R and d_{fl} on the total CO_2 emission and fuel consumption if the leading vehicle is going to stop at the TLS. At $d_{fl} = 10$ m, the CO_2 emission and fuel consumption levels for all values of S_R are almost the same because the vehicles are close to each other. In this case, the following vehicle must decelerate to S_{Rl} regardless of the value of S_R. At $d_{fl} = 100$ m, the vehicles are still close to each other. However, $d_{fl} > h_{min_1}$, which means that the following vehicle will travel at S_R, then decelerate to S_{Rl} when the distance between it and its leading vehicle reaches h_{min_1}. The minimum CO_2 and fuel consumption happen when $S_R = S_{Rl}$ because at all values of S_R the vehicle will stop; thus, traveling at the lowest speed with zero acceleration produces less CO_2 emission and fuel consumption. With increasing S_R, the CO_2 emission and fuel consumption increase slightly since the vehicles are close to each other, making the following vehicle travel at S_R for a short time. As a result, changing S_R's value does not clearly affect CO_2 emission and fuel consumption.

The interpretations of the remaining results are similar. For example, when $d_{fl} = 200$ m, the optimum value of S_R equals 40.8 km/h since the value of CO_2 emission and fuel consumption are minimal. At this value, the vehicle will not be affected at all by its leader; also, it will not stop (Scenario 1). The CO_2 emission and fuel consumption increase when $S_R <$ optimum S_R although the vehicle remains unaffected by the leading one because

Table 5.4: Conclusions of the results.

d_{fl} (m)	Optimum S_R (km/h) if the leader will not stop at TLS	Optimum S_R (km/h) if the leader will stop at TLS
10	51.3	40
50	52.6	40
100	54.2	40
200	57.3	40.8
250	58.9	42.6
300	60	44.4

the vehicle would need more acceleration, to S_{max}, after passing the TLS if it traveled at lower speeds. Scenario 3 happens when the vehicle travels at $S_R >$ optimum S_R. In this scenario, high S_R results in low S_x, which leads to high acceleration to S_{max}. As a result, CO_2 emission and fuel consumption increase with increasing S_R. The vehicle will follow Scenario 4 if it travels at $S_R \geq 48$ km/h. The conclusions of the results are shown in Table 5.4.

In conclusion, accelerating and speeding are the main actions that increase fuel consumption and CO_2 emission. Three important remarks from the results of this example are summarized as follows:

- The optimum S_R is S_{Rl} if the vehicle will be affected by the leading one once the former increases its speed to more than S_{Rl}.
- The optimum S_R ranges between $S_{Rl} \leq S_R^* \leq S_{max}$ if the vehicle is able to increase its speed to more than S_{Rl} without being affected by its leader.
- The optimum S_R is S_{min} if the vehicle has to stop anyway, because lower speeds with zero acceleration consume less fuel and produce fewer emissions.

5.5 Summary

This chapter has developed a comprehensive optimization model for V2V and TLS2V as a special case with the objective of minimizing fuel consumption and emissions from vehicles approaching a TLS. This objective is achieved by controlling the speed to the optimum S_R, which helps vehicles avoid having to stop, making lengthy accelerations, and running at

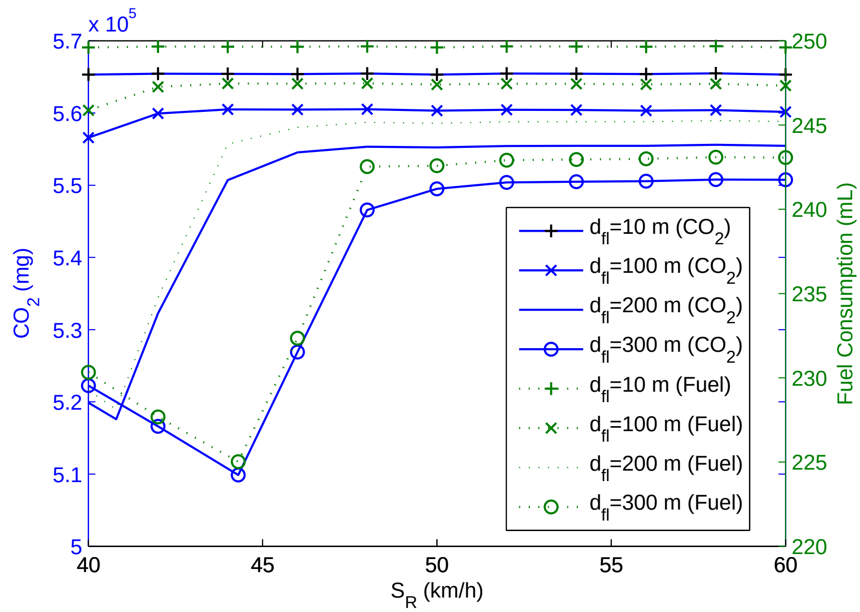

Figure 5.6: Total vehicle CO_2 emission and fuel consumption versus the recommended speed of V_2 if the leading vehicle will stop at the TLS

unnecessarily excessive speed. Therefore, the optimum S_R, as shown in the results, equals S_{Rl} if the vehicle, once it increases its speed to more than S_{Rl}, will be affected by its leader; the optimum S_R equals S_{min} if the vehicle has to stop anyway; the optimum S_R is within the range $S_{Rl} \leq S_R^* \leq S_{max}$ if the vehicle is able to increase its speed to more than S_{Rl} without being affected by its leader. The minimum fuel consumption and emissions can be achieved if the vehicle travels at the optimum S_R.

Chapter 6

Heuristic expressions to compute optimum or near-optimum S_R value

This chapter proposes expressions to compute the optimum or near-optimum recommended speed (S_R) of the leading and following vehicles. These expressions have been proposed based on the observations drawn from Chapter 5's results, which are: (1) the optimum S_R should be the maximum possible speed that allows the vehicle to pass the traffic light signal (TLS) without stopping or decelerating; (2) if the vehicle has to stop, the result of the optimum S_R equals S_{min}; (3) the optimum S_R must equal S_{max} if the vehicle is close to the green TLS and can catch it. The next sections show the computation of S_R for the leading vehicle (V_1) and its follower (V_2) as shown in Figure 6.1. This work has been published as a journal paper in IEEE Transactions on Intelligent Transportation Systems [63] and a conference paper in IEEE Intelligent Transportation Systems Conference [64].

6.1 Computation of S_R for leading vehicle (V_1)

Vehicle V_1 is the closest vehicle to the TLS as shown in Figure 6.1. To achieve the maximum possible speed that allows the vehicle to pass the TLS without stopping or decelerating, the required delay of the vehicle to be able to pass the TLS should equal the time interval for the vehicle to reach a location where the distance to reach the TLS equals the minimum space headway (h_{min}). Equation 6.1 shows the case if the TLS sends the message when it

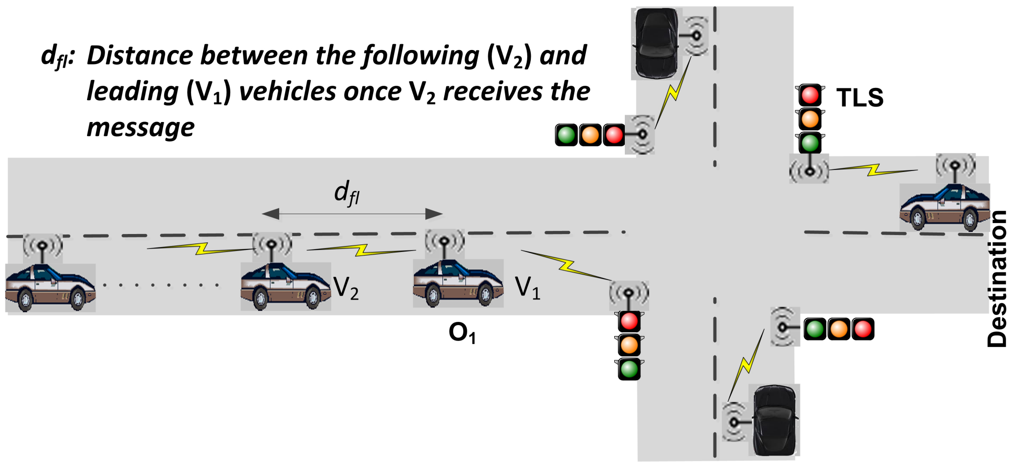

Figure 6.1: Vehicles V_1 and V_2 approaching a TLS

is **green**.

$$\underbrace{(N_g - 1) \cdot C_L + L_g + T_y + T_r - D}_{\substack{\text{Required delay to pass the TLS if the} \\ \text{message is sent when the TLS is green}}} = \underbrace{\frac{d - d_{dec} - h_{min}}{S_R} + \alpha}_{\substack{\text{Required delay to be} \\ h_{min} \text{ away from the} \\ \text{TLS, while the speed} \\ \text{is adapted to } S_R}} \tag{6.1}$$

where $N_g = \max(\lceil \frac{|d/S_{max} - L_g|}{C_L} \rceil, 1)$;
$C_L = T_g + T_y + T_r$;
$\alpha = \frac{S_{max} - S_R}{\delta}$;
$d_{dec} = \frac{S_{max} + S_R}{2} \cdot \frac{S_{max} - S_R}{\delta}$;
$h_{min} = \frac{S_R^2}{2 \cdot \delta}$.
The parameters are defined in Table 6.1.

From Equation 6.1, S_R can be formulated as in Equation 6.2.

$$S_R = \max(\frac{d - d_{dec} - h_{min} + \alpha \cdot S_R}{(N_g - 1) \cdot C_L + L_g + T_y + T_r - D}, S_{min}) \tag{6.2}$$

Table 6.1: Definition of the parameters

L_g	Time remaining to switch from green to yellow
L_y	Time remaining to switch from yellow to red
L_r	Time remaining to switch from red to green
C_L	TLS cycle length
d	Distance between the vehicle and the TLS after receiving the message
D	Packet delay
α	Time the vehicle has to comfortably decelerate from S_{max} to S_R
d_{dec}	Distance traveled during the deceleration from S_{max} to S_R
δ	Deceleration rate (kph/s)
N_g	Light cycles that will be completed before passing the TLS if the message is sent when the TLS is green
N_r	Light cycles that will be completed before passing the TLS if the message is sent when the TLS is red
N_y	Light cycles that will be completed before passing the TLS if the message is sent when the TLS is yellow
T_{l_1}	Time for a leading vehicle to reach the TLS (s). It is sent by the leading vehicle based on its selected scenario.
T_{l_2}	Time for a leading vehicle to pass the TLS (s). It is sent by the leading vehicle based on its selected scenario
h_{min_1}	Minimum safe space headway when the following vehicle travels at S_R and the leading vehicle travels at S_{Rl}
h_{min_2}	Minimum safe space headway when the following vehicle travels at S_R and the leader is stopped
d_{fl_n}	Distance between the following and the leading vehicles (m) after the the former adjusts its speed to S_R
S_{Rl}	Recommended speed of the leading vehicle

In another situation, the equivalent of Equation 6.1 if the TLS sends the message when it is **red** is the following equation:

$$\underbrace{(N_r - 1) \cdot C_L + L_r - D}_{\substack{\text{Required delay to pass the TLS if the} \\ \text{message is sent when the TLS is red}}} = \underbrace{\frac{d - d_{dec} - h_{min}}{S_R} + \alpha}_{\substack{\text{Required delay to be} \\ h_{min} \text{ away from the} \\ \text{TLS, while the speed} \\ \text{is adapted to } S_R}} \tag{6.3}$$

where $N_r = \max(\lceil \frac{|d/S_{max} - L_r|}{C_L} \rceil, 1)$. The calculation of S_R is according to Equation 6.4:

$$S_R = \max(\frac{d - d_{dec} - h_{min} + \alpha \cdot S_R}{(N_r - 1) \cdot C_L + L_r - D}, S_{min}) \tag{6.4}$$

In addition, if the TLS sends the message when it is **yellow**, the equality as in Equation 6.5 has to be satisfied in order to achieve the maximum possible speed that allows the vehicle to pass the TLS without stopping or decelerating.

$$\underbrace{(N_y - 1) \cdot C_L + L_y + T_r - D}_{\substack{\text{Required delay to pass the TLS if the} \\ \text{message is sent when the TLS is} \\ \text{yellow}}} = \underbrace{\frac{d - d_{dec} - h_{min}}{S_R} + \alpha}_{\substack{\text{Required delay to be} \\ h_{min} \text{ away from the} \\ \text{TLS, while the speed} \\ \text{is adapted to } S_R}} \tag{6.5}$$

where $N_y = \max(\lceil \frac{|d/S_{max} - L_y - T_r|}{C_L} \rceil, 1)$. S_R can be formulated as in the following equation.

$$S_R = \max(\frac{d - d_{dec} - h_{min} + \alpha \cdot S_R}{(N_y - 1) \cdot C_L + L_y + T_r - D}, S_{min}) \tag{6.6}$$

6.1.1 Results and Discussions

This section presents the results of S_R and vehicle CO_2 emissions of vehicle V_1, using the optimization model and the heuristic expression for S_R. Since fuel consumption is proportional to CO_2 emissions, the figures of the fuel and CO_2 will look similar. Therefore, the results of fuel consumption are not presented in this section. The model has been analyzed for V_1 traveling from origin (O_1) to destination (D) as shown in Figure 6.1,

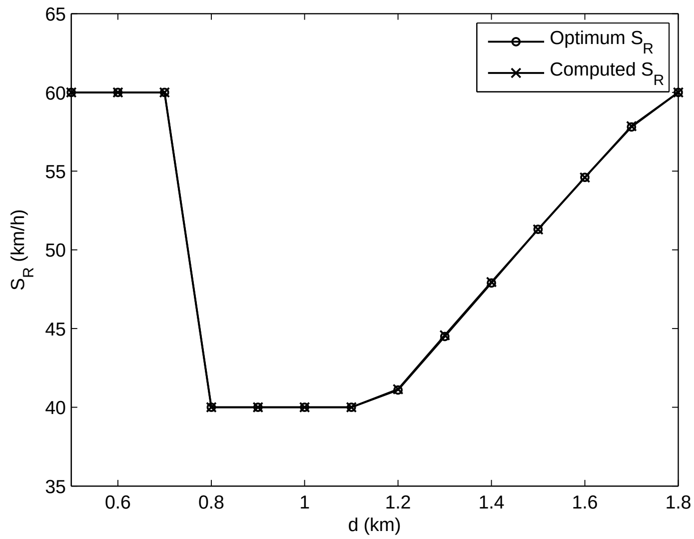

Figure 6.2: S_R vs. dis. b/w the vehicle and the TLS after receiving the msg

where the distance between O_1 and D equals 2.5 km. The rest of the parameters are specified as presented in Section 5.4.

From Figures 6.2 and 6.3, one can notice the following. At $d = 0.5$, 0.6, and 0.7 km, the vehicle can pass the green TLS if it travels at S_{max}. Thus, both optimum and computed S_R equal 60 km/h. In this case, no action is required from the vehicle since it is already traveling at S_{max}. Consequently, the CO_2 emissions are the same as shown in Fig. 6.3. At $d = 0.8$ to 1.1 km, the optimum and computed S_R are 40 km/h. This is the case when the vehicle has to stop. It can be noticed that larger d results in less CO_2 emissions, the result of vehicle receiving the message earlier at larger d. Thus, the vehicle can take action early. At $d = 1.2$ to 1.7 km, the vehicle will follow Scenario 1 or Scenario 3 (without stopping) when d increases, as discussed in Section 5.1. Therefore, CO_2 emissions decrease when d increases. Finally, optimum and computed S_R are equal to S_{max} again when $d = 1.8$ km.

6.2 Computation of S_R for the following vehicle (V_2)

Vehicle V_2 follows vehicle V_1 as shown in Figure 6.1. To compute S_R of V_2, we need to know whether V_1 will stop at the TLS or not. This information is sent from V_1 to V_2.

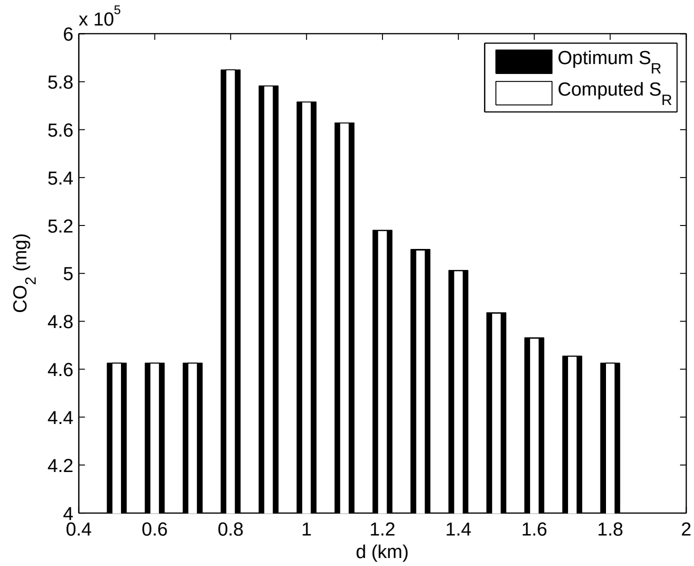

Figure 6.3: Total CO_2 emissions vs. d

6.2.1 If the leading vehicle will not stop at the TLS

As observed in the previous chapter, the optimum S_R should be the maximum possible speed that allows the vehicle to pass the TLS without having to stop or decelerate at the TLS. The vehicle is not affected by its leader if both are traveling at the same speed. Therefore, the optimum S_R falls within the following range: $S_{Rl} \leq S_R^* \leq S_{max}$. The expression is presented as follows.

$$S_R = \min(\max(S_{Rl} + \frac{d_{fln} - h_{min_1}}{T_{l_1} - \alpha}, S_{Rl}), S_{max}) \tag{6.7}$$

The addition term after S_{Rl} is the amount of speed that can be added to S_{Rl} without causing the vehicle to be affected by its leader. The formula guarantees that S_R does not exceed S_{max} and does not stay under S_{Rl}. Note that notations are defined in Table 6.1.

6.2.2 If the leading vehicle will stop at the TLS

As observed from Figure 5.6, the optimum S_R is the maximum possible speed that allows the vehicle to pass the TLS without stopping or slowing. However, if the vehicle has to stop anyway, the optimum S_R is S_{min}, which equals S_{Rl} since the leading vehicle will travel at S_{min} if it has to stop anyway, as shown in Fig. 5.4. To achieve the maximum possible speed that allows the vehicle to pass the TLS without stopping or slowing, the delay required for the leading vehicle to pass the TLS should equal the time the following vehicle needs to reach the point where the distance to the TLS equals the minimum space headway (h_{min_2}) as in Equation 6.8. Note that notations are defined in Table 6.1.

$$\underbrace{(T_{l_2} - \alpha)}_{\substack{\text{Required delay for the} \\ \text{leading vehicle to pass} \\ \text{the TLS}}} = \underbrace{\frac{d - d_{dec_1} - h_{min_2}}{S_R}}_{\substack{\text{Required delay for the following} \\ \text{vehicle to be } h_{min_2} \text{ away from the} \\ \text{TLS, while the speed is adapted to } S_R}} \tag{6.8}$$

From Equation 6.8, S_R can be formulated as in Equation 6.9.

$$S_R = \min(\max(\frac{d - d_{dec_1} - h_{min_2}}{T_{l_2} - \alpha}, S_{Rl}), S_{max}) \tag{6.9}$$

6.2.3 Results and Discussions

Setting parameters and the system model as presented in Section 5.4, Fig. 6.4 shows the optimum and computed S_R for V_2. It is clear that the computed S_R is almost equal to the optimum one. The slight difference occurs because, in the optimization, we consider a one-decimal degree of accuracy; however, in the computed S_R, it is a four-decimal degree of accuracy. The values could be exactly the same if a one-decimal degree is considered for both optimization and computation.

As shown in Fig. 6.4, when the distance between the following (V_2) and leading (V_1) vehicles (d_{fl}) is short, both the optimum and computed S_R are close to the speed of the lead vehicle ($S_{Rl} = 51.1$ km/h). However, as d_{fl} increases, V_2 will be able to increase its speed without being affected by its leader. Eventually, the vehicle will be able to travel at the free flow speed (maximum speed limit).

Similar to Fig. 6.4, Fig. 6.5 shows that the optimum and computed S_R are almost equal, both being equal to S_{min} at $d_{fl} \leq 170$ m. This is the case when the vehicle has to stop. As d_{fl} increases, the optimum and computed S_R increase to help the vehicle pass the TLS with minimum CO_2 emissions.

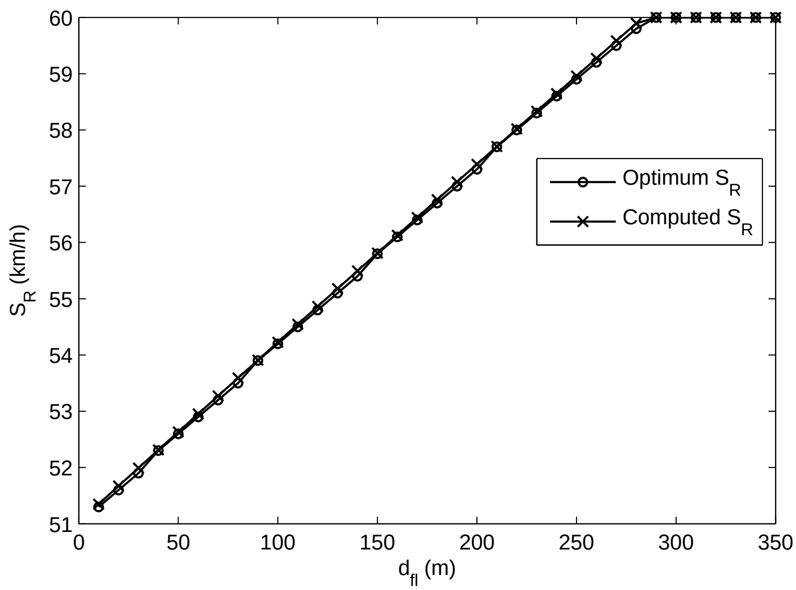

Figure 6.4: Optimum and computed S_R vs. d_{fl} if the leading vehicle does not stop at the TLS

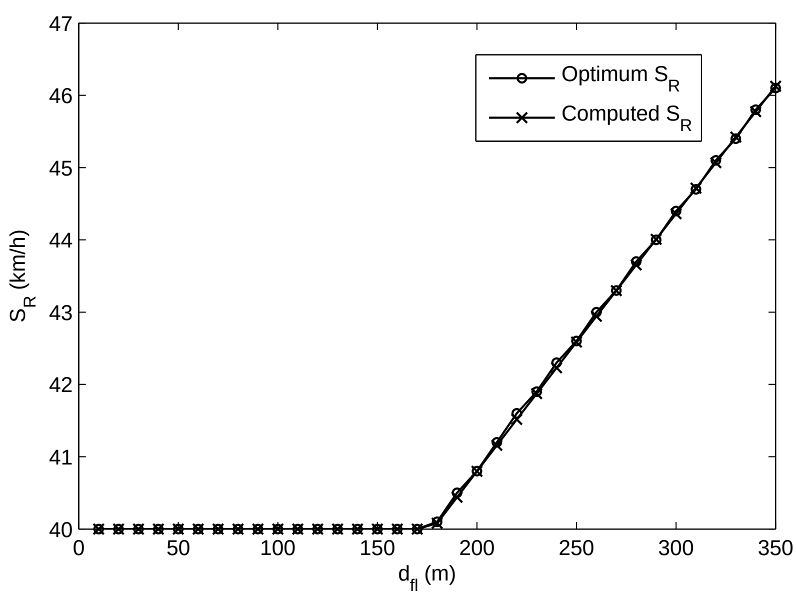

Figure 6.5: Optimum and computed S_R vs. d_{fl} if the leading vehicle will stop at the TLS

6.3 Summary

In this chapter, we have proposed heuristic expressions that can achieve the optimum or near-optimum recommended speed. This speed could lead to the maximum reduction of vehicle fuel consumption and CO_2 emission. These expressions have been proposed based on the observations of the optimization results shown in Chapter 5: (1) the optimum S_R should be the maximum possible speed that allows the vehicle to pass the traffic light signal (TLS) without stopping or decelerating; (2) if the vehicle has to stop, the result of the optimum S_R equals S_{min}; (3) the optimum S_R must equal S_{max} if the vehicle is close to the green TLS and can catch it. The analytical results showed that our proposed heuristic expressions can achieve a value that is almost equal to the optimum S_R.

Chapter 7

Performance Evaluation

While the focus of the previous two chapters was to evaluate the maximum environmental benefit from TLS2V and V2V communications for a single vehicle, this chapter presents results of a scale-up simulation study using a modeled real-world network of urban and suburban areas in the city of Waterloo, Ontario, Canada, as shown in Figure 7.1. The considered streets are as highlighted in Figures 7.2 and 7.3 for suburban and urban environments, respectively. The main street for the suburban area is Northfield Drive, and for the urban area is University Avenue. For each environment, our proposed Economical and Environmentally Friendly Geocast (EEFG) protocol has been evaluated in two traffic-volume hours based on real-data counted by the Regional Municipality of Waterloo [66]: (1) the minimum traffic volume hour of the day (off-peak hour); (2) the maximum traffic volume hour of the day (peak hour). For the signalized intersections, real signal timings, provided by the Regional Municipality of Waterloo, are used.

7.1 Suburban Environment

Suburban streets are those with low-density driveway access on the periphery of an urban area. Signalized intersections in suburban areas are not close to one another. Therefore, they are isolated (independent) intersections. This section studies the performance of the EEFG protocol for three consecutive intersections on Northfield Drive in Waterloo, as shown in Figure 7.2. These intersections are Northfield Drive and Bridge Street, Northfield Drive and University Avenue, and Northfield Drive and Sawmill Road. The lengths of the street sections have been measured using the Google Earth program [67]. Based on real-data counted by the Regional Municipality of Waterloo in 2010, 2012 and 2013, the off-peak

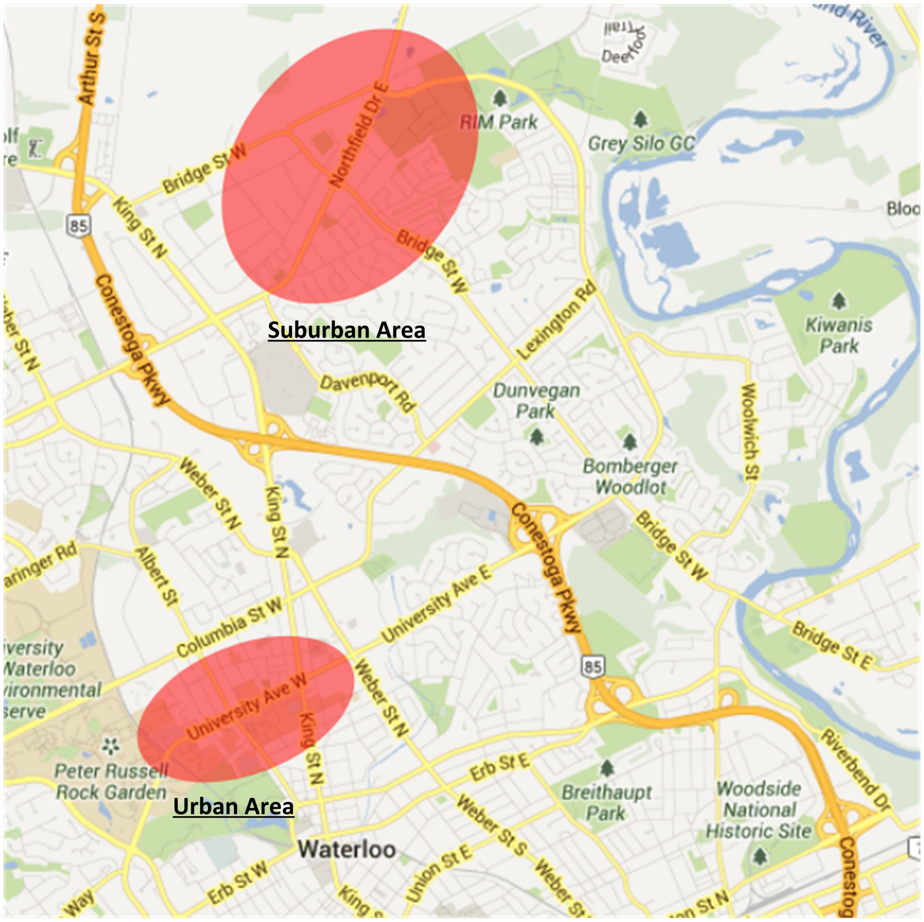

Figure 7.1: A suburban and an urban areas in the city of Waterloo, Ontario, Canada

hour of the day is from 9:30 am to 10:30 am, while the peak hour is from 4:45 pm to 5:45 pm.

7.1.1 Minimum Traffic Volume Hour (9:30 am - 10:30 am)

Vehicles enter the system as a Poisson process with a rate of λ vehicle/hour/lane from Origins (O_i) and leave from Destinations (D_i), where $i = 1, 2, ..., 8$ as shown in Figure 7.4. Table 7.1 summarizes the data of each intersection and street. Taking the intersection of Northfield and Bridge as an example, vehicles approaching the intersection toward the east are on Northfield, which has one lane, S_{max} = 60 km/h, and S_{min} = 40 km/h. In reality, S_{min} has not been specified for these streets. However, we assumed that S_{min} is

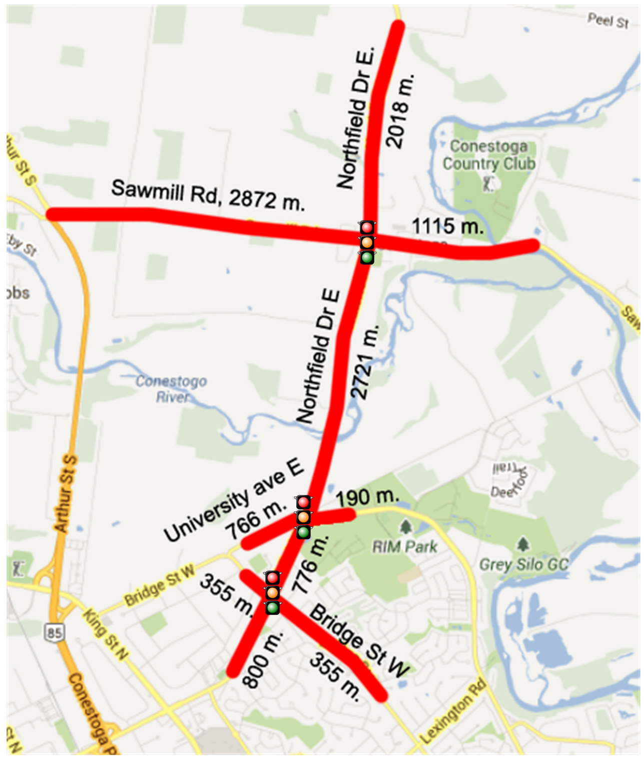

Figure 7.2: Suburban Streets: an extract of the city of Waterloo

20 km/h below S_{max}. Of those vehicles, 9% are turning left at the intersection, 41% are going through, and 50% are turning right. Most of the signals have multiple timing plans throughout the day. Signals in a suburban environment generally operate independently from one another. In reality, the signals are semi-actuated; however, we consider the maximum green phase time, and do not consider the green arrow light. Offsets are a percentage of the cycle length and relate to the beginning of the Northfield Drive green. For example, if the TLS at Northfield and Bridge switches to green at time t = 5 and the offset is 93% for the TLS at Northfield and University, the TLS at Northfield and University will switch to green at time t = 85. Table 7.2 shows the TLS phase times and offsets.

The simulation stops when 500 vehicles have arrived at destinations in ten different movement scenarios. The simulation results exclude vehicles that have not yet reached a destination when the simulation stops. The proposed EEFG protocol has been evaluated based on economical and environmentally friendly measures (vehicle fuel consumption and CO_2 emission) using the optimum and computed S_R. The protocol has been compared

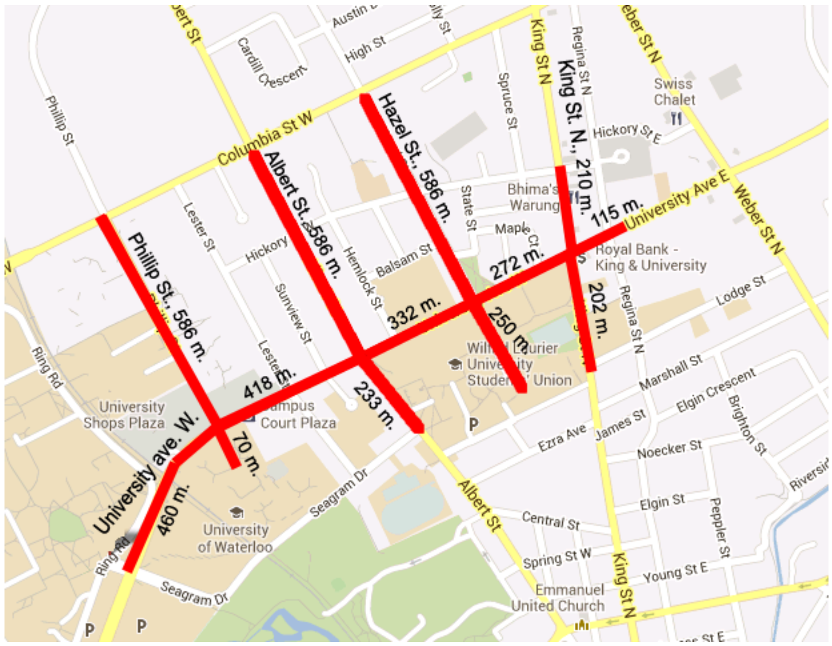

Figure 7.3: Urban Streets: an extract of the city of Waterloo

with a case where no vehicular network is applied. In this case, a vehicle enters the system at a speed that is drawn from the discrete uniform distribution on the interval $[S_{min}, S_{max}]$. Moreover, the impact of communication measures (e.g., message delay and delivery ratio) and quality of travel metrics (e.g., vehicle idling times) on the reduction of CO_2 emission and fuel consumption are presented.

The average CO_2 emission and fuel consumption from traveling vehicles have been computed with different vehicles' transmission ranges. Figure 7.5 shows the benefit of the EEFG protocol on the amount of vehicle CO_2 emission and fuel consumption. With no EEFG, these amounts are independent of the vehicles' transmission range since no communication occurs. Zero transmission range means there is no vehicle-to-vehicle communications. However, vehicles receive packets from the TLS, where the transmission range of the TLSs is 1 km. As the vehicles' transmission range increases, the vehicles receive a packet early. Also, the chance of packet delivery increases. These advantages help vehicles avoid uneconomical and environmentally unfriendly (UEU) actions. As a result, the amount of CO_2 emission and fuel consumption decreases as the vehicles' transmission range increases, as shown in Figure 7.5.

It can be noticed from Figure 7.5 that CO_2 emission and fuel consumption using the optimum S_R are equal to those using computed S_R when vehicles receive packets only

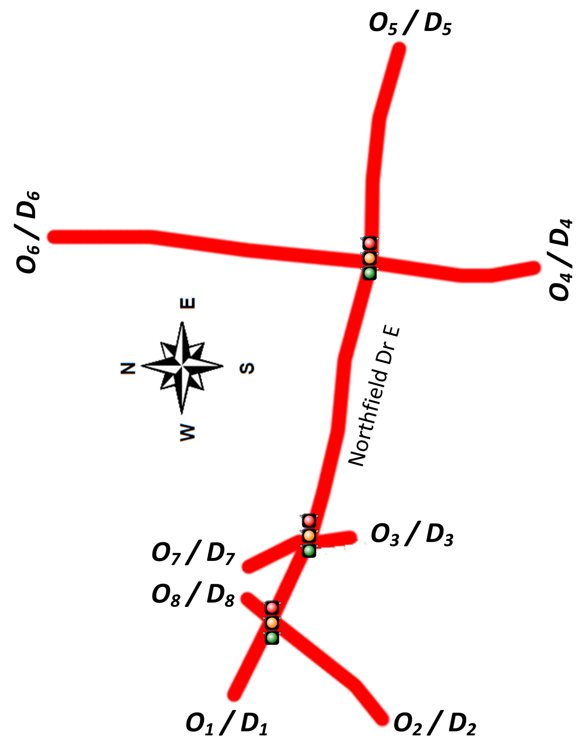

Figure 7.4: Vehicles' origins and destinations

from the TLS. However, they are slightly different when V2V communication is involved because a vehicle receiving has no leading vehicle or is not affected by its leading vehicle. In other words, Scenarios 2 and 4, as discussed in Section 5.1, do not occur. On the other hand, these scenarios could happen when a vehicle receives from its leader. In these scenarios, the computed S_R of a vehicle is equal to the recommended speed of its leader (S_{Rl}) if the vehicle is going to be affected by that leader. In this case, the vehicle decreases its speed to S_{Rl} immediately after receiving the message. In some cases, the computed S_R equals optimum S_R as we observed in Chapter 6, but not always, because of many factors, including speed-limit, current speed value, S_{Rl} value, distance between the vehicles, distance to the TLS, TLS phase times, time spent idling, and duration of deceleration. These factors are considered in the optimization model. When the transmission range increases, the CO_2 emission and fuel consumption using the optimum and computed S_R are the same because the scenarios in which a vehicle affected by its leader (Scenario 2 and 4) rarely happen.

Another way to evaluate the performance of the protocol is by presenting the average

Table 7.1: Traffic information for suburban intersections and streets (9:30 am - 10:30 am)

Northfield Dr. & Bridge St.				
	EASTBOUND (O_1)	NORTHBOUND (O_2)	SOUTHBOUND (O_8)	WESTBOUND (Not Origin)
Left turn (%)	9	56	18	7
Through (%)	41	36	59	83
Right turn (%)	50	8	23	10
λ (vph/lane)	376	284	111	–
# of lanes	1	1	1	1
S_{max} (km/h)	60	50	50	60
S_{min} (km/h)	40	30	30	40
Northfield Dr. & University Ave.				
	EASTBOUND (Not Origin)	NORTHBOUND (O_3)	SOUTHBOUND (O_7)	WESTBOUND (Not Origin)
Left turn (%)	1	49	35	17
Through (%)	52	20	46	76
Right turn (%)	47	31	19	7
λ (vph/lane)	–	85	37	–
# of lanes	1	2	1	1
S_{max} (km/h)	60	50	50	60
S_{min} (km/h)	40	30	30	40
Northfield Dr. & Sawmill Rd.				
	EASTBOUND (Not Origin)	NORTHBOUND (O_4)	SOUTHBOUND (O_6)	WESTBOUND (O_5)
Left turn (%)	16	11	9	61
Through (%)	59	49	75	34
Right turn (%)	25	40	16	5
λ (vph/lane)	–	197	212	259
# of lanes	1	1	1	1
S_{max} (km/h)	80	50	80	80
S_{min} (km/h)	60	30	60	60

vehicle saving in CO_2 emission and fuel consumption. Figure 7.6 shows the average CO_2 and fuel saving per vehicle versus vehicles' transmission range. The savings using the optimum S_R and computed S_R are equal if only TLS2V communication and large transmission ranges are considered. Otherwise, the savings using the optimum S_R are more than those using the computed S_R.

Figure 7.7 shows how the EEFG protocol can decrease the time vehicles must idle. It is clear that in the absence of a vehicular network, the average vehicle's idling time is around 11 seconds. This time would be shortened if the idea of vehicular networks is applied. With the EEFG protocol, increasing the transmission range can decrease vehicular idling time to a minimum of 3.5 seconds.

The average vehicle idling times with EEFG using optimum S_R are almost equal to those with EEFG using the computed S_R. Thus, if the stop-and-go conditions of a vehicle can be avoided using the optimization model to obtain S_R, it is going to be avoided as well using the heuristic expressions.

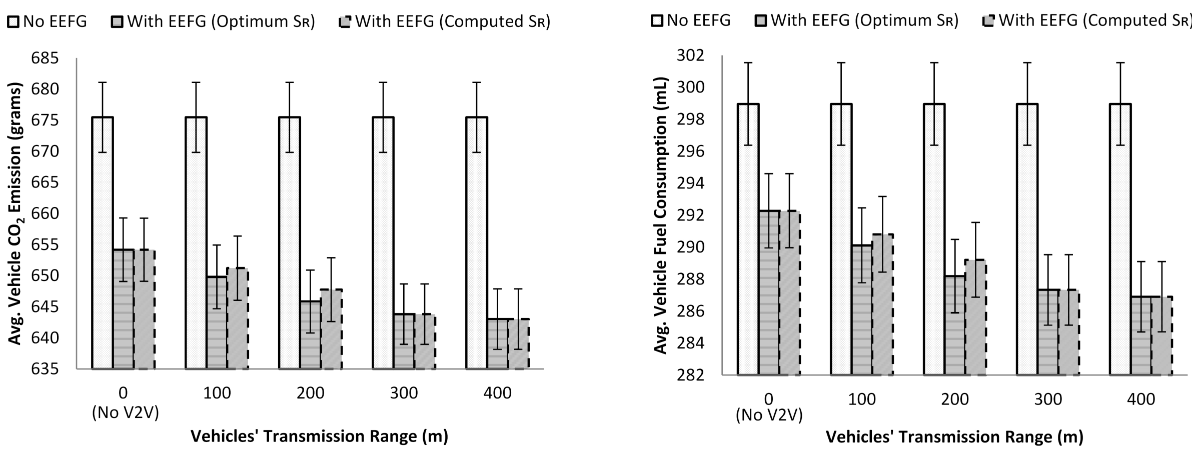

Figure 7.5: Average vehicle CO_2 emission and fuel consumption versus vehicles' transmission range in the suburban environment (9:30 am - 10:30 am)

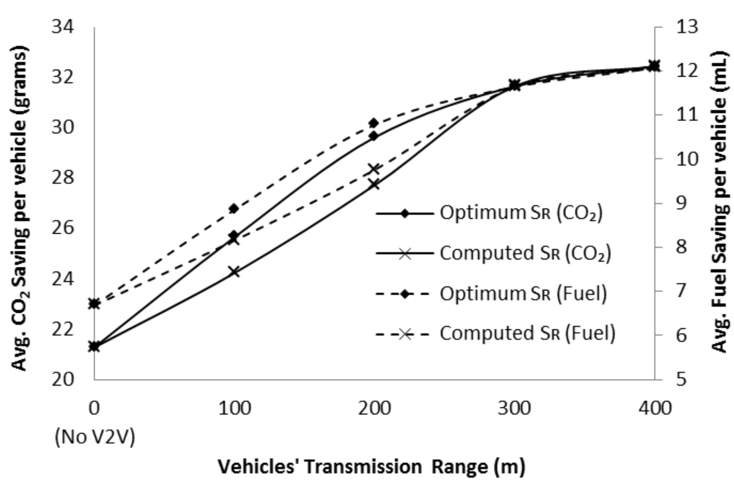

Figure 7.6: Average vehicle saving in CO_2 emission and fuel consumption versus vehicles' transmission range in the suburban environment (9:30 am - 10:30 am)

Table 7.2: Signal timing for suburban intersections (9:30 am -10:30 am)

Northfield Dr. & Bridge St.				
	Green (sec)	Yellow (sec)	Red (sec)	Offset (%)
Northfield Drive	35	4	33	–
Bridge Street	29	4	39	–
Northfield Dr. & University Ave.				
	Green (sec)	Yellow (sec)	Red (sec)	Offset (%)
Northfield Drive	48	4	34	93
University Avenue	30	4	52	–
Northfield Dr. & Sawmill Rd.				
	Green (sec)	Yellow (sec)	Red (sec)	Offset (%)
Northfield Drive	26	4	34	0
Sawmill Road	30	4	30	–

For each destination node, packet delay (D) is defined as the difference between the time of receiving the packet and the time of initiating the packet from the TLS. This work considers only buffering delay, since transmission, processing, and propagation delays are small values that do not impact the results. Also, we assume ideal MAC and PHY layers. It is clear that increasing the vehicles' transmission range helps reduce packet delay. In fact, fast packet delivery enables earlier vehicle actions, thereby achieving greater CO_2-emission and fuel-consumption reductions. Figure 7.8 shows the relationship between the average packet delay of all traveling vehicles and the transmission range. It can be noticed from Figures 7.5 and 7.8 that the amount of CO_2 emission and fuel consumption are directly proportional to packet delay as shown in Figure 7.9. A minimum average delay of around 6 seconds has to exist even if we have large transmission ranges because a vehicle does not send the received packet until it adjusts its speed to the recommended one. During the adjustment period, the packet will be buffered. This delay increases with an increased number of hops. For example, a vehicle receiving from a TLS takes 3 seconds to adjust its speed to S_R and send the packet to its following vehicle, which might itself need 2 seconds to adjust its speed to its S_R and send its packet. As a result, the total buffering delay for the following vehicle is 5 seconds. On the other hand, it is 3 seconds for the leading vehicle.

Figure 7.10 demonstrates the average ratio of cars that were supposed to receive a packet but did not due to the short vehicle transmission range. When the transmission

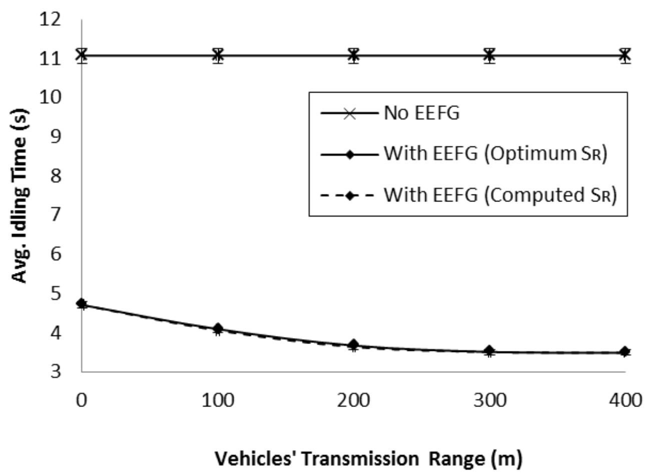

Figure 7.7: Average vehicle stops delay versus vehicles' transmission range

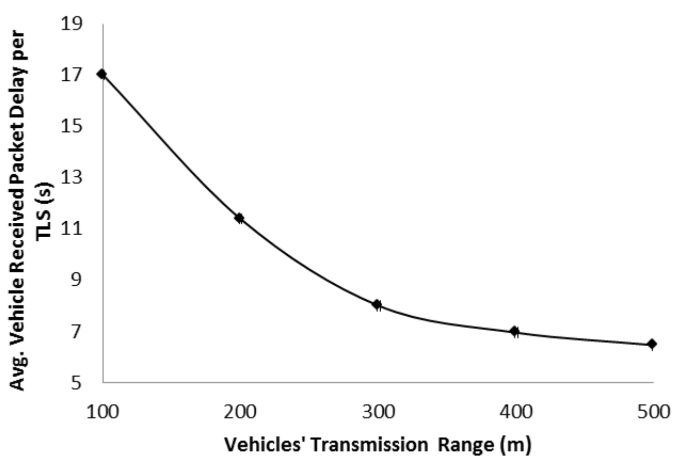

Figure 7.8: Average vehicle received packet delay versus vehicles' transmission range

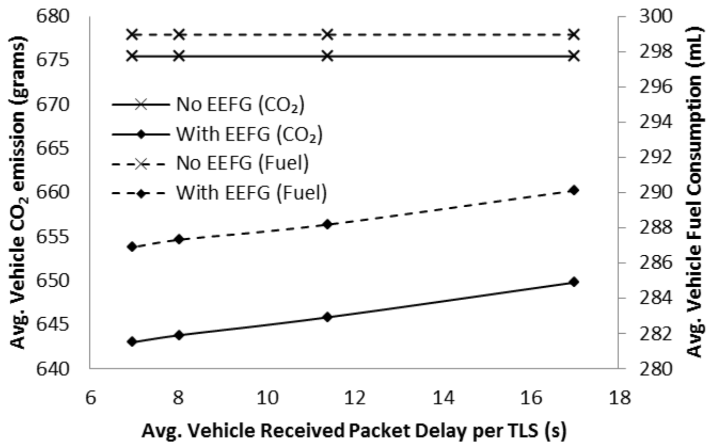

Figure 7.9: Average vehicle CO_2 emission and fuel consumption versus average received packet delay

range (T_x) equals zero, there is only communication from the TLS to vehicles. Therefore, around 40% of the vehicles received a packet although T_x=0. Similar to packet delay, this ratio is directly proportional to the amount of CO_2 emission and fuel consumption, as shown in Figure 7.11. Therefore, it is desirable to design a geocast protocol that has a short packet delay and high packet delivery ratio for the reduction of CO_2 and fuel consumption.

7.1.2 Maximum Traffic Volume Hour (4:45 pm - 5:45 pm)

This subsection evaluates the EEFG protocol during the peak hour. The traffic information of the intersections and streets are summarized in Table 7.3. In addition, Table 7.4 shows the phase times and offsets of each TLS. Assumptions and simulation settings are as in Subsection 7.1.1.

Similar to the results obtained in Subsection 7.1.1, vehicles can save fuel and reduce emissions using the EEFG protocol. As shown in Figure 7.12, the CO_2 emission and fuel consumption decrease with a vehicle's increasing transmission range. Unlike the results in Subsection 7.1.1, the CO_2 emission and fuel consumption using the optimum and computed S_R are not equal when the transmission range increases. At the peak hour, increasing transmission range might not have a significant effect on CO_2 and fuel since the distance

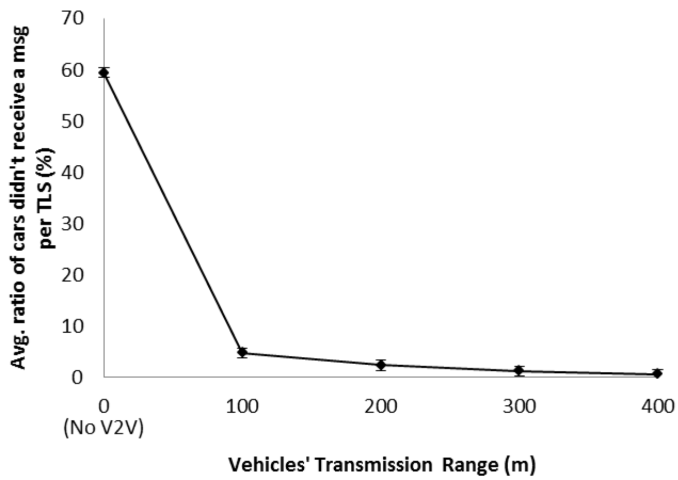

Figure 7.10: Average ratio of cars unable to receive a packet per TLS

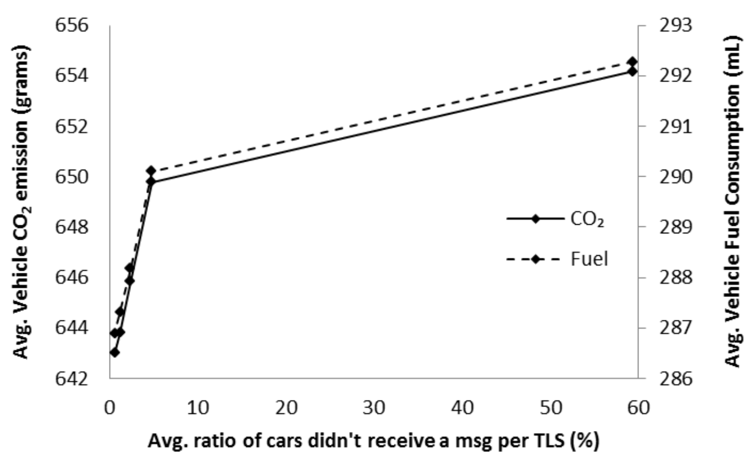

Figure 7.11: Average CO_2 emission and fuel consumption vs. ratio of cars not able to receive a packet per TLS

Table 7.3: Traffic information for suburban intersections and streets (4:45 pm -5:45 pm)

Northfield Dr. & Bridge St.				
	EASTBOUND (O_1)	NORTHBOUND (O_2)	SOUTHBOUND (O_8)	WESTBOUND (Not Origin)
Left turn (%)	2	63	17	8
Through (%)	50	28	68	87
Right turn (%)	48	9	15	5
λ (vph/lane)	1045	529	474	–
# of lanes	1	1	1	1
Northfield Dr. & University Ave.				
	EASTBOUND (Not Origin)	NORTHBOUND (O_3)	SOUTHBOUND (O_7)	WESTBOUND (Not Origin)
Left turn (%)	0	46	72	22
Through (%)	78	21	25	70
Right turn (%)	22	33	3	3
λ (vph/lane)	–	229	216	–
# of lanes	1	2	1	1
Northfield Dr. & Sawmill Rd.				
	EASTBOUND (Not Origin)	NORTHBOUND (O_4)	SOUTHBOUND (O_6)	WESTBOUND (O_5)
Left turn (%)	17	8	12	50
Through (%)	65	40	69	47
Right turn (%)	18	52	19	3
λ (vph/lane)	–	861	264	328
# of lanes	1	1	1	1

between the sender and receiver might already be less than the transmission range. Therefore, scenarios in which a vehicle is affected by its leader (Scenario 2 and 4) can happen even though the transmission range is large. As a result, the CO_2 emission and fuel consumption using the optimum and computed S_R differ even with a large transmission range.

Figure 7.13 shows the average saving of CO_2 and fuel using the EEFG protocol with different transmission ranges. As the transmission range increases, the vehicles receive a packet early. Also, the chance of packet delivery increases. As a result, the saving of CO_2 emission and fuel consumption increases as the vehicles' transmission range increases.

7.2 Urban Environment

Urban streets are those with a relatively high density of driveway access, and located in an urban area. Signalized intersections in urban areas are close to one another. Therefore, they might be coordinated (dependent) intersections. This section studies the performance of the EEFG protocol for four consecutive intersections (Figure 7.3) on University Avenue in Waterloo, Canada: University Avenue and Phillip Street, University Avenue and Albert

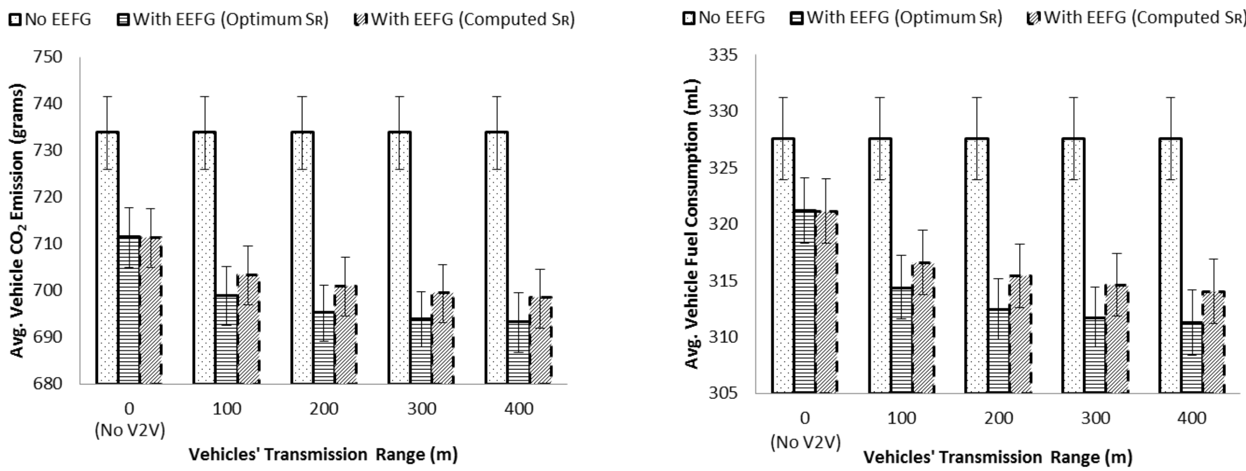

Figure 7.12: Average vehicle CO_2 emission and fuel consumption versus vehicles' transmission range in suburban environment (4:45 pm - 5:45 pm)

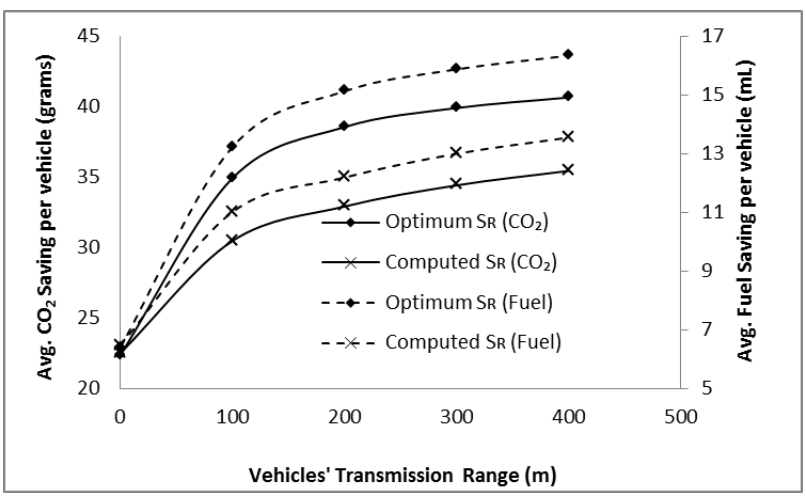

Figure 7.13: Average vehicle saving in CO_2 emission and fuel consumption versus vehicles' transmission range in suburban environment (4:45 pm - 5:45 pm)

Table 7.4: Signal timing for suburban intersections (4:45 pm -5:45 pm)

Northfield Dr. & Bridge St.				
	Green (sec)	Yellow (sec)	Red (sec)	Offset (%)
Northfield Drive	31	4	37	–
Bridge Street	33	4	35	–
Northfield Dr. & University Ave.				
	Green (sec)	Yellow (sec)	Red (sec)	Offset (%)
Northfield Drive	56	4	36	74
University Avenue	32	4	60	–
Northfield Dr. & Sawmill Rd.				
	Green (sec)	Yellow (sec)	Red (sec)	Offset (%)
Northfield Drive	29	4	30	0
Sawmill Road	26	4	33	–

Street, University Avenue and Hazel Street, and University Avenue and King Street. The lengths of the street sections have been measured using the Google Earth program [67]. Based on real-data counted by the Regional Municipality of Waterloo in 2010 and 2012, the off-peak hour of the day is from 9:30 am to 10:30 am, while the peak hour is from 4:45 pm to 5:45 pm.

7.2.1 Minimum Traffic Volume Hour (9:30 am - 10:30 am)

Vehicles enter the system as a Poisson process with a rate of λ vehicle/hour/lane from Origins (O_i) and leave from Destinations (D_i), where $i = 1, 2, ..., 10$ as shown in Figure 7.14. Table 7.5 summarizes the data of each intersection and street. Most of the signals have multiple timing plans throughout the day. Signals in an urban environment are generally coordinated. In reality, the signals are semi-actuated; however, we consider the maximum green phase time, and do not consider the green arrow light. Offsets are a percentage of the cycle length and relate to the beginning of the University Avenue green. Table 7.5 shows the TLS phase times and offsets.

As shown in Figure 7.15, CO_2 emission and fuel consumption can be reduced by using the EEFG protocol in urban streets. The amount of CO_2 emission and fuel consumption decrease as vehicles' transmission range increases. Because the TLSs are relatively close to one another, the amount of CO_2 emission and fuel consumption start to reach a constant

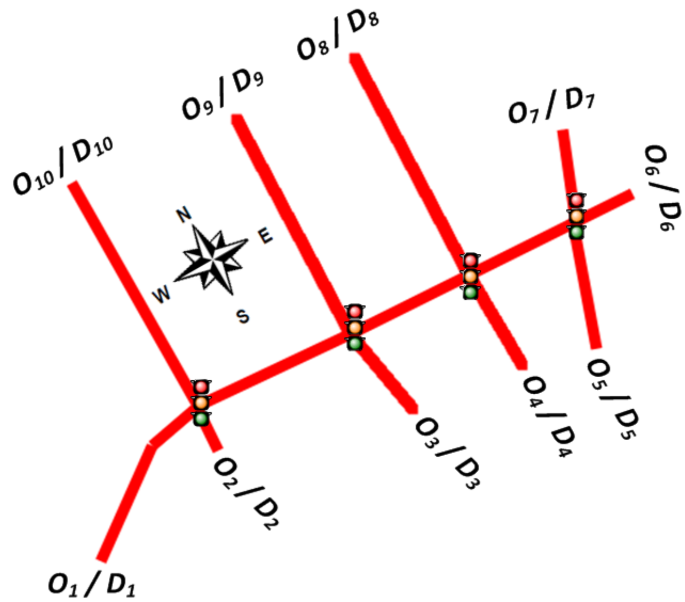

Figure 7.14: Vehicles' origins and destinations

state after 200 m transmission range, indicating that the network becomes connected all the time when the range is greater than or equal 200 m.

As discussed in the previous results, CO_2 emission and fuel consumption using the optimum S_R are equal to those using computed S_R when vehicles receive only from the TLS. However, they are slightly different when V2V communication is involved because the scenarios where a vehicle is affected by its leader (Scenario 2 and 4) are most likely to happen in the urban streets even at the off-peak hour since the distances between intersections are not great. Figure 7.16 shows the average saving of CO_2 emission and fuel consumption when using the EEFG protocol for the optimum and computed S_R.

7.2.2 Maximum Traffic Volume Hour (4:45 pm - 5:45 pm)

This subsection evaluates the EEFG protocol during the peak hour in the urban area. The traffic information for the intersections and streets is summarized in Table 7.7. In addition, Table 7.8 shows the phase times and offsets of each TLS. Assumptions and simulation settings are as in Subsection 7.2.1.

In the urban areas, using the EEFG protocol can save fuel and reduce emissions at the peak hour as shown in Figure 7.17. Increasing the transmission range helps to reduce

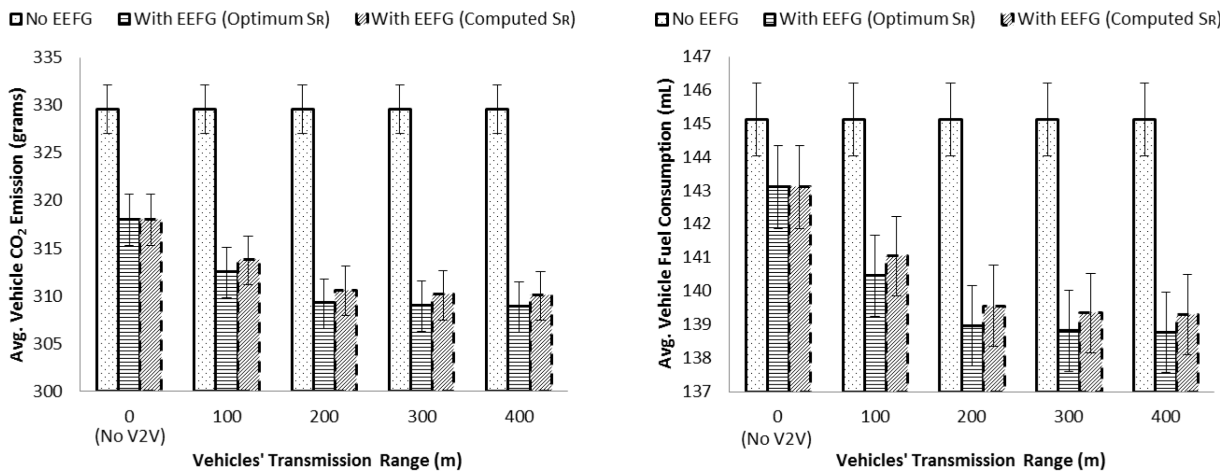

Figure 7.15: Average vehicle CO_2 emission and fuel consumption versus vehicles' transmission range in urban environment (9:30 am - 10:30 am)

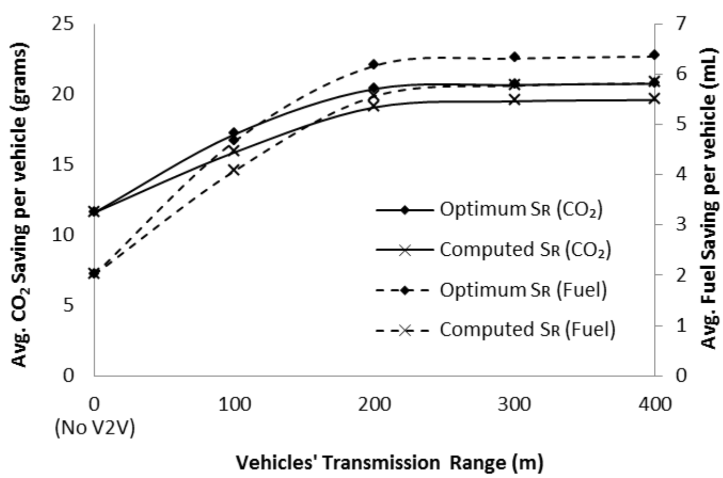

Figure 7.16: Average vehicle saving in CO_2 emission and fuel consumption versus vehicles' transmission range in urban environment (9:30 am - 10:30 am)

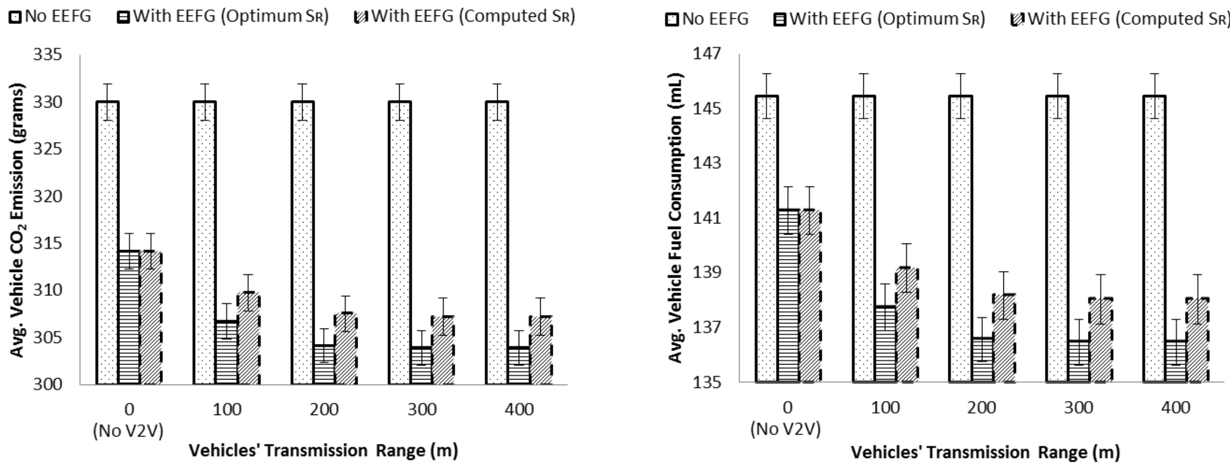

Figure 7.17: Average vehicle CO_2 emission and fuel consumption versus vehicles' transmission range in urban environment (4:45 pm - 5:45 pm)

fuel and emissions. Similar to the results obtained in Subsections 7.1.1, 7.1.2, and 7.2.1, the optimum S_R equals the computed S_R if the V2V communication is not involved. On the other hand, a difference in the optimum and computed S_R could happen if a vehicle received from its leader and was affected by it. Figure 7.18 shows the possible average saving per vehicle.

7.3 Interpretation of Results

Based on the traffic information presented in Tables 7.1 and 7.3, the total average number of vehicles that enter the suburban road network is 1546 vehicles at the off-peak hour and 4175 vehicles at the peak hour. Considering 400 m transmission range, the average CO_2 reduction is 32.5 g/vehicle at the off-peak hour and 40.7 g/vehicle at the peak hour as shown in Figures 7.6 and 7.13. Therefore, the total average CO_2 emission from the vehicles is 50.2 kg/hr at the off-peak hour and 169.72 kg/hr at the peak hour. Applying EEFG only at the off-peak and peak hours in one year, the average CO_2 reduction that can be achieved is 73.9 Mg.

For the urban environment, the average number of vehicles that enter the road network is 2878 vehicles at the off-peak hour and 7105 vehicles at the peak hour, as can be observed from Tables 7.5 and 7.7. At 400 m transmission range, the average CO_2 reduction at the

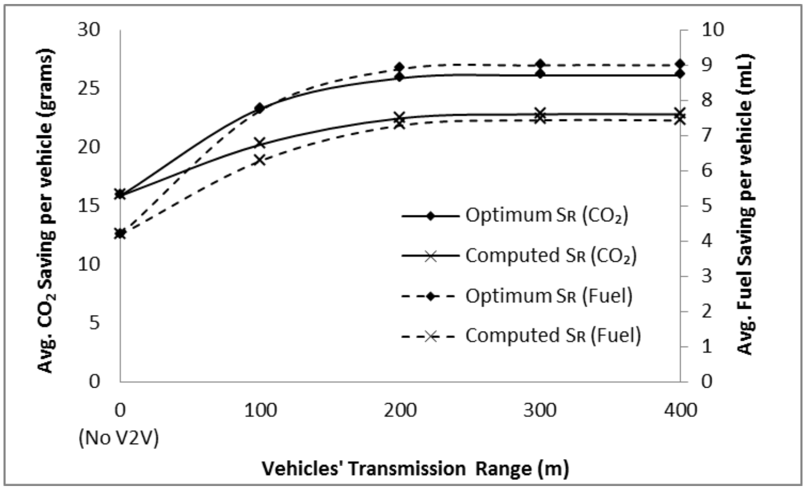

Figure 7.18: Average vehicle saving in CO_2 emission and fuel consumption versus vehicles' transmission range in urban environment (4:45 pm - 5:45 pm)

off-peak hour is 20.75 g/vehicle, and it is 26.2 g/vehicle at the peak hour. As a result, the CO_2 emitted from the vehicles is 59.9 kg/hr and 186.2 kg/hr at the off-peak hour and peak hour, respectively. Considering EEFG applied only at the off-peak and peak hours, the average CO_2 emission that can be reduced in a year is 82.8 Mg.

7.4 Summary

Four case studies have been considered in this chapter to evaluate the EEFG protocol: (1) a suburban environment at the maximum traffic volume hour of the day; (2) a suburban environment at the minimum traffic volume hour of the day; (3) an urban environment at the maximum traffic volume hour of the day; (4) an urban environment at the minimum traffic volume hour of the day. Comparing results with and without using the EEFG protocol, reduced vehicle CO_2 emission, fuel consumption, idling time can be achieved with EEFG. In the first case as an example, we demonstrate that the packet delay and packet delivery success ratio have an impact on vehicle CO_2 emission and fuel consumption.

In the case of TLS2V communication, the optimization and heuristic expressions give the same S_R results. However, the results might differ if V2V communication is involved. Based on the results obtained in this chapter, EEFG can save fuel and reduce CO_2 emission in all four cases.

Table 7.5: Traffic information for urban intersections and streets (9:30 am-10:30 am)

	University Ave. & Phillip St.			
	EASTBOUND (O_1)	NORTHBOUND (O_2)	SOUTHBOUND (O_{10})	WESTBOUND (Not Origin)
Left turn (%)	30	50	60	1
Through (%)	68	25	7	70
Right turn (%)	2	25	33	29
λ (vph/lane)	268	8	170	–
# of lanes	2	1	1	2
S_{max} (km/h)	50	50	50	50
S_{min} (km/h)	30	30	30	30
	University Ave. & Albert St.			
	EASTBOUND (Not Origin)	NORTHBOUND (O_3)	SOUTHBOUND (O_9)	WESTBOUND (Not Origin)
Left turn (%)	5	16	15	7
Through (%)	88	72	77	85
Right turn (%)	7	12	8	8
λ (vph/lane)	–	350	228	–
# of lanes	2	1	1	2
S_{max} (km/h)	50	50	50	50
S_{min} (km/h)	30	30	30	30
	University Ave. & Hazel St.			
	EASTBOUND (Not Origin)	NORTHBOUND (O_4)	SOUTHBOUND (O_8)	WESTBOUND (Not Origin)
Left turn (%)	4	38	43	6
Through (%)	88	14	15	90
Right turn (%)	8	48	42	4
λ (vph/lane)	–	52	72	–
# of lanes	2	1	1	2
S_{max} (km/h)	50	50	50	50
S_{min} (km/h)	30	30	30	30
	University Ave. & King St.			
	EASTBOUND (Not Origin)	NORTHBOUND (O_5)	SOUTHBOUND (O_7)	WESTBOUND (O_6)
Left turn (%)	23	16	17	14
Through (%)	70	67	67	75
Right turn (%)	7	17	16	11
λ (vph/lane)	–	209	198	324
# of lanes	2	2	2	2
S_{max} (km/h)	50	50	50	50
S_{min} (km/h)	30	30	30	30

Table 7.6: Signal timing for urban intersections (9:30 am -10:30 am)

University Ave. & Phillip St.				
	Green (sec)	Yellow (sec)	Red (sec)	Offset (%)
University Avenue	33	4	11	–
Phillip Street	7	4	37	–
University Ave. & Albert St.				
	Green (sec)	Yellow (sec)	Red (sec)	Offset (%)
University Avenue	37	4	33	23
Albert Street	29	4	41	–
University Ave. & Hazel St.				
	Green (sec)	Yellow (sec)	Red (sec)	Offset (%)
University Avenue	55	4	37	66
Hazel Street	33	4	59	–
University Ave. & King St.				
	Green (sec)	Yellow (sec)	Red (sec)	Offset (%)
University Avenue	31	4	31	77
King Street	27	4	35	–

Table 7.7: Traffic information for urban intersections and streets (4:45 pm -5:45 pm)

University Ave. & Phillip St.				
	EASTBOUND (O_1)	NORTHBOUND (O_2)	SOUTHBOUND (O_{10})	WESTBOUND (Not Origin)
Left turn (%)	16	36	71	1
Through (%)	83	14	1	87
Right turn (%)	1	50	28	12
λ (vph/lane)	320	36	549	–
# of lanes	2	1	1	2
University Ave. & Albert St.				
	EASTBOUND (Not Origin)	NORTHBOUND (O_3)	SOUTHBOUND (O_9)	WESTBOUND (Not Origin)
Left turn (%)	6	13	12	9
Through (%)	85	70	82	86
Right turn (%)	9	17	6	5
λ (vph/lane)	–	837	688	–
# of lanes	2	1	1	2
University Ave. & Hazel St.				
	EASTBOUND (Not Origin)	NORTHBOUND (O_4)	SOUTHBOUND (O_8)	WESTBOUND (Not Origin)
Left turn (%)	4	38	53	5
Through (%)	91	17	15	90
Right turn (%)	5	45	32	5
λ (vph/lane)	–	837	688	–
# of lanes	2	1	1	2
University Ave. & King St.				
	EASTBOUND (Not Origin)	NORTHBOUND (O_5)	SOUTHBOUND (O_7)	WESTBOUND (O_6)
Left turn (%)	14	14	19	11
Through (%)	80	77	68	79
Right turn (%)	6	9	13	10
λ (vph/lane)	–	427	446	542
# of lanes	2	2	2	2

Table 7.8: Signal timing for urban intersections (4:45 pm - 5:45 pm)

University Ave. & Phillip St.				
	Green (sec)	Yellow (sec)	Red (sec)	Offset (%)
University Avenue	49	4	11	–
Phillip Street	7	4	53	–

University Ave. & Albert St.				
	Green (sec)	Yellow (sec)	Red (sec)	Offset (%)
University Avenue	43	4	37	14
Albert Street	33	4	47	–

University Ave. & Hazel St.				
	Green (sec)	Yellow (sec)	Red (sec)	Offset (%)
University Avenue	64	4	38	90
Hazel Street	34	4	68	–

University Ave. & King St.				
	Green (sec)	Yellow (sec)	Red (sec)	Offset (%)
University Avenue	38	4	34	2
King Street	30	4	42	–

Chapter 8

Conclusions and Future Work

8.1 Summary and Conclusions

This work was motivated by the fact that applying vehicular networks in transportation systems can play a key role in reducing vehicle fuel consumption and emissions. Most applications in vehicular networks aim to reduce the number of fatalities on roads and to comfort drivers and their passengers. However, this thesis focuses on applications that can save the environment and money. With a focus on the network layer, most previous routing protocols in vehicular networks focus on improving the network-centric performance measures (e.g., message delay, packet delivery ratio, etc.) instead of focusing on improving the performance measures (e.g., fuel consumption and CO_2 emissions) that are meaningful to both the scientific community and the general public.

This work is multidisciplinary. It gathers together three different areas: (1) vehicular communication networks; (2) traffic engineering; (3) environmental engineering. Chapter 2 reviews the background and provides a literature survey of these areas. Vehicular networks are responsible for delivering useful packet information for energy saving. Based on the sent information, the movement of vehicles is changed. In response to vehicles' speeds and accelerations, the green performance measures can be determined.

The integration of the aforementioned areas is required in this work. Chapter 3 describes the system model, including its communication model, traffic model, mobility model, and performance measures. The thesis focuses on reducing uneconomical and environmentally unfriendly (UEU) actions that occur as vehicles approach a traffic light signal (TLS). Theses actions are stop-and-go conditions, unnecessary high acceleration, and unnecessary excessive speed.

The main goal of this thesis is to develop a new protocol, called Economical and Environmentally Friendly Geocast (EEFG), which can achieve the maximum reduction of CO_2 emission and fuel consumption from vehicles approaching a TLS. The EEFG protocol aims to deliver useful information to vehicles inside the region of interest (ROI) as explained in Chapter 4. Based on that information, the vehicle receiving the information controls its speed at a recommended speed (S_R), which helps the vehicle to reduce the UEU actions.

Two methods are proposed for determining the value of S_R: (1) using an optimization model as proposed in Chapter 5; (2) using heuristic expressions as proposed in Chapter 6. The objective function of the optimization is to minimize vehicle fuel consumption and emissions. This model is applicable in both traffic light signal-to-vehicle (TLS2V) and vehicle-to-vehicle communications. The heuristic expressions are also proposed in both TLS2V and V2V communications. They are developed based on the observations drawn from Chapter 5's results.These expressions can compute the optimum or near-optimum S_R.

Performance studies of the EEFG protocol have been presented in Chapter 7. Four case studies have been taken into account: (1) a suburban environment at the maximum traffic volume hour of the day; (2) a suburban environment at the minimum traffic volume hour of the day; (3) an urban environment at the maximum traffic volume hour of the day; (4) an urban environment at the minimum traffic volume hour of the day. These studies show the benefits of using EEFG: reduced vehicle CO_2 emission, fuel consumption, and idling time. Considering the first case stud as an example, the results demonstrate that the packet delay and packet delivery success ratio have an impact on vehicle CO_2 emissions and fuel consumption. In case of TLS2V, the optimization and heuristic expressions achieve the same S_R results. However, the results might differ if V2V communication is involved. As shown in the results, EEFG can save fuel and reduce CO_2 emissions in all four cases.

8.2 Future Research Work

This work can be extended in several directions, such as:

- **Considering different types of vehicles**

Vehicles manufacturers such as Honda, Toyota, and Nissan [68][69][70] have produced vehicles with either hybrid technology, in which a gasoline engine is considered the main source of power while providing an auxiliary electric motor that provides additional power, or fully electric vehicles (FEVs). In our work, the focus has been only on vehicles running on fossil fuels with the objective of reducing their fuel consumption and emissions. As a future work, the energy savings for electric or hybrid vehicles that arise using our model can be investigated.

- **Integrating the optimization of traffic light phases**

Research on using vehicular networks at signalized intersections to achieve minimum vehicle fuel consumption and emissions can be classified into two types: (1) controlling a TLS's phases based on information transmitted from approaching vehicles to the TLS [41]. The goal is to determine the optimum values of the TLS's phases; (2) controlling vehicles based on information transmitted from the TLS ahead. As proposed in this thesis, the goal is to optimize the vehicles' speed. It would be an important but challenging contribution if the two aforementioned types can be integrated or combined.

- **Trip-based optimization**

The proposed optimization model works for each individual TLS independently. For a vehicle approaching a TLS as an example, the objective is to determine the minimum fuel cost and emissions of the vehicle at the current TLS regardless of the vehicle trip. We do not guarantee that our model will achieve minimum fuel cost and emissions for the whole trip. Further research could be undertaken based on a more holistic perspective that considers a whole trip.

- **Drivers' behavior and recommended lane**

The thesis assumes the best case scenario, where the vehicle is in full control or that the driver follows the instructions precisely. In [71], we studied the performance of EEFG considering a different penetration rate (α), which is the percentage of vehicles that are equipped with communication devices. EEFG can save fuel and CO_2 emission even with low α. However, more studies are needed to enhance our model by considering driving behavior. For example, a dynamic suggestion could be provided based on driver behavior. For more reduction of emissions and fuel consumption, the EEFG protocol can be enhanced by providing vehicles with information about the best lane to travel in.

References

[1] R. Baldessari et al. *Car to Car Communication Consortium-manifesto: overview of the C2C-CC system.* version 1.1, 2007.

[2] H. Moustafa and Y. Zhang. *Vehicular networks: techniques, standards, and applications.* Auerbach Publications, 2009.

[3] F. Li and Y. Wang. Routing in vehicular ad hoc networks: a survey. *IEEE VT Magazine*, 2(2):12–22, 2007.

[4] Q. Yu and G. Heijenk. Abiding geocast for warning message dissemination in vehicular ad hoc networks. *IEEE International Conference on Communications Workshops (ICC)*, pages 400–404, 2008.

[5] C. Maihöfer, T. Leinmüller, and E. Schoch. Abiding geocast: time–stable geocast for ad hoc networks. *Proceedings of the 2nd ACM international workshop on Vehicular ad hoc networks*, pages 20–29, 2005.

[6] C. Maihöfer and R. Eberhardt. Time-stable geocast for ad hoc networks and its application with virtual warning signs. *Computer Communications*, 27(11):1065–1075, 2004.

[7] S.D. Hermann, C. Michl, and A. Wolisz. Time-Stable Geocast in Intermittently Connected IEEE 802.11 MANETs. *Proceeding of IEEE 66th Vehicular Technology Conference*, pages 1922–1926, 2007.

[8] H. Rahbar. Dynamic Time-stable Geocast Routing in Vehicular Ad Hoc Networks. *A thesis Presented to the University of Waterloo, Department of Electrical and Computer Engineering, Waterloo, Ontario, Canada*, 2009.

[9] C. Maihöfer. A Survey of Geocast Routing Protocols. *IEEE Communications Surveys and Tutorials*, 6(2):32–42, 2004.

[10] E. C. Wiebe. Gasoline Prices in Parts of Canada between 1998 and 2012. http://climate.uvic.ca/people/ewiebe/car/fuel_price.html.

[11] M. Ferreira and P.M. d'Orey. On the impact of virtual traffic lights on carbon emissions mitigation. *IEEE Transactions onIntelligent Transportation Systems*, 13(1):284–295, 2012.

[12] Organization for Economic Co-operation and Development (OECD)/ International Energy Agency (IEA), *CO_2 Emissions from Fuel Combustion Highlights*, 2009.

[13] B. Karp and H.T. Kung. GPSR: greedy perimeter stateless routing for wireless networks. In *Proceedings of the 6^{th} annual international conference on Mobile computing and networking*, pages 243–254, 2000.

[14] L. Briesemeister, L. Schafers, and G. Hommel. Disseminating messages among highly mobile hosts based on inter-vehicle communication. In *Intelligent Vehicle Symposium*, pages 522–527. IEEE, 2000.

[15] Y. B. Ko and N. H. Vaidya. Location-Aided Routing (LAR) in mobile ad hoc networks. *Wireless Networks*, 6(4):307–321, 2000.

[16] M. T. Moreno. *Inter-Vehicle Communications: Achieving Safety in a Distributed Wireless Environment: Challenges, Systems and Protocols.* Dissertation, Universittsverlag Karlsruhe, 2007.

[17] C. Maihofer and R. Eberhardt. Geocast in vehicular environments: caching and transmission range control for improved efficiency. In *Intelligent Vehicles Symposium*, pages 951–956. IEEE, 2004.

[18] M. Alsabaan, K. Naik, and A. Nayak. Applying vehicular ad hoc networks for reduced vehicle fuel consumption. *Recent Trends in Wireless and Mobile Networks*, pages 217–228, 2010.

[19] M. Alsabaan, K. Naik, T. Khalifa, and A. Nayak. Vehicular networks for reduction of fuel consumption and CO_2 emission. In *Industrial Informatics (INDIN), 8^{th} IEEE Int. Conf. on*, pages 671–676, 2010.

[20] Environmental Protection Agency: User's Guide to Mobile 6, Mobile Source Emission Factor Model. Ann Arbor, Michigan, 2002.

[21] California Air Resources Board: User's Guide to EMFAC, Calculating emission inventories for vehicles in California, 2007.

[22] M. Barth, F. An, T. Younglove, G. Scora, C. Levine, M. Ross, and T. Wenzel. Comprehensive modal emission model (CMEM) version 2.0 user's guide. Riverside, California. 2000.

[23] K. Ahn and H. Rakha. Field evaluation of energy and environmental impacts of driver route choice decisions. In *Intelligent Transportation Systems Conference, IEEE*, pages 730–735, 2007.

[24] UK Department for Environment, Food & Rural Affairs: Cold Start Advanced-user guide. iss. 1, 2008.

[25] M. Van Aerde and Ltd. Associates. INTEGRATION release 2.30 for Windows: Users Guide: Fundamental Model Features. I & II, 2005.

[26] K. Ahn, H. Rakha, A. Trani, and M. Van Aerde. Estimating vehicle fuel consumption and emissions based on instantaneous speed and acceleration levels. *Journal of Transportation Engineering*, 2(128):182–190, 2002.

[27] W. Alasmary and W. Zhuang. Mobility impact in IEEE 802.11 p infrastructureless vehicular networks. *Ad Hoc Networks*, 10(2):222–230, 2012.

[28] W. Alasmary and O. Basir. Achieving Efficiency and Fairness in 802.11-based vehicle-to-infrastructure Communications. In *Vehicular Technology Conference*, pages 1–6. IEEE, 2011.

[29] X. Chen, H. Refai, and X. Ma. On the enhancements to IEEE 802.11 MAC and their suitability for safety-critical applications in VANET. *Wireless Communications and Mobile Computing*, 10(9):1253–1269, 2010.

[30] Y. Wang, A. Ahmed, B. Krishnamachari, and K. Psounis. IEEE 802.11 p performance evaluation and protocol enhancement. In *International Conference on Vehicular Electronics and Safety*, pages 317–322. IEEE, 2008.

[31] M. Alsabaan, K. Naik, T. Khalifa, and A. Nayak. *Applying Vehicular Networks for Reduced Vehicle Fuel Consumption and CO_2 Emissions.* Book chapter in Intelligent Transportation Systems, 2011.

[32] Highway Capacity Manual.: Transportation Research Board. National Research Council, Washington, D.C., 2000.

[33] M.A. Chowdhury and A.W. Sadek. *Fundamentals of Intelligent Transportation Systems planning.* Artech House Publishers, 2003.

[34] A.D. May. *Traffic flow fundamentals*. Prentice Hall, 1990.

[35] D. Krajzewicz, G Hertkorn, P Wagner, and C. Rössel. SUMO (Simulation of Urban MObility): An Open-Source Traffic Simulation. In *Proc. 4^{th} Middle East Symp. Simulation Modeling*, pages 183–187, 2002.

[36] K. Nagel, P. Stretz, M. Pieck, R. Donnelly, and C.L. Barrett. TRANSIMS Traffic Flow Characteristics. In *Los Alamos National Lab. report (LA-UR) 97-3531*, 1999.

[37] Laboratory for Software Technology (ETH Zurich), "Realistic Vehicular Traces". http://lst.inf.ethz.ch/ad-hoc/cartraces.

[38] M. M. Artimy, W. Robertson, and W.J. Phillips. Connectivity in inter-vehicle ad hoc networks. *Proc. IEEE Canadian Conf. Elec. Comp. Eng.*, 1:293–98, 2004.

[39] T. Delot, S. Ilarri, S. Lecomte, and N. Cenerario. Sharing with caution: Managing parking spaces in vehicular networks. In *Mobile Information Systems*, volume 9, pages 69–98, 2013.

[40] B. Liu, D. Ghosal, C.N. Chuah, and H.M. Zhang. Reducing greenhouse effects via fuel consumption-aware variable speed limit (fc-vsl). *IEEE Transactions on Vehicular Technology*, 61(1):111–122, 2012.

[41] V. Gradinescu, C. Gorgorin, R. Diaconescu, V. Cristea, and L. Iftode. Adaptive traffic lights using car-to-car communication. In *Proceesing of IEEE 65^{th} Vehicular Technology Conference*, pages 21–25, 2007.

[42] T. Tielert, M. Killat, H. Hartenstein, R. Luz, S. Hausberger, and T. Benz. The impact of traffic-light-to-vehicle communication on fuel consumption and emissions. In *Internet of Things (IOT)*, pages 1–8. IEEE, 2010.

[43] K. Katsaros, R. Kernchen, M. Dianati, and D. Rieck. Performance study of a Green Light Optimized Speed Advisory (GLOSA) application using an integrated cooperative ITS simulation platform. In *IEEE International Wireless Communications and Mobile Computing Conference (IWCMC)*, pages 918–923, 2011.

[44] H. Rakha and R.K. Kamalanathsharma. Eco-driving at signalized intersections using v2i communication. In *IEEE Conference on Intelligent Transportation Systems (ITSC)*, pages 341–346, 2011.

[45] IEEE 802.11p: Wireless MAC and Physical Layer (PHY) specifications: Wireless Access in Vehicular Environments, July. 2010.

[46] IEEE Std 1609.4-2010, IEEE Standard for Wireless Access in Vehicular Environments (WAVE)-Multi-channel operation, Feb. 2011.

[47] C. L. Huang, Y. P. Fallah, R. Sengupta, and H. Krishnan. Adaptive InterVehicle Communication Control for Cooperative Safety Systems. *IEEE Network*, 24(1):6–13, 2010.

[48] Vehicle Safety Communications Consortium (VSCC), "Vehicle Safety Communications Project, Task 3 Final Report: Identify Intelligent Vehicle Safety Applications Enabled by DSRC," 2005.

[49] High Accuracy-Nationwide Differential Global Positioning System Program Fact Sheet. *U.S. Department of transportation-Federal Highway Adminstration*, Dec. 2012.

[50] M.A. Wiering, J. Veenen, J. Vreeken, and A. Koopman. Intelligent traffic light control. *Technical Report UU-CS-TR-2004-029, Institute of Information and Computing Sciences, Utrecht University*, 2004.

[51] C. Gershenson. Self-Organizing Traffic Lights. *Journal of Complex Systems*, 16(1):29–53, 2004.

[52] F. Rezaei, K. Naik, and A. Nayak. Investigation of Effective Region for Data Dissemination in Road Networks Using Vehicular Ad hoc Network. *IEEE International Conference on Fuzzy Systems*, pages 1977–1982, 2009.

[53] Manual on Uniform Traffic Control Devices (MUTCD), 2009 edition. Federal Highway Administration, U.S. Department of Transportation, December 2009. http://mutcd.fhwa.dot.gov/kno_2009.htm.

[54] A.S. Al-Ghamdi. Analysis of Time Headways on Urban Roads. *Civil Engineering and Environmental Systems*, 19(2):169–185, 2002.

[55] B. Chopard, P.O. Luthi, and P-A. Queloz. Cellular automata model of car traffic in a two-dimensional street network. *Journal of Physics A: Mathematical and General*, 29(10):2325–2336, 1996.

[56] B. Chopard, A. Dupuis, and P.O. Luthi. A cellular automata model for urban traffic and its application to the city of Geneva. *Network-Spatial-Theory*, 3:9–21, 2003.

[57] H. Rakha, M. Van Aerde, K. Ahn, and A.A. Trani. Requirements for evaluating traffic signal control impacts on energy and emissions based on instantaneous speed and acceleration measurements. In *Transportation Research Record*, volume 1738.

[58] J. Herrera and A. Bayen. Incorporation of Lagrangian measurements in freeway traffic state estimation. *Transportation Research Part B: Methodological*, 44(4):460–481, 2010.

[59] A. Hofleitner, R. Herring, P. Abbeel, and A. Bayen. Learning the dynamics of arterial traffic from probe data using a dynamic Bayesian network. *IEEE Transactions on Intelligent Transportation Systems*, 13, 2012.

[60] K. Dar, M. Bakhouya, J. Gaber, M. Wack, and P. Lorenz. Wireless communication technologies for ITS applications [Topics in Automotive Networking]. *IEEE Commun. Mag.*, 48(5):156–162, 2010.

[61] H. Rakha, K. Ahn, and A. Trani. Comparison of MOBILESa, MOBILE6, VT-MICRO, and CMEM Models for Estimating Hot-Stabilized Light-Duty Gasoline Vehicle Emissions. *Canadian Journal of Civil Engineering*, 30:1010–1021, 2003.

[62] M. Alsabaan, K. Naik, T. Abdelkader, T. Khalifa, and A. Nayak. Geocast routing in vehicular networks for reduction of CO_2 emissions. *Information and Communication on Technology for the Fight against Global Warming*, pages 26–40, 2011.

[63] M. Alsabaan, K. Naik, and T. Khalifa. Optimization of Fuel Cost and Emissions Using V2V Communications. *IEEE Transactions on Intelligent Transportation Systems*, 2013.

[64] M. Alsabaan, K. Naik, T. Khalifa, and A. Nayak. Optimization of Fuel Cost and Emissions with Vehicular Networks at Traffic Intersections. In *IEEE Intelligent Transportation Systems Conference*, pages 613–619, 2012.

[65] W. L. Winston and M. Venkataramanan. *Introduction to Mathematical Programming: Applications and Algorithms*. Duxbury, 2003.

[66] Regional Municipality of Waterloo. http://www.regionofwaterloo.ca.

[67] Google Earth, website. http://earth.google.com.

[68] Honda Plug-In Hybrid. http://world.honda.com/Hybrid.

[69] Toyota Prius 2013. http://www.toyota.com/prius-hybrid.

[70] Nissan LEAF. http://www.nissanusa.com/leaf-electric-car.

[71] M. Alsabaan, K. Naik, T. Abdelkader, T. Khalifa, and A. Nayak. Economical and Environmentally Friendly Geocast Routing in Vehicular Networks. *IEEE Systems Journal*, revised and resubmitted.

[72] IEEE. 5.9 GHz Dedicated Short Range Communications (DSRC). http://grouper.ieee.org/groups/scc32/dsrc.

[73] Statistics Canada. http://www40.statcan.gc.ca.

[74] S. Tsugawa and S. Kato. Energy ITS: another application of vehicular communications. *IEEE Comm. Magazine*, 48(11):120–126, 2010.

[75] M.L. Poulton. Alternative fuels for road vehicles. *Billerica, MA: Computational Mechanics Publications*, 1994.

[76] G. Zhang and Y. Wang. Optimizing minimum and maximum green time settings for traffic actuated control at isolated intersections. *Intelligent Transportation Systems, IEEE Transactions on*, (99):1–10, 2011.

[77] T. Delot, N. Cenerario, S. Ilarri, and S. Lecomte. A cooperative reservation protocol for parking spaces in vehicular ad hoc networks. In *Proceedings of the 6th International Conference on Mobile Technology, Application and Systems*, page 30. ACM, 2009.

[78] B. Asadi and A. Vahidi. Predictive cruise control: Utilizing upcoming traffic signal information for improving fuel economy and reducing trip time. *IEEE Transactions on Control Systems Technology*, 19(3):707 –714, 2011.

[79] M. Alsabaan, W. Alasmary, A. Albasir, and K. Naik. Vehicular Networks for a Greener Environment: A Survey. *IEEE Communications Surveys and Tutorials*, 2012.

[80] Y. P. Fallah, C. Huang, R. Sengupta, and H. Krishnan. Design of cooperative vehicle safety systems based on tight coupling of communication, computing and physical vehicle dynamics. In *Proceedings of the 1st ACM/IEEE International Conference on Cyber-Physical Systems*, pages 159–167, 2010.

[81] C. L. Huang and R. Sengupta. Analysis of Channel Access Schemes for Model-based Estimation over Multi-access Networks. In *IEEE International Symposium on Intelligent Control*, pages 408–413, 2008.